Distributed Interference Management in Unplanned Wireless Environments

Christopher Waters

Supervised by

Dr Simon Armour (Univ. of Bristol)

Prof. Angela Doufexi (Univ. of Bristol)

Dr Woon Hau Chin (Toshiba)

Dr Filippo Tosato (Toshiba)

Centre for Doctoral Training in Communications

University of Bristol

A dissertation submitted to the University of Bristol in accordance with the requirements for award of the degree of Doctor of Philosophy in the Faculty of Electronic and Electrical Engineering

PhD Communications

August 2020

Word count: 25,417

Abstract

As new applications for wireless communications are developed, system designers are turning more frequently to unplanned networks. While cheaper to deploy, such networks suffer a deficit in control and planning which have a negative impact on the network's ability to manage interference. The lack of centralised power control and scheduling increases the impact of collisions which manifest as in-band interference, negatively impacting performance. This thesis examines several aspects of interference management and determines the parameters that a system designer can manipulate to control the behaviour of the network.

First we determine the optimal update rate for a subspace-based distributed interference alignment scheme, reducing convergence time to within 100 iterations. While this improves the convergence time of the algorithm it offers no capacity improvement due to a lack of power-awareness in the algorithm. An altered algorithm is then proposed that offers power-awareness and is found to improve convergence time to less than 10 iterations at a cost to sum interference levels and network capacity.

We then propose training sequences that enables users to determine the number of antennas another user possesses with less than 1% error, using this information to recover the training signal for channel estimation. These sequences are found to perform better than the equivalent chaotic training sequences in estimating channel coefficients. This approach continues to function in channels with unequal transmit and receive antennas, permitting its use in heterogeneous networks.

Finally we derive an analytic expression for the upper bound of the likelihood an arbitrary number of neighbours can be detected by a user using SIC on transmissions from directional antenna arrays during neighbour discovery. The expression found permits the system designer to optimise system parameters such as SIR threshold, user array directivity, and transmission rate given the expected user density of the network.

Acknowledgements

I am forever indebted to the following people for their unwavering support and counsel throughout my time researching and writing this work.

To my parents for instilling in me the value of hard work and learning,

to Hannah for her encouragement to resume my work on my thesis and her help and support throughout the writing process,

to Simon for his patience and determination to see me along the path no matter how circuitous

... and to the rest of the CDT for keeping me in high spirits and knowing I'm not alone.

Declaration

I declare that the work in this dissertation was carried out in accordance with the requirements of the University's Regulations and Code of Practice for Research Degree Programmes and that it has not been submitted for any other academic award. Except where indicated by specific reference in the text, the work is the candidate's own work. Work done in collaboration with, or with the assistance of, others, is indicated as such. Any views expressed in the dissertation are those of the author.

SIGNED _____ DATE _____

Contents

List of Figures

Acronyms

$.^{[ij]}$ the ij^{th} submatrix of the larger matrix.

$\|\mathbf{X}\|_F$ The Frobenius Norm of a matrix.

$\|x\|$ The distance from the origin to a point x.

$\mathbb{E}[X]$ Expectation of the random variable X.

$\mathbf{H}_{ij}$ User indices are denoted by subscript - this example is the complex channel matrix between transmiter i and received j.

$\mathbf{I}_N$ The $N \times N$ Identity matrix.

$\mathbf{X}^H$ Conjugate transpose of the matrix $\mathbf{X}$.

$\mathbf{X}^T$ Regular transpose of the matrix $\mathbf{X}$.

$\mathbf{X}$ Matrices are denoted by a bold upright uppercase letter or character..

$\mathbf{y}$ Vectors are denoted by an bold upright lowercase letter or character..

$\mathcal{CN}(0, \sigma^2)$ Complex Gaussian distribution with mean 0 and variance σ^2.

$\mathcal{N}(0, \sigma^2)$ Gaussian distribution with mean 0 and variance σ^2.

$\mathcal{R}$ The set of Real numbers.

Bias(X) The Bias of random variable X.

Tr$(\mathbf{X})$ Trace of the matrix $\mathbf{X}$.

Var(X) The Variance of random variable X.

diag$(\mathbf{X})$ The diagonal entries of the matrix $\mathbf{X}$.

rank$(\mathbf{H})$ Rank of the matrix $\mathbf{H}$.

span$(\mathbf{X})$ span of the columns of the matrix $\mathbf{X}$.

vec$(\mathbf{X})$ The vector operator creates an $NM \times 1$ column vector from an $N \times M$ matrix.

$\otimes$ The Kronecker Product.

$\phi = \{\cdots\}$ Definition of a set.

$\phi \sqcup \psi$ The union of sets phi and psi.

$|\mathbf{h}|$, $|\Phi|$ The absolute value of a complex number or the size of a set.

x, N Scalar quantities are denoted by a italic letter or character..

AWGN Additive White Gaussian Noise.

BER Bit Error Rate.

CDF Cumulative Distribution Function.

.

CSI Channel State Information.

CSIR/T Channel State Information at the Receiver/Transmitter.

CSMA Carrier Sense Multiple Access with Collision Avoidance.

DoF Degrees of Freedom.

FM Frequency Modulation.

GDoF Generalised Degrees of Freedom.
GPS Global Positioning System.

HPBW half-power beamwidth.

IA Interference Alignment.
IC Interference Channel.
ICS Industrial Control System.
IEEE Institution of Electronic and Electrical Engineers.
IoT Internet of Things.
IT Information Technology.
ItA Iterative Alignment.

LAN Local Area Network.
LTE Long Term Evolution.

MAC Media Access Control, Multiple Access Channel.
MCS Modulation and Coding Scheme.
MIMO Multiple Input Multiple Output.
ML Maximum Likelihood.
MRRC Maximal-Ratio Receiver Combining.
MSE Mean Squared Error.

NKP Nearest Kronecker Product.
NMSE Normalised Mean Squared Error.
NR Interference to Noise Ratio.

PPP Poisson Point Process.

QoS Quality of Service.

SIC Successive Interference Cancellation.
SINR Signal to Interference plus Noise Ratio.
SISO Single Input Single Output.
SNR Signal to Noise Ratio.
SVD Singular Value Decomposition.

TIM Topological Interference Management.

TIN Treating Interference as Noise.

UCA Uniform Circular Array.

ULA Uniform Linear Array.

WLAN Wireless Local Area Network.

WLI Weighted Leakage Interference.

WSN Wireless Sensor Network.

1 Introduction

1.1 Motivation

Ubiquitous network connectivity – in particular connectivity for non-IT devices in low-power, short range networks in what is referred to as the 'Internet of Things' (IoT) – is heralded as the next phase of the information age and the beginning of the fourth industrial revolution [1]. While some IoT deployments will be carefully planned in industries or applications where reliability is a key requirements (e.g. building services, industrial processes, personal and corporate security) there will be many applications where networks will be deployed rapidly or on an ad-hoc basis. In order to meet the ever-increasing needs for wireless bandwidth, both types of networks require robust and effective interference management.

Rapidly deployed and unplanned networks face a significant challenge; such networks will likely rely on minimal infrastructure either through design or necessity, and so will rely on decentralised methods for deployment. This includes, but is no limited to:

- negotiating a media access scheme,
- channel estimation (without the assistance of a central base station, or *a priori* information on the channel)
- establishing a common modulation and coding scheme
- agreeing channel usage and user rates

Users in unplanned networks will need to be capable of adapting to the wireless environment they find themselves in, which could range from very dense to very sparse deployments, or as a secondary user in the presence of a higher-priority primary user to which no interference should be caused. Without the strict coordination between users and sophisticated multiple-access schemes available to planned networks, unplanned networks suffer the deleterious effects of co-channel interference more acutely.

System designers responsible for setting the parameters of devices before deployment face

a significant challenge; the techniques used to achieve the list of tasks above must be capable of working with a minimum of assistance from the network operator (ideally none), and also with minimal feedback from other users in the network. For this reason decentralised protocols and algorithms must operate independently but be capable of reaching solutions that enable sufficient network access for every user within the limitations set by the designers. There is therefore merit in investigating such techniques, and assessing the key parameters of algorithms used to reach workable interference management solutions within an unplanned network.

1.2 Interference Management Use Cases

The Unplanned Wireless Network

Unplanned wireless networks are typified by their distributed Media Access Control, Multiple Access Channel (MAC) layer. Examples include contention-based Wireless Local Area Network (LAN) protocols such as the IEEE 802.11 WiFi standards and IEEE 802.15 Low-Rate Wireless Networks [2, 3]. In these networks it can be safely assumed that most users are battery-powered, and so any transmissions that do not result in a successful communication are highly undesirable, as are transmissions at power levels in excess of what is required for successful communications. For this reason collisions due to contention in the network are avoided using collision avoidance protocols and self-organised scheduling between nodes that ultimately negatively impact the sum throughput of the network. The possibility that Interference Management can progress beyond these avoidance techniques and offer greater likelihood of successful communication between users with every transmission are very appealing in these applications.

Heterogeneous Cellular Networks

As cellular networks meet ever-increasing demand for high-bandwidth user terminals and begin to support the IoT they will begin to rely on low-range, high-rate small cells (often called picocells and microcells) to provide the necessary wireless resource. This is a process known

as network 'densification' and is considered a key enabler of fifth-generation (5G) and later phases of Long Term Evolution (LTE) mobile networks [4, 5]. This process allows areas of particularly high demand to be addressed without going to the trouble and expense of planning a new cell deployment. These networks will typically not be installed by the cellular provider but by businesses and home users who will not have access to the cell planning tools used by network providers to ensure co-channel interference is kept to a minimum. For this reason these deployments must be capable of avoiding becoming a source of interference to the rest of the cellular network, and themselves avoid co-channel interference from the larger cells, in order to be of any use to the customer.

1.3 Thesis structure and summary of contributions

The remainder of this thesis is structured as below:

Chapter 2 introduces the background concepts and theory required in order to understand the foreground content and contributions of the thesis. This includes the basics of MIMO transmission as well as introducing the Singular Value Decomposition (SVD) decomposition method of identifying subchannel eigenspaces in a Gaussian vector channel.

Also presented are the prior art in this field; various interference management techniques and their application to the two-user interference channel, each determined by the prevailing conditions in the Single Input Single Output (SISO) interference channel. The concept of interference alignment is then described.

Finally the concept of Stochastic Geometry is introduced, and a number of techniques from the field are demonstrated in how they can be used to estimate the parameters of an unplanned wireless network, modelled as a Poisson point process.

Chapter 3 is concerned with implementing a distributed interference management, namely the Iterative Alignment (ItA) algorithm [6]. The operation of the algorithm is measured and its performance assessed against the needs of a typical application. In particular, the instability of

the algorithm in its original form prevents its use in practical schemes.

Two modifications are proposed and their performances assessed against the 'standard' Iterative Alignment scheme. The first modification is to reduce the frequency of updates to introduce stability to the algorithm by reducing the opportunity for hysteresis within the solution. This is found to be highly effective in reducing the time taken for the users to converge on an alignment solution, albeit at a penalty to residual interference and hence network sum capacity.

The second modification is to enable a user to cease updating its coding vector coefficients when it reaches a point in which a suitable interference management scheme is possible. We determine when this can be determined using only local channel information and measure the effect this power awareness has on the performance compared to Iterative Alignment. The effects are more pronounced than simply reducing the update probability, with convergence now possible within only a few iterations. However this comes at a steeper price than selective updates, with the possibility of a feasible interference solution being less likely than the other two forms of the algorithm.

The chapter concludes with recommendations for which of the various iterative alignment schemes are best suited for a variety of applications.

Chapter 4 is concerned with estimating a key element of many interference management techniques; the number of antennas each user possesses. This is of critical importance to alignment and power control schemes in which the number of antennas of interferers form part of the achievable rate region.

In this chapter we derive a method for estimating the rank of a channel using only locally-collected information. This is achieved through the design of specific training sequences that exploit the correlation properties of the channel. The performance of the technique is found to be relatively invariant to the length of the training sequence, and requires only a few repetitions to establish adequate correlation properties. This suggests the training sequence is suitable for use in low-power networks where excessive transmissions should be avoided.

The training sequence is also demonstrated to be effective in channels that are underdetermined, for instance when the number of receiving antennas is fewer than that of the transmitter. It is also demonstrated to be an effective channel equalisation sequence, outperforming the equivalent 'chaotic' sequence from the literature. This is of significant value where both channel rank estimation and equalisation must be performed. Some of the content of this chapter was published in [7].

Chapter 5 addresses the problem of neighbour discovery during the initial configuration of an unplanned wireless network. Neighbour discovery is especially important when interference management relies upon knowledge of which of the node's neighbours are potential interferers or victims. In this chapter we propose a neighbour discovery technique for MIMO networks where the transmitters use circular arrays and Dolph-Chebyshev array patterns to create two classes of neighbour at the receiver, aligned and unaligned. Due to the ability of the Dolph-Chebyshev technique to suppress the gain of sidelobes, each class of neighbour exhibits very different channel gains. Through this construction it is possible to analyse the success likelihood of detecting multiple aligned neighbours through SIC, against a backdrop of interference from the remaining unaligned users.

This is achieved using multiple Poisson Point Processes (PPPs) to represent the two independent sets of users, those with their main lobes aligned with the receiver and those who are unaligned. Through these two PPPs we find a closed form expression for the upper bound of the success probability of detecting k neighbours simultaneously, and from it identify four network parameters that a system designer may use to 'tune' the network according to the physical attributes and performance goals of the network. These four parameters are compared and opportunities for trade-offs between them that the designer can make are identified. It is found that the upper bound is acceptable as an indication of the effects of the network user density, sidelobe suppression, and transmission probability on the success likelihood, but as the complexity of the coding scheme employed increases the bound becomes loose and is of less value to the system designer.

Finally in Chapter 6 we conclude the thesis with conclusions drawn on the impact of the previous chapters on the practicality of interference management. In addition further work in developing the techniques proposed in this thesis as well as related work is described, and predictions made as to how these developments might be able to improve the state of interference management techniques.

2 Background

This chapter outlines some of the background required in order to consider Interference Management and other related techniques. This underpins the contributions in the following chapters.

2.1 Chapter Structure

This chapter is organised as follows:

In Section 2.2 we introduce the theory and nomenclature of Multiple Input Multiple Output (MIMO) transmission. The K-user MIMO Interference Channel is also presented, a model frequently used to analyse interference in wireless networks. The Singular Value Decomposition (SVD) method of decomposing the MIMO channel into independent channels is then introduced, and we demonstrate how this manner of coding permits more sophisticated methods of interference management than those already discussed. This section introduces the concepts of Degrees of Freedom (DoF), over which alignment schemes operate, and Generalised Degrees of Freedom (GDoF), which is a measure of network performance against the behaviour of the equivalent Single Input Single Output (SISO) Interference Channel.

In Section 2.3 we introduce and compare various methods of interference management that are already widespread. We compare and contrast their capabilities and conditions for use, with a particular focus on the spatial management schemes that will be considered in this thesis.

Finally in section 2.4 we review the tools and techniques from Stochastic Geometry that can be used to predict random user placement within a wireless network. An example is then offered showing how a model of node placement can be used to make estimates of the level of interference within the network.

2.2 Wireless communication

Wireless Communication stands out as one of the defining technologies of the modern industrial revolution and advent of the information age, and one that stands to continue to influence the growth of an increasingly data-based economy [8, 9]. Modern Wireless Local Area Network (WLAN) standards have allowed the use of wireless to become commonplace in the home and workplace, having previously been the reserve of advanced technical users (amateur and packet radio), broadcasters (television and FM radio), and governmental and commercial organisations (marine, emergency services, long-distance telecommunications). Alongside the increased use of wireless networks in the home, the use of connected devices has introduced a new class of user to many corporate and industrial networks. Industrial Control System (ICS) and Internet of Things (IoT) applications have made it possible for a wide variety of sensors, actuators and processing devices to now be connected to the network. This permits new real-time monitoring, control and management applications that have been hailed as the 'fourth Industrial Revolution'. All of these have contributed to an ever-increasing demand for wireless connectivity, in new environments no longer limited to the home or office.

With this increased demand has come a significant technical challenge; as modulation schemes become more complex and communications margins become tighter the influence of interference from neighbouring users becomes greater than that of noise, the classic source of wireless transmission error. Such networks are known as *interference limited* networks, in contrast to *noise limited* networks where noise is the most significant factor in predicting system performance. In interference limited networks the typical 'link budget' approach to estimating Bit Error Rate (BER) fails to capture the necessary information to characterise performance. The likelihood of error is now influenced by probabilistic factors introduced by interference such as fading, correlation, and timing.

Various techniques have been developed to overcome some of these challenges, either allowing the effects to be overcome (e.g. reducing the likelihood of all modes of a transmitted signal experiencing fading at the same time) or to be modelled and factored into the transmission

strategy (e.g. precoding a transmission to negate the effects of a correlated source or interferer). These will be discussed in later sections of this chapter.

2.2.1 MIMO Transmission

The concept of harnessing multiple antenna elements to influence the properties of a transmitter or receiver has prevailed since almost the beginning of radio, and has been used to enhance signal power and directivity in phased arrays and steerable Radar systems since the early 20th century. These approaches are appropriately known as *beamforming* approaches, as they are primarily used to alter the transmission power envelope to form a 'beam' of concentrated energy in the direction of the desired receiver. Conversely this technique can also be used to steer 'nulls', regions of low energy directivity, towards undesired receivers. Such techniques do not take into account the scattering or phasing effects of the environment between transmitter and receiver, and so are employed in applications where the scattering environment does not change or has little influence on the link budget.

Around the turn of the 21st century the idea was introduced of using separate transmitter chains associated with each element in the transmitter array to make use of the scattering characteristics of the channel. This began with demonstrating how transmitter diversity could be used to improve resistance to multipath fading in a Maximal-Ratio Receiver Combining (MRRC) system [10]. Separate receiver chains allow further manipulation of the received signals to maximise system performance. By exploiting the diversity inherent in the link between each pair of transmitter and receiver antenna, a complex matrix of channel coefficients can be created. Such systems with both multiple transmit and multiple receive antennas are known as Multiple Input Multiple Output (MIMO) systems.

By altering the phase and amplitude of the signal before transmission through each antenna (i.e. precoding) or after (i.e. postcoding), the channel can provide one of two characteristics: *Spatial diversity* provides protection from the effects of fading by spreading energy across a number of different transmission modes which, given suitable conditions, are not affected by the

same frequency or spatial variations at the same time. *Spatial multiplexing* splits the complex MIMO channel into multiple spatially (in the sense of mathematical eigenspaces, as opposed to physical space) separated channels, each of which has the capacity of a SISO channel with its own channel characteristics. These channels can then be effectively treated as independent channels, and transmissions coordinated between them according to the transmission strategy chosen.

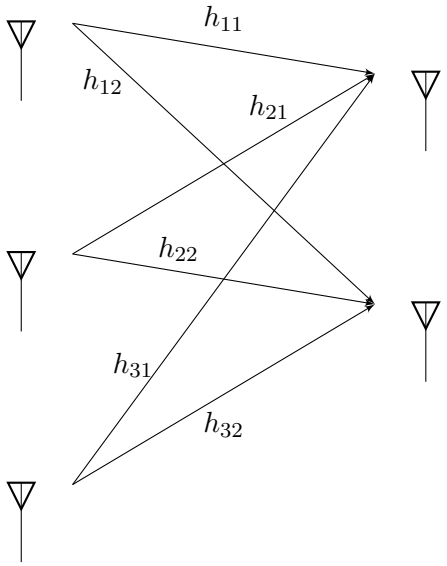

Figure 2.1: A 3×2 MIMO Channel demonstrating six channel coefficients between each pair of transmit and receive antenna

2.2.2 Spatial Multiplexing

The transmission schemes discussed in this thesis are based around spatial multiplexing, i.e. maximising the number of simultaneous streams that can be transmitted in the network. For this reason we shall restrict our discussion of MIMO to these schemes. Spatial diversity schemes are discussed in depth in [11].

In this thesis we consider the narrowband (i.e. non-dispersive) K-user MIMO channel model, where K describes the number of users in the channel. Figure 2.1 depicts a single instance of the MIMO channel between a single transmitter and receiver. In the multiuser MIMO network many of these channels exist, between each transmitter and receiver pair. Each channel has dimension

$N \times M$, where N represents the number of receiving antennas, and M the transmitting antennas. In the case of the K-user MIMO channel each individual channel between transmitter i and receiver j is completely described by the channel matrix $\mathbf{H_{ij}}$. Each instance is a vector Gaussian channel, where each element of the channel matrix h_{kl} is a complex Gaussian random variable with unity power, and describes the channel gain from transmit antenna k to receive antenna l. This corresponds to a frequency-flat Rayleigh fading channel with no correlation at either transmitter or receiver. The time index will be omitted from further discussion as we assume that the channel exhibits a coherence time greater than the time taken to transmit the sequence $\mathbf{x}$ [12], and channel estimation is performed for each 'realisation' of the channel independently of all others over time.

The output of the $M \times N$ MIMO channel is

$$\mathbf{y_j} = \mathbf{H_{ij}x_i} \tag{2.1}$$

where $\mathbf{y}$ is the received message, $\mathbf{x}$ is the transmitted message and $\mathbf{H}$ is the complex channel matrix.

By applying precoding and postcoding vectors $\mathbf{V}$ and $\mathbf{U}^H$ to the transmitted and received signals respectively it is possible to manipulate what is sent through the channel to the receiver.

We derive the coding vectors from the unitary rotation matrices generated by performing Singular Value Decomposition (SVD) on the channel matrix:

$$\mathbf{H} = \mathbf{U}\mathbf{\Lambda}\mathbf{V}^H \tag{2.2}$$

$$= \begin{bmatrix} \mathbf{u}_1 & \mathbf{u}_2 & \mathbf{u}_3 \\ \vdots & \vdots & \vdots \end{bmatrix} \begin{bmatrix} \lambda_1 & 0 & 0 & 0 \\ 0 & \lambda_2 & 0 & 0 \\ 0 & 0 & \lambda_3 & 0 \end{bmatrix} \begin{bmatrix} \mathbf{v}_1^H & \dots \\ \mathbf{v}_2^H & \dots \\ \mathbf{v}_3^H & \dots \\ \mathbf{v}_4^H & \dots \end{bmatrix} \tag{2.3}$$

$$= \sum_{\max M,N} \mathbf{u_l} \lambda_l \mathbf{v_l^H} \tag{2.4}$$

where $\mathbf{\Lambda}$ is an $N \times M$ matrix whose diagonal entries are the ordered singular values of the channel matrix $\mathbf{H}$. If the eigenvectors corresponding to the eigenvalues of the channel (i.e. the matrices $\mathbf{V}^H$ and $\mathbf{U}$) are known to both parties it is possible to treat each individual stream as a separate channel, each with a gain of $\lambda_i \quad i = 1, \dots d$ This result is known as the Singular Value Decomposition of the MIMO channel.

The maximum number of independent channels that can be generated in this manner is limited to the smaller of the dimensions of $\mathbf{H}$, i.e. $d = \min(M, N)$ and is equal to the rank of the matrix Λ. This gives rise to the Degrees of Freedom (DoF) of the channel, expressed as the number of individual eigenchannels created by the combinations of coding vectors $\mathbf{u}$ and $\mathbf{v}$ and gain values λ.

Consider the single-user MIMO channel with perfect Channel State Information (CSI). By using the SVD-derived eigenvectors as coding matrices it is possible to express the received message as a simple sum of the transmitted messages. In this case the transmitted signal $\mathbf{x}' = \mathbf{V}\mathbf{x}$ is precoded before transmission. The postcoded signal $\mathbf{y}' = \mathbf{U}^H\mathbf{y}$ at the receiver therefore has the form

$$\begin{aligned}\mathbf{y}' &= \mathbf{U}^H\mathbf{y} \\ &= \mathbf{U}^H(\mathbf{H}\mathbf{x}' + \mathbf{n}) \\ &= \mathbf{U}^H(\mathbf{U}\mathbf{\Lambda}\mathbf{V}^H\mathbf{V}\mathbf{x} + \mathbf{n}) \\ &= \mathbf{\Lambda}\mathbf{x} + \mathbf{U}\mathbf{n} \\ &= \mathbf{\Lambda}\mathbf{x} + \mathbf{n}' \end{aligned} \tag{2.5}$$

where $\mathbf{n}$ is the additive white gaussian noise encountered in the channel, which has unity power and auto correlation matrix $\mathbf{n}\mathbf{n}^H \sim \mathcal{N}(0, I_N)$, and $\mathbf{n}'$ represents the postcoded noise vector. Since $\mathbf{U}^H$ is a rotation matrix the power of the noise received is unaffected, but is 'steered' into a particular eigenspace.

The SVD decomposition and eigenchannel transmission method demonstrates a powerful capability of MIMO transmission: by directing individual symbol streams and splitting the power into particular eigenspaces, the throughput of a channel use can be arbitrarily selected subject to the limits imposed by the individual gains of each eigenchannel. As will be discussed in later sections it is also possible to allow interference between the eigenchannels, allowing throughput and interference to be traded against each other in pursuit of the optimal transmission strategy for a given channel. These techniques requires precise channel knowledge at both transmitter (CSIT) and receiver (CSIR) in order to compute the correct precoder and postcoder matrices.

2.2.3 Generalised Degrees of Freedom

The sum and symmetric capacity of a network is often stated in units of 'Generalised Degrees of Freedom' (GDoF). GDoF is a metric introduced in [13] to describe the symmetric rate achieved in an interference channel as a fraction of the channel capacity of the equivalent Additive White Gaussian Noise (AWGN) channel with no interference. GDoF can be described as thus:

$$d_{sym}(\alpha) := \lim_{\mathrm{SNR,INR}\to\infty;\frac{\log\mathrm{INR}}{\log\mathrm{SNR}}=\alpha} \frac{C_{sym}(\mathrm{INR},\mathrm{SNR})}{\mathrm{C_{awgn}(SNR)}} \tag{2.6}$$

The GDoF 'W curve', which demonstrates the achievable region for the channel given the strategies above, is shown in Figure 2.2. This provides an intuitive interpretation of the effect of interference on channel capacity; if there was no interference then the capacity of each link would equal the AWGN channel capacity and $d_{sym}(0) = 1$. The effect of noise on the achievable rate of the channel is therefore abstracted away from the discussion of interference. As such, optimisation of GDoF alone does not ensure successful communication through the channel.

In the low interference regime (i.e. $\alpha = \frac{\log\mathrm{INR}}{\log\mathrm{SNR}} < 0.5$) the authors identify that the optimal transmission strategy is simply to treat interference as noise (TIN). The GDoF achievable in this region follows intuitively then, that as the interference grows from $\alpha = 0$ (no interference) TIN offers diminishing returns. In the medium interference channel ($0.5 < \alpha < 2$) the authors identify that a power-splitting technique is the optimal strategy, with a simple Han-Kobayashi scheme (see Section 2.3.3) able to achieve the entire rate region to within 1/bit/sec/Hz). Within the region $0.5 < \alpha < 1$ it is also still possible to use TIN as transmission strategy, subject to the same diminishing returns observed in the low interference regime. In the high interference regime where the interference power is significantly greater than the desired signal (i.e. $\alpha \geq 2$ then the receiver would be capable of decoding the interfering signals first and subtract it from the aggregate signal. This allows the full AWGN channel capacity (represented by a GDoF=1) to be achieved in the desired link.

It is clear that there is no single optimal transmission strategy for interference channels, and some channel knowledge will be necessary to be able to make the best use of the resources available (e.g. where a power-splitting technique is required). These techniques will be the topic of discussion in the next section.

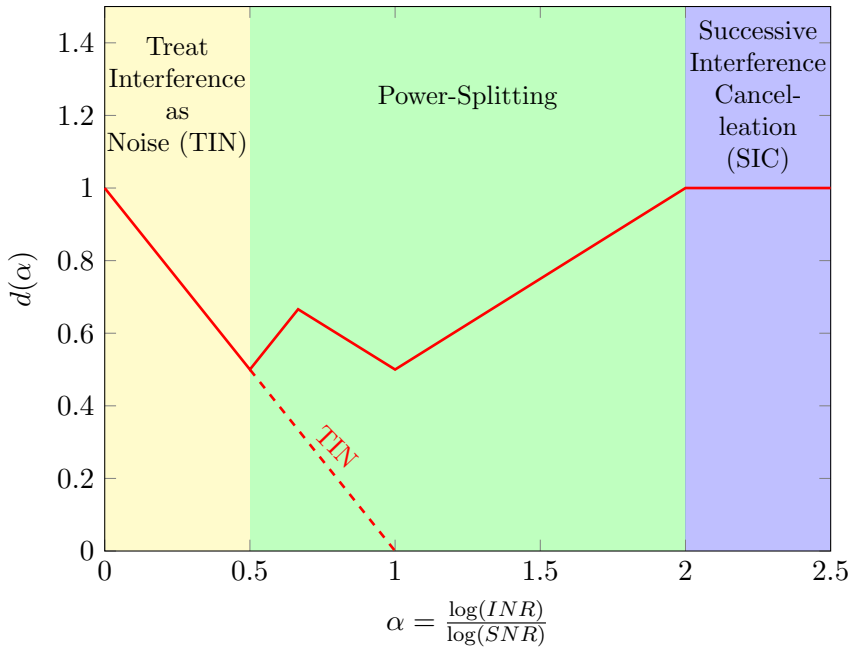

Figure 2.2: The GDoF 'W' curve for the two-user symmetric Gaussian interference channel showing the optimal transmission strategy according to [13]

2.3 Interference Management

This section describes several methods of interference management, listed in approximate order of complexity. In practice, several of these solutions may be used in response to the prevailing conditions within the network.

The simplest method of Interference Management is to prevent it from happening in the first instance. This can be achieved through three mechanisms; power control, transmission control, and spectrum allocation. However, since these are avoidance techniques they ultimately sacrifice user access to the channel to prevent interference.

Where interference is unavoidable, or where a control mechanism is unable to function correctly (e.g. decentralised networks or especially large networks where transmissions between users at the extremities of the network are difficult to coordinate) it may be appropriate to simply treat the interference as noise, and suffer the penalty to the desired messages' SNRs in exchange for a low-complexity solution. This is known to be the case in the low interfer-

ence regime, where the influence of interference in the channel is less than that of the noise encountered.

Where desired and undesired signal levels are of comparable power levels, the use of superposition coding enables transmission schemes where the undesired messages are decoded in the same manner as the desired ones. Users in the channel can decode this intentional interference and subtract it from the received signal to reveal the desired message, in a technique called Successive Interference Cancellation. In such schemes messages are formed out of two codebooks, one which is intended to be received by all users and is allocated sufficient power that it can be decoded and removed from the aggregated received signals at all receivers.

Some methods for interference management take a more 'cognitive' approach to transmission control; most transmission strategies exhibit greedy behaviour, attempting to make the best use out of the channel individually. This has been demonstrated to be less effective than transmitters taking cognisance of the interference they generate, and by backing off on their channel usage users can actually improve overall system performance [14, 15, 16]. This is achieved by permitting interference to be introduced into the network, albeit at lower power than if a greedy power control algorithm were used. MIMO coding of these interfering messages is steered into a subspace within the eigenspaces of both intended and unintended channels, with the outcome being some of the available DoF is lost to interference, but leaves the remainder of the channel interference free.

As will become apparent in the course of this section of the thesis there is no single transmission strategy that is optimal over the entire range of scenarios that may be encountered within the network; the prevailing conditions of interferers and desired transmissions will determine the best course of action. It is also clear that each strategy has its own drawbacks and challenges; some may not necessarily be perfectly suited to operation in an unplanned wireless network, while some may be capable of operation but with significant restrictions or have onerous requirements in order to be usable.

Table 2.1: Resource allocation techniques

Signalling dimension	Allocation technique
Time	Time Division Multiple Access
Space	Antenna directivity
Frequency	Frequency Division Multiple Access
Eigenspace	Spatial multiplexing

2.3.1 Avoidance Techniques

Power Control is the mechanism by which interference is minimised in a network by limiting the power of transmissions such that they meet the Quality of Service (QoS) required 'and no more'. In most wireless networks it can be assumed that users rely on limited power sources (normally batteries) and so efficient use of transmit power is crucial. Power limitations might also be imposed due to licensing restrictions. Power control is achieved usually through link adaptation, where the user alters its transmission power given the error rates of its previous transmissions. In a wireless network it is also crucial that transmitters only use sufficient power to ensure successful communications, as excess power emitted into the network has greater potential to interfere with other users' communications. Distributed power control is a difficult task, and is often performed in an iterative manner depending on the error rates experienced by users in isolation with no cooperation between transmitters. [17] proposes a distributed power control algorithm that optimises SINR with the aid of CSIT, for instance.

The most frequently used and relevant avoidance technique to wireless networks is spectrum allocation. By assigning a defined portion of the wireless resource to each user for their exclusive use, interference is avoided for the majority of cases (synchronisation errors and MAC-level collisions notwithstanding). In Multiple Access networks this translates to essentially 'orthogonalising' the signalling subspaces each user is assigned within the network. These subspaces can be a combination of space, time, frequency, or eigenspace. Table 2.1 lists allocation techniques for each of these dimensions.

In the centralised case each user is able to achieve a symmetric rate equal to $1/K$ of the single-user channel capacity (where K is the number of users in the network), assuming equal

resource-sharing. Centralised schemes are capable of dynamic resource allocation, as signalled by the users to the controlling base station. This technique is widely used in technologies such as Long Term Evolution (LTE), where users can be dynamically allocated subcarriers depending on their service requirements [18].

Finally interference can be avoided using MAC-layer mechanisms, where transmissions are scheduled in such a manner so as to avoid two nodes transmitting (and thus interfering with each other) at the same time. Such schemes have evolved from the ALOHA protocol [19] originally proposed for ALOHANET, and are commonly used in IEEE Wireless Local Area Network protocols such as 802.11 (WiFi) in the form of Carrier Sense Multiple Access with Collision Avoidance (CSMA).

Such protocols are not immune from interference; to the contrary, rather than attempt to recover the signal the entire frame is considered lost should a collision occur. Many MAC protocols however have built-in detection and correction techniques to reduce the likelihood of further collisions. The symmetric rate possible through an entirely probabilistic MAC scheme such as ALOHA is hard to determine, and even when some structure is imposed on the scheme (e.g. slotted ALOHA) the throughput must be estimated using models that simplify some aspects of the MAC protocol.

2.3.2 Treating interference as noise

The two-user Gaussian interference channel as shown in Figure 2.3 is considered in the next few sections.

In the noise-limited regime, the interference experienced by the receiver is less than the noise power. It is known that in this regime that Treating Interference as Noise (TIN) is the optimal strategy, and leads to simple channel codebooks that are well understood and have well-defined performance boundaries. However, even for the most simple schemes the rate region is not trivial and relies on channel information in order to determine the optimal power levels for each transmitter [20].

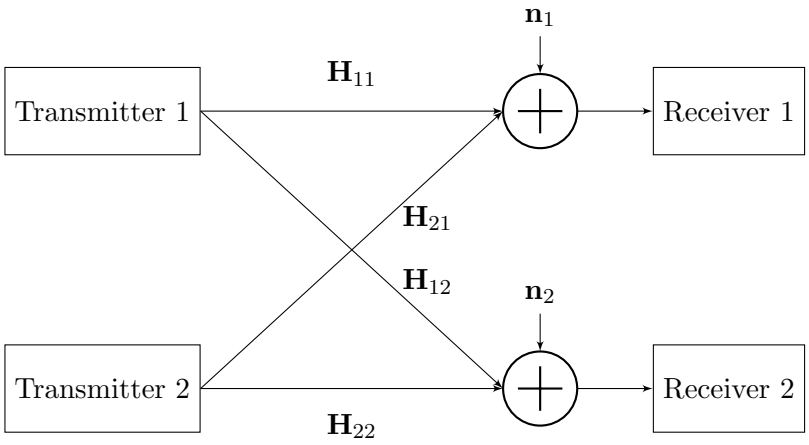

Figure 2.3: The Two-user MIMO Interference Channel

Many results examining TIN apply only to the two-user interference channel; the literature makes frequent use of the two-channel interference channel to determine new bounds for the GDoF of a channel, but most approaches would need to be applied simultaneously between each pairwise match of users within the network. This would not be feasible without significant information transfer between users, and causes non-linearity in the emergent behaviour of many users executing the algorithm independently. [21] investigates the optimality of TIN in the K-user Gaussian interference channel, in an attempt to determine the criteria where TIN could be applied globally and be known to be optimal. The authors determine that TIN is the optimal strategy, achieving all points in the capacity region to within a constant gap, when for each user the desired signal power is no less than the sum of the strengths of the strongest interference from this user and the strongest interference to this user.

2.3.3 Han-Kobayashi schemes

Efforts have been made to alleviate the effect of Multiple Access capacity degradation with the use of multiuser cancellation techniques. These techniques permit users to interfere with each other in such a manner that a suitably-equipped receiver is capable of removing this interference. *Successive Interference Cancellation* enables a receiver to successively decode each interfering signal (starting with the most powerful), removing it from the combined received signal leaving the remaining signals to be decoded in the same manner. This can be repeated until the desired

signal is detected and, SINR permitting, decoded. Many schemes employ a 'Han-Kobayashi' scheme, so named after the authors of [22].

The Han-Kobayashi scheme is based off the transmission of two symbol streams simultaneously, using superposition coding to combine them in a single codebook. These streams are called 'user' creating a virtual user W, and 'common' creating a virtual user U. Common streams are intended to be decoded by all users who receive them; once decoded, the remaining signals will be the user streams, of which only the desired message need be decoded. The user messages not intended for that particular receiver are treated as noise. In the two-user Gaussian interference channel this duality allows the interference channel to be treated as two separate multiple access channels.

Consider the two-user interference channel depicted in Figure 2.3, where each user is equipped with only SISO capabilities. This is done only for clarity; Han-Kobayashi schemes are equally applicable to MIMO schemes as demonstrated in [23]. In order for both users to be able to communicate they both must transmit at private and public rates achievable within their respective Multiple Access Channels; the achievable rate region of the interference channel can thus be defined as the union of the achievable rate regions of both Multiple Access Channels.

Each user transmits two streams, one public (W_1 and W_2) and one private (U_1 and U_2). They are allocated powers P_{w1},P_{w2},P_{u1},P_{u2} and achieve rates R_{w1},R_{w2},R_{u1},R_{u2} respectively.

The signals at receivers 1 and 2 are thus

$$y_1 = h_{11}w_1 + h_{11}u_1 + h_{21}w_2 + h_{21}u_2 + \sigma_1 \tag{2.7}$$

$$y_2 = h_{12}w_1 + h_{12}u_1 + h_{22}w_2 + h_{22}u_2 + \sigma_2 \tag{2.8}$$

where σ_i is the AWGN noise term apparent at receiver i. Thus the rates of the user streams are defined as the rates $R_1 = R_{u1} + R_{w1}$ and $R_2 = R_{u2} + R_{w2}$ that exist in both regions shown in Figure 2.4.

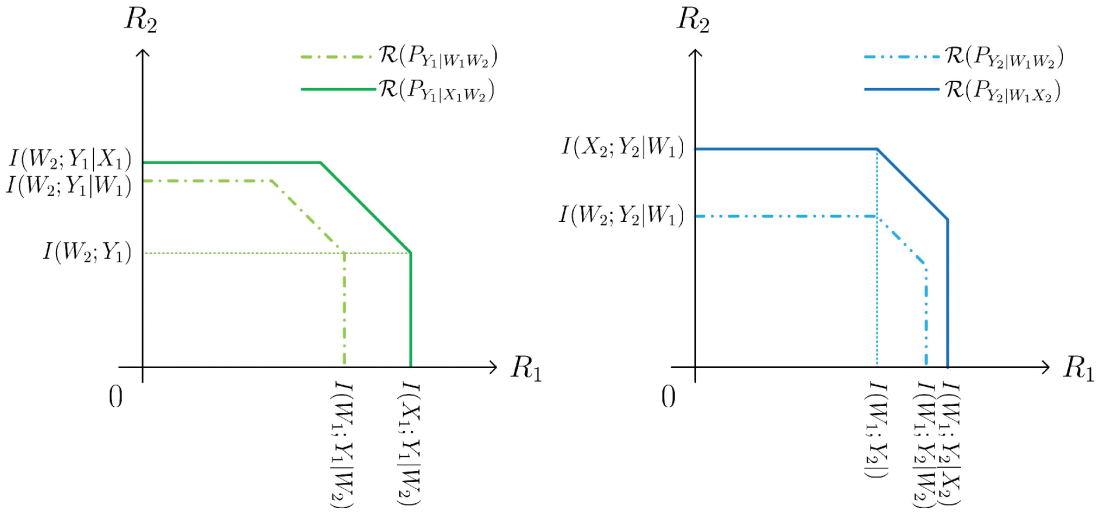

Figure 2.4: Illustration of the achievable rate regions available in a two-user interference channel through the creation of Multipl-Access Channels by a Han-Kobayashi scheme. The combined public and private messages of the users are described as X_1, X_2 and the public messages W_1, W_2 (from [24])

While this is a powerful tool that can dramatically improve the symmetric rate of the channel [25] this requires additional side information (signal powers, positions in the power 'ranking') to be made known to the transmitters and receivers. It is also possible to perform joint decoding of the public and private streams [26], which yields better resilience against erroneous decoding of the unwanted common stream but requires knowledge of the codebooks required *a priori*.

2.3.4 Interference Alignment

With the advent of adaptive signal processing and MIMO architectures Interference Alignment (IA) has become a feasible management technique that approaches interference from a different perspective. Much information theoretical work has been carried out to find bounds for the performance of IA in different channels. These includes the MIMO X Channel [27] and, most important for this discussion, the K-user Interference Channel [28].

Indeed, it is the interference channel that offers one of the most interesting results from the theory of Interference Alignment; with perfect alignment, and sufficiently high Degrees of Freedom (DoF) and Signal to Noise Ratio (SNR), it is possible for the sum rate of the system to scale linearly with the number of users K without bound. In addition, each user receives half the

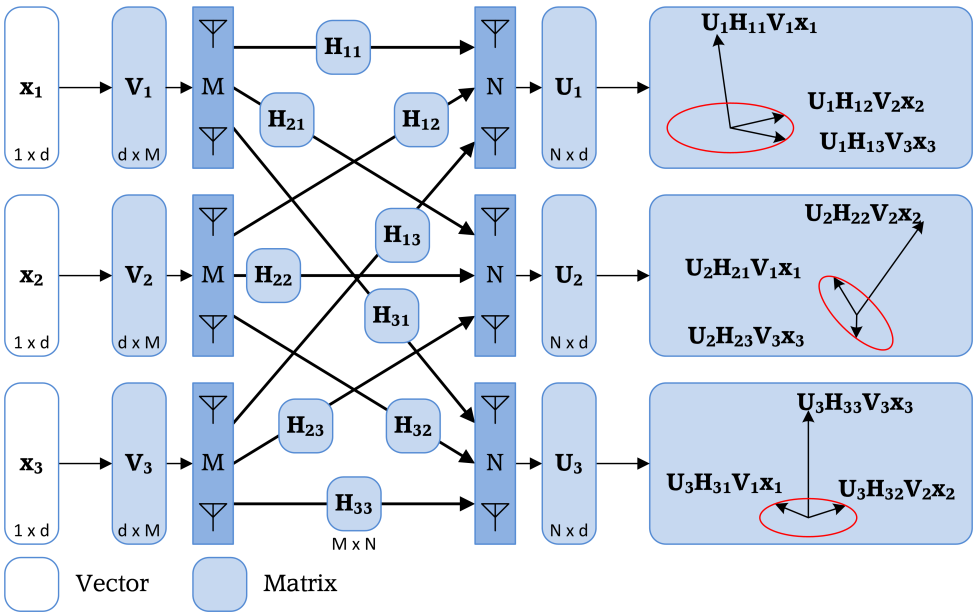

Figure 2.5: Interference Alignment in a 3-user Interference Channel using linear precoding

single-user capacity of the channel. This leads to a startling result; provided there are sufficient signalling dimensions (i.e. Degrees of Freedom) available over which to align the interference, the sum capacity of the system is *unbounded* and scales linearly with K.

Interference Alignment steers the transmissions of users in such a manner that the interference at the receivers is diverted into a smaller signalling space than that available to the desired signal, as shown in Figure 2.5. This subspace is totally interference-free and thus the effects of interference are avoided at the expense of the signalling space available. The signalling space can be any of the dimensions normally used for spectrum allocation; this has been performed in space and time using time-varying MIMO channels [28], frequency, and time using propagation delays [29].

The linear alignment scheme uses the precoding and filtering matrices $\mathbf{U}$ and $\mathbf{V}$ (as introduced in section 2.2.1). Full and perfect Channel State Information, delivered instantly, is assumed at the transmitters (CSIT).

Consider the received signals at receiver 1 in the three-user MIMO Interference Channel, which has been filtered with the beamforming matrix $\mathbf{U}_1^H$:

$$\mathbf{y}_1 = \mathbf{U}_1^H \mathbf{y}_1' = \mathbf{U}_1^H \mathbf{H}_{11}\mathbf{V}_1\mathbf{x}_1 + \mathbf{U}_1^H \mathbf{H}_{21}\mathbf{V}_2\mathbf{x}_2 + \mathbf{U}_1^H \mathbf{H}_{31}\mathbf{V}_3\mathbf{x}_3 + \mathbf{n}_i \tag{2.9}$$

For each receiver to cancel the interference $\mathbf{U}_1$ is used to eliminate the interference from the other undesired transmitters, i.e.

$$\mathbf{U}_j^H \mathbf{H}_{jk}\mathbf{V}_k = \mathbf{0} \qquad \forall j \neq k \tag{2.10}$$

It is assumed that the MIMO antennas are suitably uncorrelated to produce independent channels between the users, and so the channel matrix is well-conditioned and has full rank [11].

$$\text{rank}(\mathbf{U}_k^H \mathbf{H}_{kk}\mathbf{V}_k) = d_k \tag{2.11}$$

where d_k is the number of independent streams sent from transmitter k and represents the DoF available for transmissions through the desired channel.

In order for alignment to be possible, sufficient DoF for each desired channel to be received interference-free is required. The remaining DoF is used to contain the interference messages from the other two transmitters, expressed as the following:

$$\text{span}(\mathbf{H}_{21}\mathbf{V}_2) = \text{span}(\mathbf{H}_{31}\mathbf{V}_3) \tag{2.12}$$

$$\mathbf{H}_{12}\mathbf{V}_1 = \mathbf{H}_{32}\mathbf{V}_3 \tag{2.13}$$

$$\mathbf{H}_{13}\mathbf{V}_1 = \mathbf{H}_{23}\mathbf{V}_2 \tag{2.14}$$

i.e. the transmissions from users 2 and 3 occupy the same signalling subspace at receiver 1, and simultaneously at receivers 2 and 3 the dimensions of the interference must be equal. The calculation of the solutions to (2.12) – (2.14) using zero-forcing and a full proof of the achievable

DoF in this channel is presented in [28]. The criteria in Equations (2.10) and (2.11) are necessary for there to exist a perfect alignment solution; the most crucial being the rank requirements of the overall channel. Without sufficiently independent eigenchannels for the streams present in the channel there can be no possibility of alignment.

[30] leads to the intuition that as long as

$$\max_k(d_k) = d \leq \frac{M+N}{K+1} \tag{2.15}$$

there exists a set of polynomial equations that can be used to compute $\mathbf{V}$ for each user. Once beyond this bound, insufficient simultaneous equations exist to be able to resolve all the streams present in the channel, and a solution that achieves both criteria cannot be found.

While linear alignment offers a powerful tool for removing interference, it has onerous CSIT requirements. In order for alignment to be performed the precoder calculations require channel information from the other receivers which is unlikely to be possible in a distributed system. This information not only has to be collected but it is possible by the time it is acquired the channel coefficients have changed. For this reason a large body of work exists investigating what can be achieved with imperfect CSIT.

The need for perfect CSI comes from linear alignment's 'blindness' to signal power; interference is treated equally regardless of the actual strength of the various signalling subspaces. By applying power control and 'splitting' the DoF between users and permitting leakage between the subspaces better results can be achieved. By restricting the power transmitted, e.g. by applying a Han-Kobayashi scheme to the transmitted signals, then the need for perfect alignment can be relaxed. This also permits the demand for perfect CSI to be relaxed as well. This is demonstrated in the partial alignment scheme by Karmakar et al in [31].

2.3.5 Interference Alignment with Imperfect Channel State Information

CSIT can be considered imperfect for many reasons; it can be too low resolution (thus incurring quantisation noise), noisy from repeated transmission, out of date, limited or not strictly based on channel state (e.g. channel statistics) or simply non-existent. For many of these cases alignment schemes have been devised.

Out of date CSIT has been proven to be useful in alignment schemes; [32] proposes a scheme called *Retrospective Alignment* in which the transmission happens in two stages; randomly-generated precoders are used in the first stage of transmission. The second stage begins once the delayed CSIT (which may only be valid for the duration of stage 1) is received. The second stage uses a linear combination of the data, the previous precoders and the outdated CSI to allow each receiver to resolve the precoders used previously, permitting alignment. In the three-user Interference Channel Retrospective Alignment is capable of achieving a sum DoF of 9/8.

In some networks it may not be practical to transmit full channel coefficients (which are prone to noise in the reverse channel which would limit the effectiveness of the alignment solution). It may however be possible to measure statistics of the channel either directly or passively. Of particular interest are the channel coherence statistics in time and frequency, which were exploited in [33] to propose *Blind Interference Alignment*. This scheme achieves alignment by scheduling transmissions over the length of a 'supersymbol', exploiting differences in the correlation times/bandwidths of different users to create new Degrees of Freedom (any operation that yields new independent channel coefficients in the network creates new DoF). The supersymbol structure resulting from a channel in which one user is time-selective and one is frequency-selective is shown in Figure 2.6. Blind Alignment is capable of creating $K/2$ sum DoF, effectively performing as well as linear alignment without the need for full CSIT.

A more active approach to blind alignment is proposed in [34]; with knowledge of the channel coherence times it is possible to create the DoF required for alignment by forcibly switching between antennas. It was found that providing the estimates of coherence time are correct, a

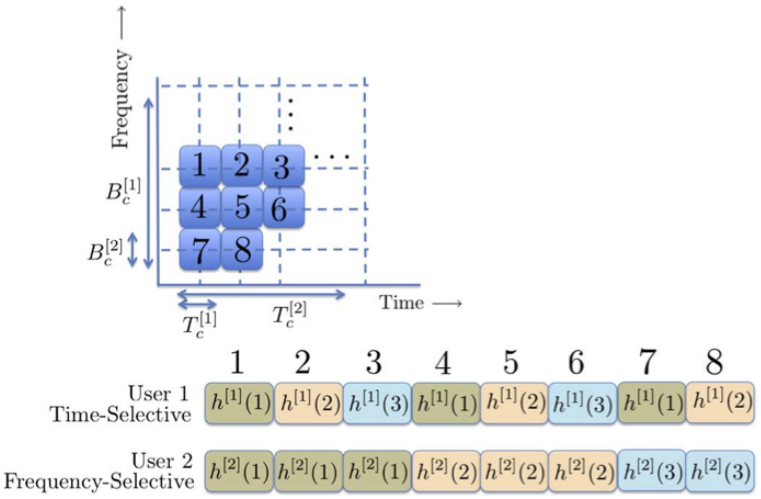

Figure 2.6: 'Blind' Interference Alignment performed between a frequency-selective user and a time-selective user (from [33])

total of $\frac{MK}{M+K-1}$ DoF can be created.

A more passive method of exploiting channel coherence is the *Ergodic Alignment* approach proposed in [35]. This method makes the assumption that the channels between the users exhibit an ergodic fading process and, at some point in the future, the channel will exhibit a response which is the inverse of that at the current time. These 'pairs' of channel instances can thereby be used to cancel out interference at the receivers. However, for this to be feasible full CSIT is required, in which case it is hard to see the benefit over linear alignment.

2.4 Stochastic Geometry

The tools within Stochastic Geometry (namely the analysis of point processes modelling user locations) have powerful applications in the study of wireless networks. By providing a stochastic model for the locations of users within the network it is possible to model parameters of the network related to the relative locations of users from each other in a manner that permits predictions to be made. The most relevant to this thesis is the estimation of interference levels experienced at a node. When coupled with the estimated desired signal power the Signal to Interference plus Noise Ratio (SINR) experienced by a user and thus the probability of outage

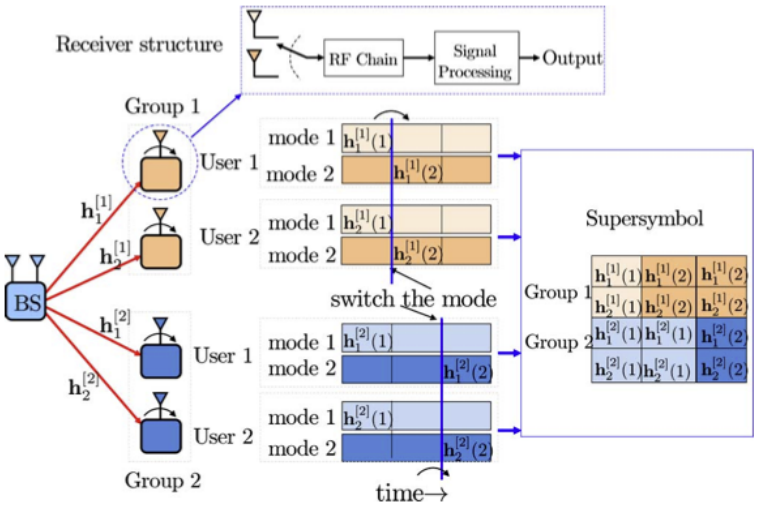

Figure 2.7: 'Blind' Interference Alignment achieved through antenna switching (from [34])

can be predicted.

In the analysis of neighbour discovery in ad-hoc networks this knowledge is invaluable, and can place a realistic, analytically-derived limit on the number of neighbours a user may realistically have for a given network density. Point processes (in particular the Poisson Point Process - PPP) have features and properties that offer analytical results for the estimation of signal powers. They also lend themselves to manipulation, emulating the effect of transmission timing and movements within the network, while preserving many of these features.

An excellent introduction to this field in the context of wireless networks is [36] by Haenggi. Another is the set of monographs by Baccelli and Błaszczyszyn [37, 38]. For this reason only the elements of this significant field of study relevant to this thesis are discussed in this section.

2.4.1 Modelling node location as a point process

As the name suggests, Stochastic Geometry is a stochastic method of analysing networks based on the relative positions of users from each other. As such, the estimates for signal powers encountered in such networks are formulated 'in the mean', and describe the long-term behaviours of a network over multiple channel uses and MAC time periods.

Node positions in the network are modelled using a Poisson Point Process (PPP) in two dimensions; although the tools of stochastic geometry are applicable at general dimensions two is usually chosen for analysis as it accurately models node position without the complications of representing 3D geometry in written work. This thesis uses both the random set and random measure formalisms to describe the point process, in that the process can be defined as a simple set $\phi = \{x_1, x_2, ...\} \subset \mathbb{R}^d$ is characterised by considering the number of points contained within a Borel set B. The number of points within each set B is a random variable $N(B)$. In the case of the PPP this random variable has a Poisson distribution.

A PPP defined on $\mathbb{R}^d$ with intensity measure Λ has the property

$$\mathbb{P}(N(B) = k) = \exp\left(-\int_B \lambda(x)dx\right) \frac{(\int_B \lambda(x)dx)^k}{k!} \tag{2.16}$$

A homogeneous PPP is one in which the intensity measure is uniform across the point process, i.e. $\Lambda(B) = \lambda|B|$. The point process depicted in Figure 2.8 is *not* a homogeneous process by virtue of being bounded by a square; its intensity can therefore not be considered uniform across $\mathbb{R}^2$. However, it is often the case that prevailing network conditions (e.g. the fading coefficient) are such that results from a sufficiently large simulation can be found to match those predictions made by models that assume an infinitely large network.

2.4.2 Point process operations

As an analytical tool for estimating network performance, point processes also possesses some convenient features that can be used to model network operations. Many of these are particular to the PPP, which is favoured by investigators due to its tractability and relative simplicity in having closed-form expressions for key network parameters already derived. There are other operations and transformations that can be applied to point processes but the ones detailed below have been used in this thesis and are considered necessary to understand the work therein.

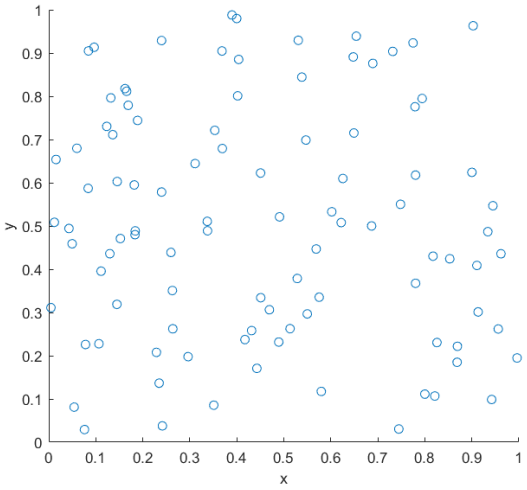

Figure 2.8: User locations in an instance of the point process with intensity $\lambda = 100$

2.4.2.1 Thinning

Thinning a point process removes certain points from the process. If the removal of each point in a stationary PPP is random with probability $1 - p$ independent of the others, the resulting point process is a PPP with intensity function $\lambda(1 - p)$.

This operation can be used to model the ALOHA MAC, in which each user independently determines if it will transmit at a given time. The resulting point process from the thinning operation then represents the users intending to transmit in the next time period.

2.4.3 Displacement

In order to model the movement of users within the network (of significant advantage where the network is composed of mobile devices) a method of displacing the users is required. The 'Poisson-ness' of the PPP is preserved when the individual nodes are displaced in a random manner, which can be used to model the movements of many independent users.

This is achieved by defining the displaced point process ϕ' as

$$\phi' = x \in \phi : x + \Delta_x \tag{2.17}$$

where Δ_x is a random displacement vector. The displacement kernel $p(x, y)$ describes the joint pdf of the new point positions. The displaced point process is a PPP with the intensity function

$$\lambda'(y) = \int_{\mathbb{R}^d} \lambda(x)p(x, y)dx \tag{2.18}$$

2.4.3.1 Mapping

A common operation in the analysis of signal powers in a wireless network is determining the received signal power based on node locations. This has an equivalent in the point process in the form of a *mapping* operation. This maps one point in a process to another point based on a mapping function f. This mapping is not restricted to the same dimensional space as the original process e.g. mapping the point location (in $\mathbb{R}^2$) to the distance of the point from the origin (in $\mathbb{R}$).

If the PPP $\phi = \{x_i\}$ defined on $\mathbb{R}^2$ with intensity function λ is mapped onto $\mathbb{R}$ with the function $f(x) = ||x||$ then

$$\phi' = f(\phi) = \cup_{x_i \in \phi} \{f(x_i)\} = \cup_{x_i \in \phi} \{||x||\} \tag{2.19}$$

has intensity measure (over the region B defined as a ball or radius r centred on the origin)

$$\Lambda'(B') = \Lambda(f^{-1}(B')) = \int_{b(o,r)} \lambda dx = \lambda \pi r^2 \tag{2.20}$$

The preservation of the PPP, albeit transformed into a different space, allows for predictions to be made on signal powers or other parameters that can be calculated from the point positions.

3 'Cognitive' Modifications to a Distributed Interference Management Scheme

3.1 Motivation

As previously discussed in Section 1.1, wireless networks can be broadly characterised as being centralised or decentralised. The tools available to both types of network for the purposes of interference mitigation are broadly the same, however the manner in which they are deployed differs significantly between the two types.

One such technique is the use of linear precoders and postcoders for the purposes of interference alignment. The 'pure' form of interference alignment described in Section 2.3.4 relies on a theoretical channel capable of transmitting instantaneous, perfect Channel State Information (CSI) to the users. Such systems are often referred to as 'genie'-assisted, as if a genie was able to inform users of the interference landscape and how to coordinate their transmissions to ensure low-interference transmissions. In practical systems this genie is provided by a high-bandwidth wired connection [39] between a central base station and the various mobile users. This type of CSI delivery may be suitable for cellular and planned networks; for instance Coordinated Multipoint systems and Massive MIMO make use of such alignment techniques to achieve high-bandwidth links by coordinating communications between multiple base stations. However this is unlikely to be feasible for unplanned environments. The 'genie' assisted application of Interference Alignment is still often used as a baseline against which to compare other alignment schemes however.

Other applications make use of a feedback mechanism between the users as part of the channel training phase [40]. Such a system however may cause additional delay in reaching a solution due to the time taken for the dissemination of feedback, but permits a significant increase in spectral efficiency due to the improved interference management possible. In an unplanned environment the back-channel genie is not present, and without prior knowledge of network parameters such

as the number of users in the network or any form of time synchronisation it can be a challenge to operate protocols with several phases of training and feedback. Each individual user must compute for themselves the best coding matrices, according to their own interference goals, without coordination with the other users within the network. In a highly mobile network or where the frequency of communication is low, these users may not be the same between channel uses.

We focus in this chapter on the 'Iterative Alignment' (ItA) algorithm described in [6]. Iterative Alignment is a subspace-based (i.e. diverting power into the various subspaces of the channel created by MIMO systems) algorithm that permit simultaneous transmission for all users, making use of multiple antennas in order to generate the necessary Degrees of Freedom (DoF). The algorithm takes advantage of channel reciprocity to iteratively compute the coding matrices for each user independently.

In general, individual users have the opportunity to pursue two different interference goals, often differentiated as 'greedy' and 'cognitive'. In 'greedy' networks users are free to act according to their own interference goals independent of each other [41]. Users are motivated to maximise their desired transmission capacity through optimising their desired path with little consideration for other users in the network. This is in contrast to 'cognitive' networks where each user adjusts its transmissions (e.g. adjusts power levels, spatial footprint) to avoid causing interference to, or to avoid the interference that it encounters from, other users. Users must make do with the remaining channel resource or accept that interference will be caused when this threshold is exceeded.

The latter strategy is of the most interest in this chapter; unplanned wireless networks stand to benefit greatly from an interference management strategy that can provide access to the channel without causing undue harm to other users' rates, in a way that requires no additional coordination with aforementioned users. Such a strategy is in line with its namesake Cognitive Radio, where secondary users make opportunistic use of existing channel resource in a manner that must not interfere with the performance of the primary (often licensed) users of

the spectrum.

When operating in a reciprocal channel (i.e. the channel eigenspaces of the forward and reverse channels between nodes are the same), Iterative Alignment allows both approaches to be the case; by aligning both transmit and receive subspaces along the same eigenchannels interference caused is minimised as well as interference received, since each user is trying to avoid the subspaces occupied by other simultaneous users.

3.1.1 The Iterative Alignment Algorithm

ItA is an iterative algorithm for the calculation of the linear transmit precoder $\mathbf{V}$ and receiver postcoder $\mathbf{U}$ using the interference covariance matrix observed by each user. By relying on channel reciprocity the receive postcoder coefficients are updated to minimise the leakage of interference from unwanted users, then the same coefficients as are used as the precoder to transmit in the opposite direction. Interference between the users is controlled by computing the interference covariance matrix $\mathbf{Q}$ of the received signal and identifying the subspaces that exhibit the least interference.

$$\mathbf{Q}_k = \sum_{j \in \mathcal{K}} \frac{P_k}{d_k} \mathbf{H}_{jk} \mathbf{V}_j \mathbf{V}_j^H \mathbf{H}_{jk}^H \tag{3.1}$$

The receiver minimises inteference observed by postcoding the received symboles with matrix $\mathbf{U}$, which is composed of the eigenvectors corresponding to the d_k smallest eigenvalues of the interference covariance $\mathbf{Q}$, where d_k is the number of signalling dimensions 'consumed' by user k's transmission. This matrix therefore 'exposes' the signalling subspace that exhibits the *least* interference between the d_k subspaces. By repeating this operation the algorithm iteratively, the algorithm 'tunes' the transmit and receive coding vectors alternately after each channel use, and is shown to reduce the observed interference at each user with every iteration [6]. Given sufficient Degrees of Freedom are available (i.e. condition (2.10) is met), it is possible to arrive at a perfect alignment scheme. The algorithm is summarised as below:

1. Start with arbitrary transmit matrices $\mathbf{V}_k$ at each user such that $\mathbf{V}_k\mathbf{V}_k^H = \mathbf{I}_{d_k}$ i.e. the precoder is unitary matrix and transmit training sequence.

   Each node performs steps 2 and 3 independently:
2. Compute the interference covariance matrix $\mathbf{Q_k}$ (3.1) of the received training signal.
3. Compute the interference-suppressing receive matrix at each receiver, given by $\mathbf{U}_k^{\star d} = \nu_d[\mathbf{Q}_k], d = 1, \ldots, d_k \quad \forall k \in \mathcal{K}$ where $\nu_d[\mathbf{A}]$ is the d^{th} smallest eigenvector of matrix $\mathbf{A}$.
4. Reverse the communications direction and set the transmit matrix to the previous iteration's receive matrix $\overleftarrow{\mathbf{V}}_k = \mathbf{U}_k$.
5. Repeat steps 2 to 4 for the reverse channel with the matrices swapped.
6. Repeat this process until the solution converges, or if a set limit is reached.

The calculation of the interference covariance matrix is possible through identifying the desired transmission and separating it from the interference, which in certain interference regimes is possible through conventional decoding and equalisation techniques. These conditions can be identified by considering the Generalised Degrees of Freedom (GDoF) curve of the 2-user interference channel, shown in Figure 2.2. As indicated, a user is capable of decoding a signal without side information in two regions; where interference is sufficiently strong ($\alpha > 2$, where Successive Interference Cancellation (SIC) is the optimal strategy) and where interference is sufficiently weak ($0 < \alpha < 1$, where treating interference as noise permits decoding at a rate inversely proportional to interference power). Using only local CSI requires no side information – neither from interfering users nor the other partner in the current user pair – and so permits the algorithm to be run locally and concurrently on each user.

While the authors prove that the algorithm is capable of reducing the sum interference in the network, measured by the Weighted Leakage Interference (WLI) (see (3.2)), they do not discuss the practicalities of multiple nodes acting in their own interests concurrently.

This brings rise to one deficiency; the convergence time of ItA is observed to be slow in practice, if convergence is reached at all. With no communication between the users it is not possible to coordinate the update of channel coefficients, which can prevent the system as a

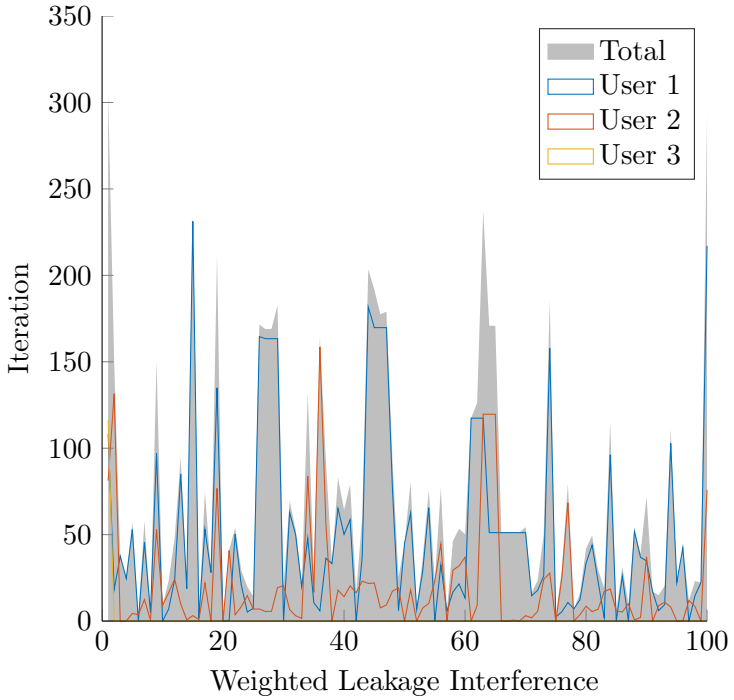

Figure 3.1: Convergence of Iterative Alignment scheme in a 3-user 4×4 MIMO Interference Channel with update probability $p = 1$. Each user attempts to use one DoF within their respective channel.

whole reaching a steady state.

Figure 3.1 shows the WLI experienced by the users in a 3-user 4×4 MIMO channel implementing ItA and demonstrates a typical situation where the users performing the algorithm simultaneously make adjustments that compensate for alterations made by another user. In the situation depicted, User 3 has determined its optimal postcoder early in the alignment process and experiences no interference; this leaves the remaining DoF to be shared between Users 1 and 2. These two users vary their interference management solutions in response to the interference experienced in the previous iteration of the algorithm. Such behaviour can lead to a lack of convergence in the overall interference in the network, where the users are unable to come to a stable solution together. This is not uncommon; in Figure 3.3 the performance of the original ItA demonstrates that even given a long convergence time, many solutions offer imperfect alignment solutions.

This has two potential negative outcomes; given that the node will have to cease channel

training at some point, this may be a point when the sum interference in the channel represents a non-optimal solution. As is shown in the example of Figure 3.1 the magnitude of interference experienced can vary significantly between iterations. It is also possible that estimation will cease when the solution overall is optimal, but not all users experience low interference and reliable reception of the payload is still not possible. As the sum of all interference experienced in the network, WLI is a poor measure of actual network performance. It is however sufficient for independent users to determine their own performance, providing that the interference also permits the desired signal to be identified and isolated. This is the price of a completely distributed algorithm; solutions may only be locally optimal, and each individual user is only capable of making decisions on the quality of its own interference alignment solution.

Depending on the network's application and operating parameters this poses a potential issue; in cognitive radio applications where causing interference to the primary users is prohibited, spending a significant time training to yield an unusable channel is a wasteful practice, but so is extending the training period to yield only a marginal improvement in interference suppression. There is therefore significant merit in being able to reduce the time taken to reach an acceptable solution, or determine with a high degree of confidence that alignment isn't possible given the original starting steering coefficients.

Another drawback of the algorithm (and one that is considered by the authors) is the inability of subspace-based schemes to determine if interference is in fact harmful; the ItA scheme is unable to assess the relative powers in each signal subspace. This has the effect that all interference is treated with the same severity, regardless of the power observed at the receiver. It is also treated the same regardless of the intended signal power, which may not be sufficient in all cases to support the transmission rate demanded by the user. It is possible then that the precoder matrices calculated by each user do not make the best use of the channels available to them when their sole purpose is to reduce the interference observed – even when the rate required by the user does not require any improvement in SINR past what has already been achieved.

Users are also unable to make full use of the array gain that it is afforded in MIMO networks,

as the algorithm makes no attempt to maximise desired channel gain. This is addressed by the authors in proposing the 'MaxSINR' algorithm [6], that maximises the SINR of each individual stream. While the MaxSINR algorithm produces overall higher sum rates over the network, it does so at the expense of power being transmitted into undesired signal spaces. This is clearly not ideal, and the system designer must take into consideration what the overall objective of the system is; to make use of MIMO techniques to improve individual throughput, or to minimise interference?

The lack of regard for interference leakage would also preclude the use of MaxSINR in many cognitive radio applications, where causing interference to the primary users of the channel must be strictly controlled. It also only partially solves the problem of wasting resources; as a 'greedy' algorithm MaxSINR seeks only to maximise the SINR for each user. This can be to the network's detriment if a user enters an interference regime that is not suitable for a distributed network, and so prevents other users being able to use the channel. This may prevent a greater waste of channel resource than had every user been able to make use of the channel concurrently, albeit at a reduced SINR and thus lower throughput.

The ItA scheme is capable however of a degree of 'cognitive' ability in its original form; each user only adjusts the precoders necessary to meet the DoF required, and therefore steers its transmissions away from signal spaces not used by its own channel. The authors do not suggest any DoF-splitting techniques for use with the algorithm; likely since the agreement of a symbol extension or Han-Kobayashi scheme that would permit this is difficult to organise without prior configuration (e.g. during production) or side information being shared during operation. In our examination of the ItA algorithm only integer-value DoF are made use of, provided by the use of MIMO coding techniques.

3.2 Implementation and Measurement of the Iterative Alignment Algorithm

3.2.1 System Model

We consider the K-user, $M \times N$ interference channel. Each user transmission has the input-output relationship $\mathbf{Y}_i = \sum_j \mathbf{H}_{ji}\mathbf{X}_j + \mathbf{N}_i \quad \forall i, j \in K$. The channels between each user pair $\mathbf{H}_{ji}$ are $M_j \times N_i$ Additive White Gaussian Noise (AWGN), i.e. $\mathbf{N}_i \sim \mathcal{CN}(0, \mathrm{I}_{N_i})$

Each user transmits using a Gaussian codebook with power constraint $\mathbb{E}[|\mathbf{X}_j|^2] \leq P_t =$ 10dB. Degrees of Freedom are provided by independently encoded messages (using a Gaussian codebook) assigned to multiple eigenchannels provided by antennas within the MIMO array. Where the desired rate requires transmission across multiple DoF d, the power is split equally, i.e. each codeword receives P_t/d. The transmit and receive precoders at each node $\mathbf{V}_j$ and $\mathbf{U}_i$ therefore have dimensions $M_j \times d_j$ and $N_i \times d_i$ respectively. Each channel between transmitter and receiver is modelled as an AWGN with unit variance.

Discussion of 'achievable' transmission in this chapter is limited to ones in which a transmission and coding scheme are feasible with no *a priori* information. Therefore, an 'achievable' scheme with a significant GDoF is still no guarantee that the channel yields sufficient capacity to be of any use, i.e. the equivalent AWGN to an interference channel may yield little to no capacity due to natural attenuation.

3.2.2 Simulation methodology

In order to permit a direct comparison between the original and modified ItA schemes, the same channel coefficients were used between each modification. Channel coefficients were randomly generated in accordance with the AWGN channel model employed. So that the algorithms' ability to achieve alignment could be tested, each user only transmitted DoF such that criterion (2.15) is met and a fully-aligned solution is at least theoretically possible.

It is assumed that no predetermined power-splitting scheme is in place at the commencement of channel training. For this reason signals received that fall into the GDoF region $1 < \alpha < 2$ are not decodable. It is therefore not possible to separate the desired signal from the interference, permitting the Interference Covariance Matrix to be calculated. In such cases no updates to the coding matrices can be made, and steps 2 to 4 of the ItA algorithm are not performed.

User coding matrices are also not updated when the interferers experienced at the receiver are not sufficiently separated in power to permit successive decoding, i.e. $\alpha > 2$ but the SINR of each interferer in order of power level is insufficient to decode and identify the training sequence. In simulations the SINR threshold required to be able to decode and cancel each interferer was set to 0 dB.

3.2.3 Measuring alignment performance

The quality of the alignment solution can be determined by two quantities; the sum of the leakage interference experienced by each user individually, and the time taken for convergence to occur within the solution.

The quality of alignment at each receiver can be measured using the Weighted Leakage Interference (WLI) experienced as defined in (3.2). As the sum of the signal power leaked from the signal spaces of unintended transmissions into the subspace of the desired signal at the receiver, a WLI of zero at all users indicates a fully aligned, interference-free network. A non-zero WLI indicates that interference from one or more users has leaked into the same subspace as the desired signal for that user.

$$\mathrm{WLI}_i = \sum_{j=1}^{K} \frac{P_j}{d_j} \mathrm{Tr}\left[\mathbf{U_i}^H \mathbf{H}_{ji} \mathbf{V_i} \mathbf{V}_i^H \mathbf{H}_{ji}^H \mathbf{U}_i\right] \tag{3.2}$$

However, this only gives the view of the network from each individual user's perspective, and as a metric of actual system performance fails to give the full picture. A better measure of whole-network performance is the sum capacity of the network, determined by the SINR of

each users' intended transmissions. This takes into account conditions where the interference suffered by a user is non-zero but sufficiently low to permit decoding of a transmission. Like the ability to identify and address interference, decoding a transmission requires the interference at the receiver to be such that the intended message can be identified and decoded, i.e. $\alpha > 2$ or $0 < \alpha < 1$.

The time taken by the network to converge on a solution can be difficult to identify; the network is considered to have converged if the angle of deflection had reduced below a threshold (i.e. the angle between sequential iterations of every user's precoder or postcoder do not exceed a threshold over multiple iterations). For the purposes of measuring performance in this chapter convergence was considered to have been achieved if the angle of deflection is zero for more than four iterations.

3.3 Random seelective Filter Updates

As shown in Figure 3.1, a network comprised of multiple users each executing the same algorithm concurrently can result in instability within the solution. This manifests in each user repeatedly updating its filter coefficients to the same small set of values without reaching a steady state solution.

This is undesirable for two reasons; firstly it is possible that a more optimal solution is available, but inaccessible due to each user's optimisation of only its own parameters. Hysteresis also prevents the detection of a local optimum within the solutions space; in the case of the Iterative Alignment scheme if all users have reached a steady state it is highly likely a local optimum has been reached; it serves no purpose to continue executing the algorithm in this case. Hysteresis could potentially be avoided by reducing the number of nodes simultaneously changing their coefficients at the same time; this can be achieved by permitting updates of the coding matrix coefficients only to happen on a proportion of cycles. For the purposes of this investigation this was achieved by adopting the update probability model from the ALOHA protocol, with varying values of the update probability p.

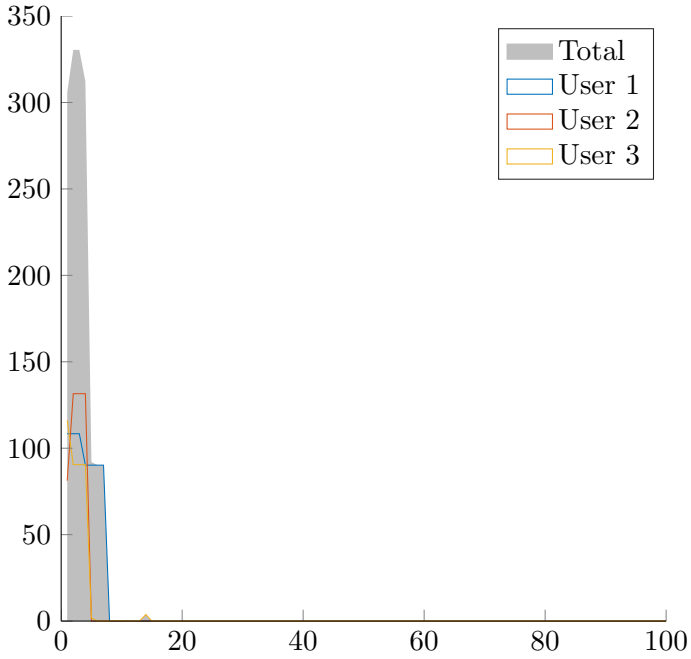

Figure 3.2: Convergence of Iterative Alignment scheme in a 3-user 4×4 MIMO Interference Channel with update probability $p = 0.4$, where convergence is observed to be reached after 21 iterations.

This would replace step 4. in the ItA algorithm with:

4a. with probability p : Reverse the communications direction and set the transmit matrix to the previous iteration's receive matrix $\overleftarrow{\mathbf{V}}_k = \mathbf{U}_k$.

4b. With probability $1-p$: Reverse the communications direction and set the transmit matrix to the same as before $\overleftarrow{\mathbf{V}}_k = \overleftarrow{\mathbf{V}}_k$.

The effect of this selectivity is shown in Figure 3.2, where three users execute the modified algorithm with $p = 0.4$ in the same interference channel as that encountered in Figure 3.1, allowing a direct comparison between the performance of the two algorithms. Since each user updates their coding matrices less often, there are more opportunities for the other users to tune their solutions while the interference received from each user remains the same. The result is a solution where each user is able to make use of the channel with zero interference, and the solution is considered to have converged after only 21 iterations of the algorithm.

Figure 3.3 maps over 1000 different channel instances the effect of various values of p on the convergence time and WLI experienced within the network. These are measured by comparing

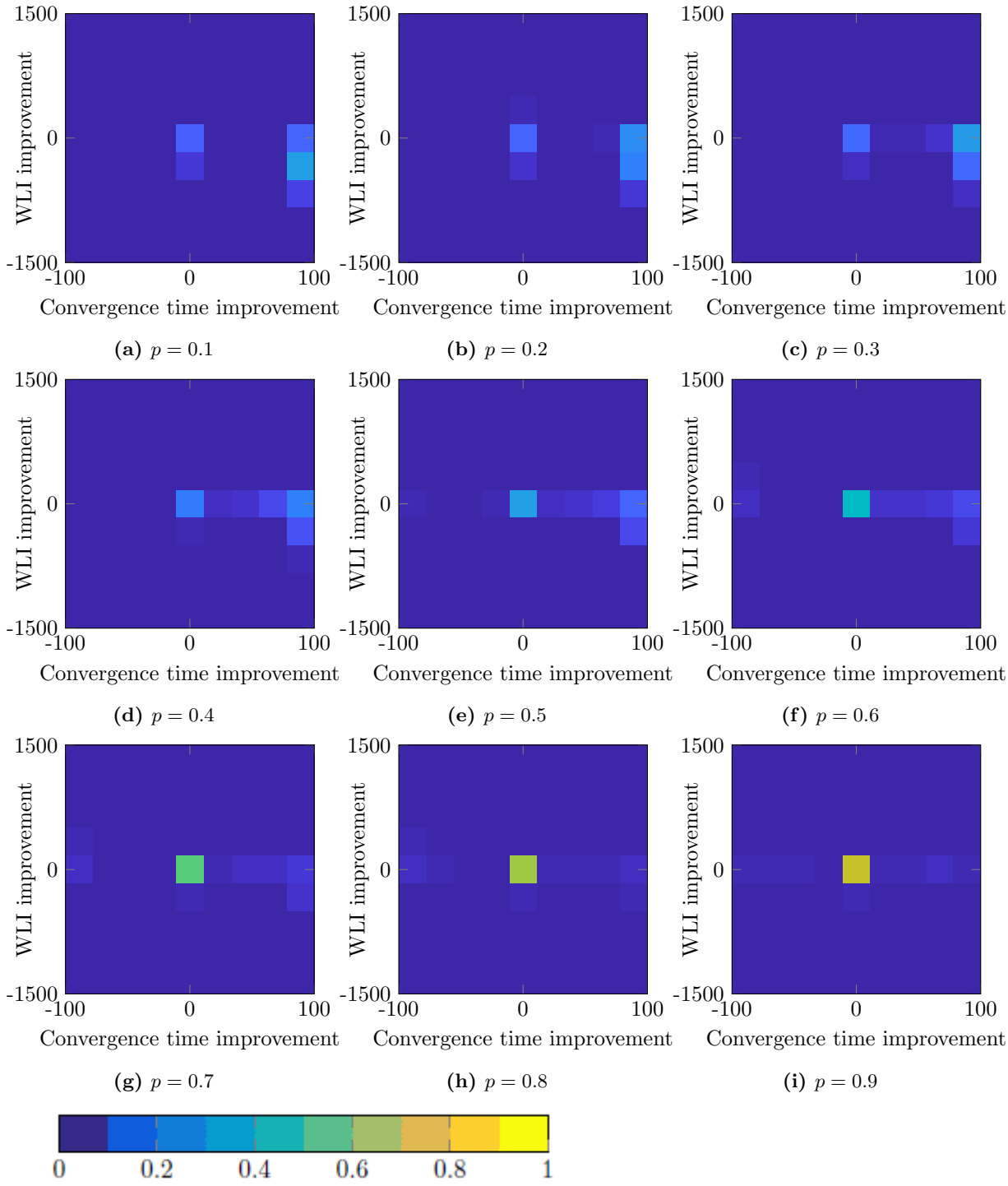

(a) $p = 0.1$ **(b)** $p = 0.2$ **(c)** $p = 0.3$

(d) $p = 0.4$ **(e)** $p = 0.5$ **(f)** $p = 0.6$

(g) $p = 0.7$ **(h)** $p = 0.8$ **(i)** $p = 0.9$

Figure 3.3: Heatmaps showing convergence time and WLI achieved in 1000 channel instances for various values of $p < 1$ compared to the original Iterative Alignment algorithm ($p = 1$)

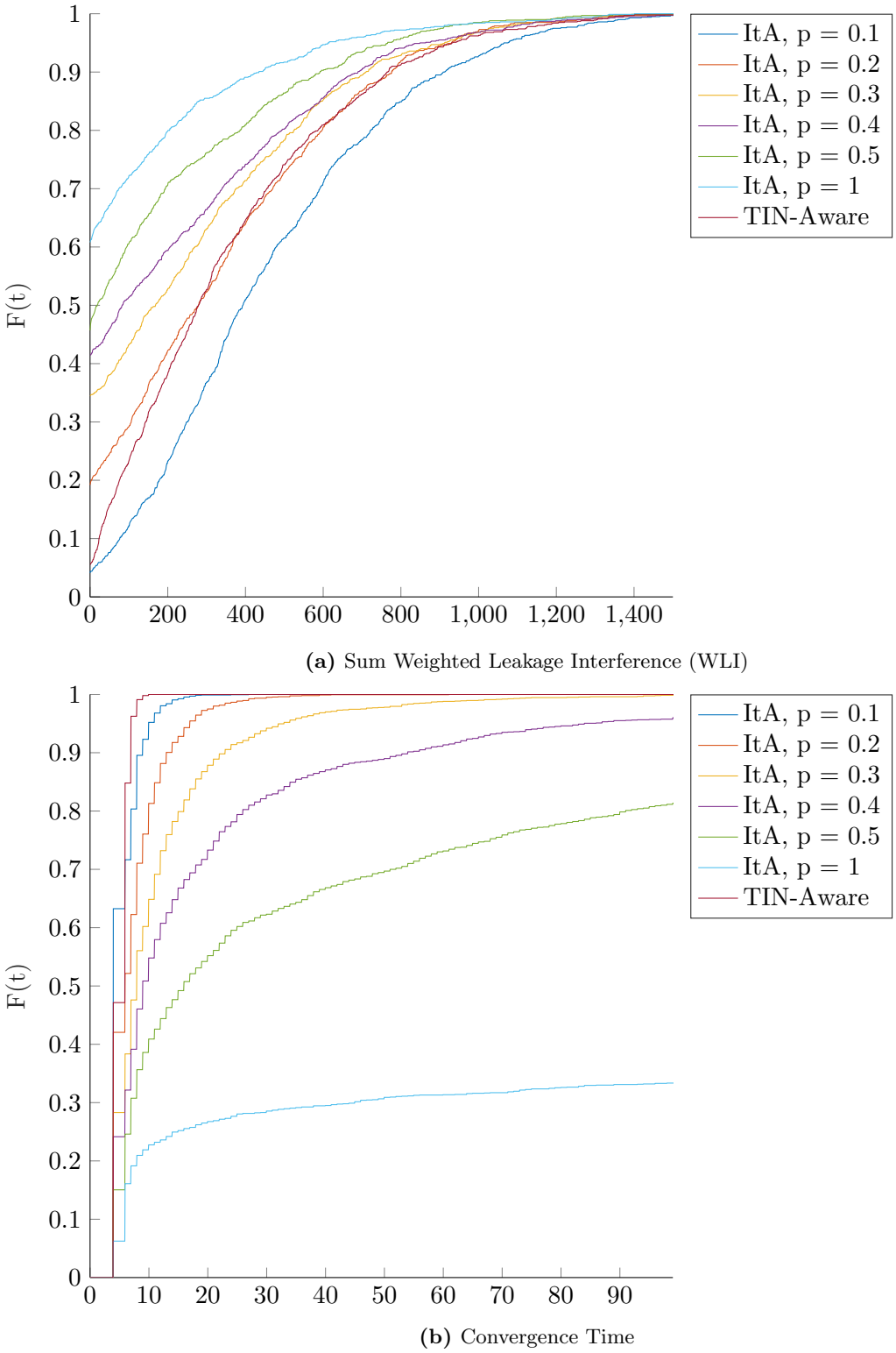

(a) Sum Weighted Leakage Interference (WLI)

(b) Convergence Time

Figure 3.4: Cumulative distribution of WLI and convergence time in a 3-user 4×4 MIMO IC

the performance of the original (i.e. $p = 1$) Iterative Alignment algorithm and the performance of the modified versions on the same channel instances.

As the update probability is reduced it is observed that the algorithm offers little improvement or detriment to the result of the algorithm compared to the original; for values of $0.9 > p > 0.5$ it is as likely for the algorithm to yield a poorer alignment solution as a better one, with little change in the convergence time. For this reason discussion of selective updates will be limited to $p < 0.5$ from this point.

Figure 3.4a shows the CDF of leakage interference for various update probabilities $p \leq 0.5$ while Figure 3.4b shows the effect of update probability on convergence time.

At $p = 0.5$ the low likelihood of update begins to yield a different result; convergence time begins to be greatly affected, with a much higher proportion of channels yielding faster results. This is however at the expense of alignment solution quality, where it is observed that the proportion of channels yielding negative WLI 'improvements' (i.e. WLI is greater than the original algorithm's solution) begins to increase significantly.

From these results it is immediately apparent that the ItA algorithm in its original form is not practical for use in a real channel estimation protocol. Within 100 iterations the likelihood of convergence when $p = 1$ is very low (less than 35%). The convergence behaviour of the selective Iterative Alignment algorithm is inversely proportional to the update probability; as the likelihood of updates is reduced, the likelihood of coming to a conclusion within 100 iterations is increased. This stands to reason, since the threshold for convergence as described in Section 3.2.3 is only four iterations with no change from any user. By reducing the frequency of precoder updates it is therefore possible to trade off between the quality of alignment quality for speed of convergence.

However, as discussed in Section 3.2.3 the WLI measure does not offer a full picture of the outcome of channel equalisation, blind to power as it is. For the true effect on system performance we must examine the sum capacity achieved by all users throughout the network,

and examine if there is a better way to direct a user to update or not depending on the SIR experienced each iteration.

3.4 Power-aware Selective Filter Updates

As discussed in Section 2.2.3 treating interference as noise is the optimal transmission strategy in the two-user interference channel within the region

$$0 \leq \frac{\log INR}{\log SNR} \leq 0.5 \tag{3.3}$$

'Optimality' in this sense is a transmission scheme that achieves the entire capacity region of the channel. [42] elaborates further, proving that in the K-user Interference Channel, this is the optimal strategy *for all users* is the following condition is met in all users:

$$\alpha_{ii} \geq \max_j(\alpha_{ij}) + \max_j(\alpha_{ji}) \quad \forall i \neq j \tag{3.4}$$

where $\alpha_{ii} = \frac{\log SNR_i}{\log P}$ and $\alpha_{ji} = \frac{\log INR_{ji}}{\log P}$

i.e. treating interference as noise is optimal when each user's desired signal power is greater than the *sum* of the largest source of interference from another user plus the largest interference signal emitted by user k.

In the high INR ($\alpha \geq 2$) and high SNR regimes ($\alpha \leq 1$) the receiver is capable of identifying the desired signal, either by SIC or treating the interference as noise respectively. This permits the calculation of (3.3) using only information gained at the receiver. (3.4), in contrast, requires knowledge of the interference *caused* by the user, which usually cannot be known without co-operation between the users. In the case of a symmetric interference channel it is likely that interference levels between the forward and reverse communications paths are equal, and the interference caused by the receiving user can be predicted. This channel knowledge can be gained

only if SIC is used to separately decode and equalise individual interference streams; there is therefore merit in considering only α as defined in (3.3) since it can be calculated in a wider range of interference scenarios.

Following [21], treating interference as noise is the optimal strategy in the K-user interference channel when condition (3.4) is met. In a symmetric K-user interference channel where iterative alignment is performed the SNRs and INRs of the forward and reverse channels will be equal, allowing (3.4) to be expressed as

$$\begin{aligned} \alpha_{ii} &\geq 2\max_j(\alpha_{ji}) = 2\max_j(\alpha_{ij}) \\ \frac{\log(\mathrm{SNR}_i)}{\log P} &\geq 2\max_j\left(\frac{\log(\mathrm{INR}_{ji})}{\log P}\right) \\ \log_P(\mathrm{SNR}_i) &\geq 2\max_j(\log_P(\mathrm{INR}_{ji})) \\ 1 &\geq 2\,\frac{\max_j(\log_P(\mathrm{INR}_{ji}))}{\log_P(\mathrm{SNR}_i)} \\ \frac{\max_j(\log_P(\mathrm{INR}_{ji}))}{\log_P(\mathrm{SNR}_i)} &\leq 0.5 \end{aligned} \tag{3.5}$$

At a receiver with only local knowledge of the channel and the signal and interference powers, only $\alpha_i = \frac{\log(\mathrm{INR}i)}{\log(\mathrm{SNR}i)}$ is known. If $0 < \alpha < 1$ the signal can be separated from the interference so the SNR and sum INR is known. At receiver i, ordering the interfering nodes $j \neq i \in K$ in order of descending interference power permits INR_i to be expressed as

$$\begin{aligned} \log_P(\mathrm{INR}_i) &= \log_P(\sum_{j\neq i}^{K}\mathrm{INR}_{ji}) \\ &= \log_P(\mathrm{INR}_{1i}) + \log\left(1 + \frac{\sum_{j=2,j\neq i}^{K}(\mathrm{INR}_{ji})}{\mathrm{INR}_{1i}}\right) \\ &\geq \max_j(\log_P(\mathrm{INR}_{ji})) \end{aligned} \tag{3.6}$$

Table 3.1: Power-aware node behaviour depending on level of interference detected

Interference regime	Action
$\alpha \leq 0.5$	TIN is optimal; do not update precoders.
$0.5 < \alpha \leq 1$	Use TIN to identify desired signal and use covariance matrix to update precoders.
$1 < \alpha \leq 2$	Cannot identify desired signal, no action possible.
$\alpha > 2$	Use SIC to identify desired signal and use interference covariance matrix to update precoders.

By substituting (3.6) into (3.5) the TIN-optimal condition can therefore be expressed as

$$\frac{\max_j(\log_P(\mathrm{INR}_{ji}))}{\log_P(\mathrm{SNR}_i)} \leq \frac{\log_P(\mathrm{INR}_{1i}) + \log\left(1 + \frac{\sum_{j=2,j\neq i}^{K}(\mathrm{INR}_{ji})}{\mathrm{INR}_{1i}}\right)}{\log_P(\mathrm{SNR}_i)} \leq 0.5 \tag{3.7}$$

Informed by the information gathered by the node, the node's precoder updates are guided by the level of interference observed during the previous iteration of the algorithm. These behaviours are listed in Table 3.1.

Being power-aware, users now have the opportunity to not update their coefficients in an effort to remain in the high interference regime, conditioned on the fact that the desired signal is separable from the interference. This gives rise to much greater levels of sum leakage interference, but the channel is still usable by the intended nodes. Since the transmission power is not informed by the algorithm no commentary can be made on the power efficiency of the algorithm, but it is not beyond the imagination that once an alignment solution has been converged upon that an distributed power optimisation stage could be carried out. This would permit the transmitting user to more economically use its transmit power where required, i.e. in signal subspaces with weaker eigenchannel gains. It may also be possible that the power-aware algorithm is run alternately with an iterative power allocation algorithm, permitting even greater spectral efficiency by iteratively aligning eigenchannels and adjusting the power transmitted into them. This approach is considered in [17], which proposes combining the Iterative Alignment algorithm with a power optimisation step. However, this was proposed as a separate feedback mechanism between users which is not discussed further or suggestions made how this would be

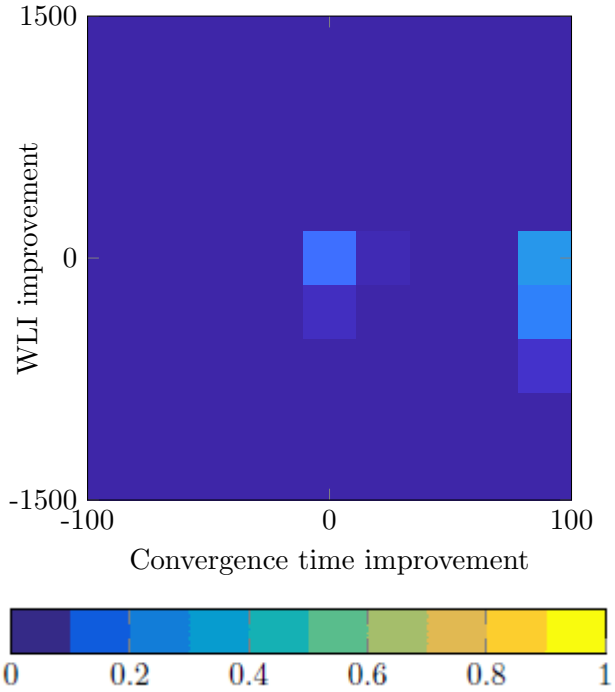

Figure 3.5: Heatmap showing convergence time and WLI achieved in 1000 channel instances for the power-aware algorithm compared to the original Iterative Alignment algorithm ($p = 1$)

implemented.

Figure 3.5 shows a heatmap of 1000 trials of the power-aware Iterative Alignment algorithm showing the effect of power-awareness on sum WLI and convergence time. From this two regions along the convergence time axis is apparent;

The first region corresponds to the scenario where no convergence time improvement is recorded; this can be attributed to channel instances in which the original ItA algorithm has acceptable convergence behaviour. While the majority of instances in this region show no change in interference performance a small number of channels record a negative impact (i.e. greater sum WLI) on interference compared to the original ItA algorithm.

The second region shows a significant convergence time improvement, which can be attributed to the power-aware algorithm reaching a point where all users are able to use the channel within a very short time. It is observed however that a much greater proportion of channel instances record a significant negative impact on interference levels.

A marked difference in the results of the power-aware ItA compared to the selective update versions is the lack of solutions that *improve* sum interference. An insignificant proportion of instances (0.16%) see an interference improvement, which is to be expected since the goal of the power-aware algorithm is not to minimise interference, but to preserve achievable channel rate.

For this reason we must also take the sum capacity achieved in each channel instance into consideration. Figure 3.7 plots a bivariate histogram over 1000 channel instances of the effect of the power-aware algorithm on the sum capacity achieved in the channel and the convergence time compared to the original ItA algorithm. From this histogram two regions of interest become apparent:

The region coloured blue where no convergence improvement is achieved corresponds to the first region identified in Figure 3.5. While this suggested no improvement was made it is observed that the power-aware algorithm is equally capable of delivering sum capacity improvements in this region as it is delivering very poor sum capacity solutions. Instances in this region where the power-aware algorithm negatively influenced convergence time were rare, making up less than 2% of the trials.

The region coloured yellow represents the second region in which using the power-aware algorithm offered an improvement of over 90% compared to the original ItA. In this region the proportion of solutions that have a negative impact on sum capacity is much higher, with the outcome reducing capacity by more than 50% occurring nearly 40% of the time overall.

The proportion of simulations that resulted in no workable alignment solutions (represented by the highest yellow column in Figure 3.7) using the power-aware algorithm was 22% compared to the original ItA scheme, which yielded an unusable result only 0.7% of the time. Figure 3.6 also shows the CDF of the power-aware algorithm's sum capacity compared to the various update probabilities of the selective ItA algorithm discussed in Section 3.3.

This demonstrates that the effect of the TIN-aware algorithm is often a lower sum capacity, but the time to reach convergence is improved significantly; nearly all simulations of the TIN-

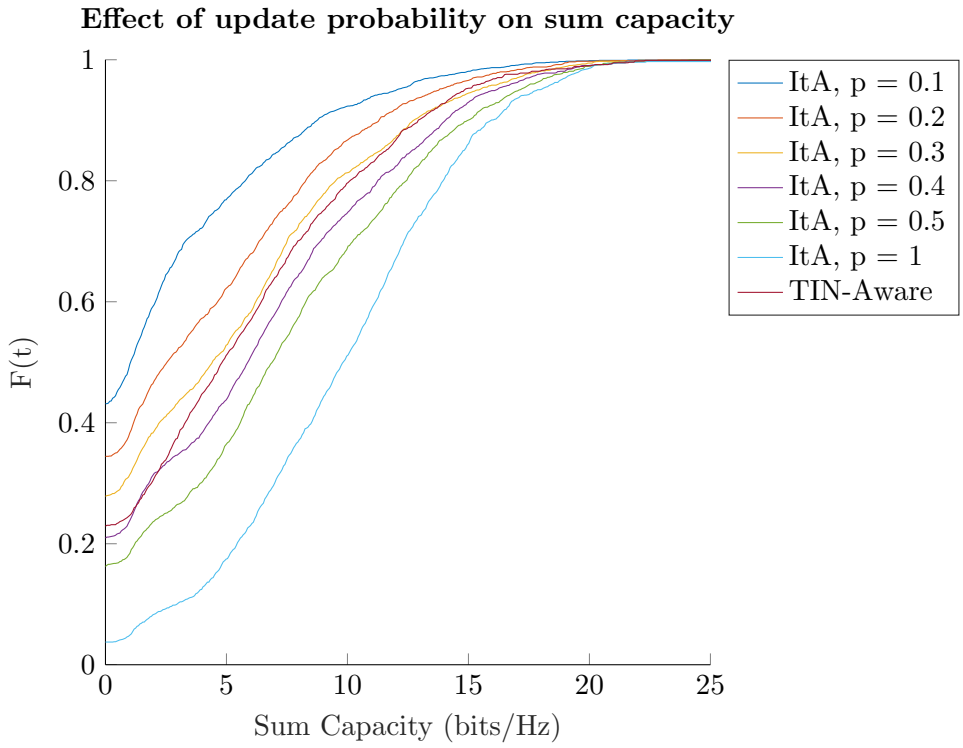

Figure 3.6: Effect of selective updates with various values of update probability p and power-awareness on sum capacity in a 3-user 4×4 MIMO Interference Channel

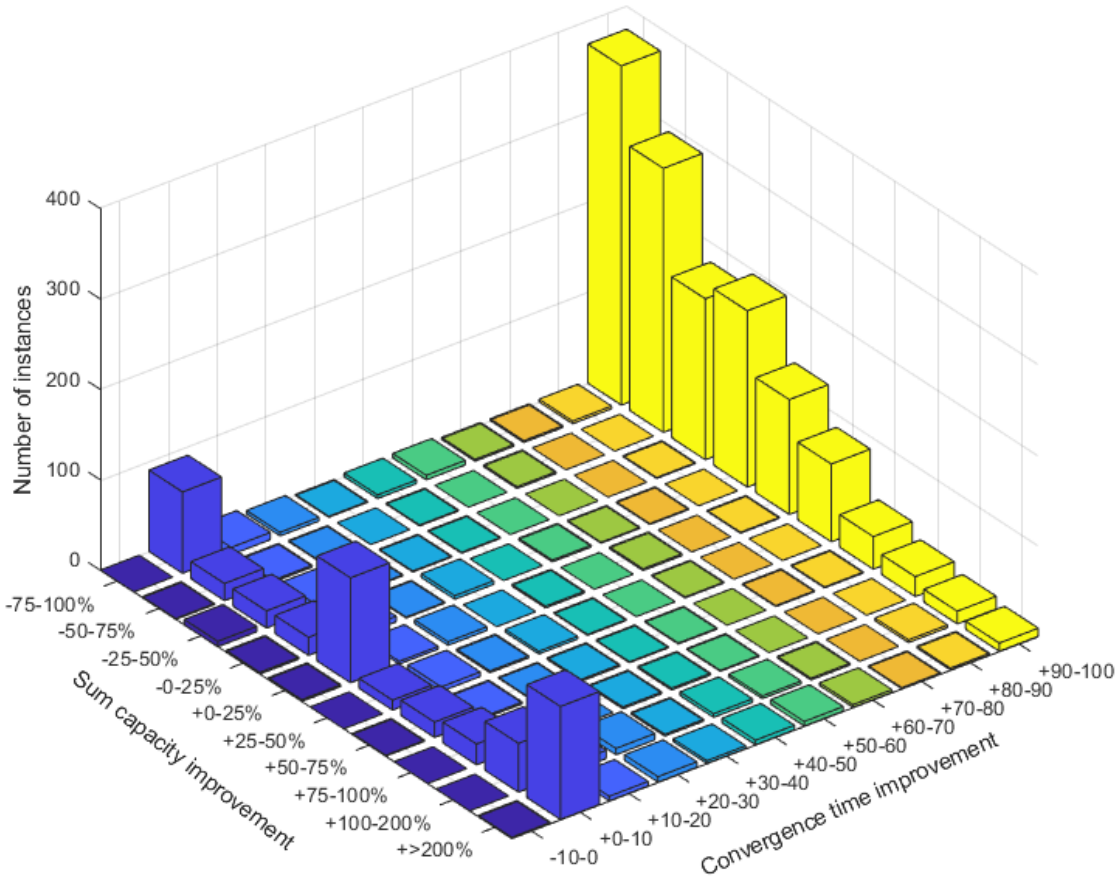

Figure 3.7: Sum capacity and convergence improvement of power-aware Iterative Alignment scheme compared to standard Iterative Alignment scheme

aware algorithm converge within only ten iterations, compared to ItA ($p = 1$), which rarely converged within 100 iterations. Even comparing the closest-performing selective ItA mode ($p = 0.4$), the CDF of convergence times in Figure 3.4b shows it is not guaranteed to converge within 100 iterations.

3.5 Conclusions

Iterative Alignment offers a functioning distributed interference management scheme with known and easily measured performance. In its original form however, it is clear that is suffers from poor convergence performance – either through being unable to converge at all, or reaching a solution that does not allow every user a feasible channel for communications. While clearly capable of arriving at an alignment solution the algorithm's inability to take signal power or channel subspace gain into account means there is no guarantee the solution is actually usable for every user. In this chapter we have considered the Iterative Alignment algorithm's drawbacks and applied two modifications to the algorithm in an effort to counter these.

The first modification is to only update the alignment precoders on some iterations, those iterations determined randomly and independently between the users on the network. This has the effect of increasing the likelihood of convergence within a short period, although at high update probabilities ($p > 0.5$) a significant proportion of simulations resulted in no convergence within 100 iterations. The results show a correlation between convergence time and update probability, with convergence time decreasing with the update probability. Reducing the update probability is not without its own drawbacks – the quality of the alignment solution, measured using the sum capacity achieved, is negatively affected. There is therefore a trade-off between the desired convergence behaviour and network performance, as depicted in Figure 3.8; depending on the network's requirements and application reducing the capacity of the network for a faster solution may be an acceptable compromise. This may be the case in applications with high user mobility or channel volatility, in which the interference solution may only be valid for a very short time. There is therefore merit in being able to reach a solution quickly and make use of the channel before the channel requires training again.

The second modification is to let the nodes in the network determine independently whether or not to update their alignment matrices. This is done by taking into consideration the received signal and interference levels observed at each iteration. The user should cease trying to improve its alignment solution when the desired signal's Signal to Interference plus Noise Ratio is such

that communication is possible using a simple decoding scheme. This the case in the low interference regime, where interference can be treated as noise, and in the high interference regime where Successive Interference Cancellation can be used to extract the desired signal. The effect of this modification is profound. Convergence times measured in simulation are very short; nearly all simulations result in convergence within ten iterations, compared to the original algorithm which frequently did not converge within 100 iterations. This yields very fast alignment solutions, albeit again at a considerable penalty to sum capacity. The impact on capacity is greater however than in the case of reducing the update probability. The proportion of solutions that yield no usable channel is also significantly higher using this modification, although with such fast convergence it would be possible to run the algorithm and reach a new solution multiple times in the time taken to run the original.

The system designer must therefore take into account what is the end goal of reducing interference within the network before an optimal algorithm choice can be made. While not a zero-sum compromise, there are three driving factors that influence the choice of algorithm.

- If the intention is to *eliminate interference* then the original algorithm ($p = 1$) offers the best option, since it yields the greatest proportion of zero-interference alignment solutions.
- If the intention is to *maximise throughput* multiple options may be suitable; while the original algorithm yields the best capacity performance, selective ItA with $p = 0.5$ suffers only a minor capacity reduction but improves the likelihood of converging within 100 iterations more than double.
- If the intention is to *achieve the fastest solution* in a highly-dynamic environment, then the power-aware algorithm is the optimal strategy since it achieves convergence fastest than any other option.

A realistic scenario in which this tradeoff may be made is in a cognitive radio application. In the case of a secondary user that may make use of a channel on the condition it causes no interference to the primary user, the elimination of interference is the primary concern of the alignment algorithm. Two approaches could be taken here; the first is to implement the original

($p = 1$) ItA algorithm in the hope that the algorithm reaches a zero-interference solution. This is likely to occur (60% of instances yield a zero-interference solution) but the likelihood that the solution will converge within 100 iterations is low (around 30%). This poses a significant risk that the solution embarked upon at the beginning of the channel training stage yields a solution that cannot be used, and this is only learned after a significant length of time has expired. The second approach is to 'fail fast and try again'; utilising the power-aware algorithm offers a very fast result (nearly 100% instances converge within ten iterations) that has a narrow chance (approximately 6%) of yielding an interference-free solution. However, since the algorithm could be run multiple times within the same time as one run of the original, multiple attempts could be made with different starting channel coefficients to find a zero-interference solution. This could also be attempted to a lesser extent with the selective ($p = 0.2$) algorithm, which is much more likely to find a zero-interference solution (19%) within approximately 30 iterations.

A second scenario is interference alignment is used to maximise the sum capacity of the network in a static or slowly-changing environment. In this case there is a clear preferred approach, which is to use the ($p = 0.5$) selective algorithm, which is more than twice as likely to yield a converged solution within 50 iterations as the original algorithm, and 70% likely to yield a converged solution within 100 iterations. This is achieved at the expense of sum capacity compared to the original algorithm, but given the much improved convergence behaviour can be easily justified. Another scenario is the same application in a highly-dynamic environment. In this case the power-aware algorithm is the preferred solution, given it offers middling capacity performance similar to that of $p = 0.4$ but with much faster convergence. Interference is not a consideration in such a network which allows such a 'noisy' option to be used.

The final realistic scenario is where interference alignment is being performed to achieve user density in a low-power 'scatternet' application. The actual sum capacity of the network is off less importance in this scenario, but convergence time will be of highest importance in order to minimise the time spent channel training and thus energy spent. In this scenario the power-aware algorithm is the clear choice here, since it minimises the time required to achieve an alignment solution and provides an adequate-capacity channel, which is all that is required.

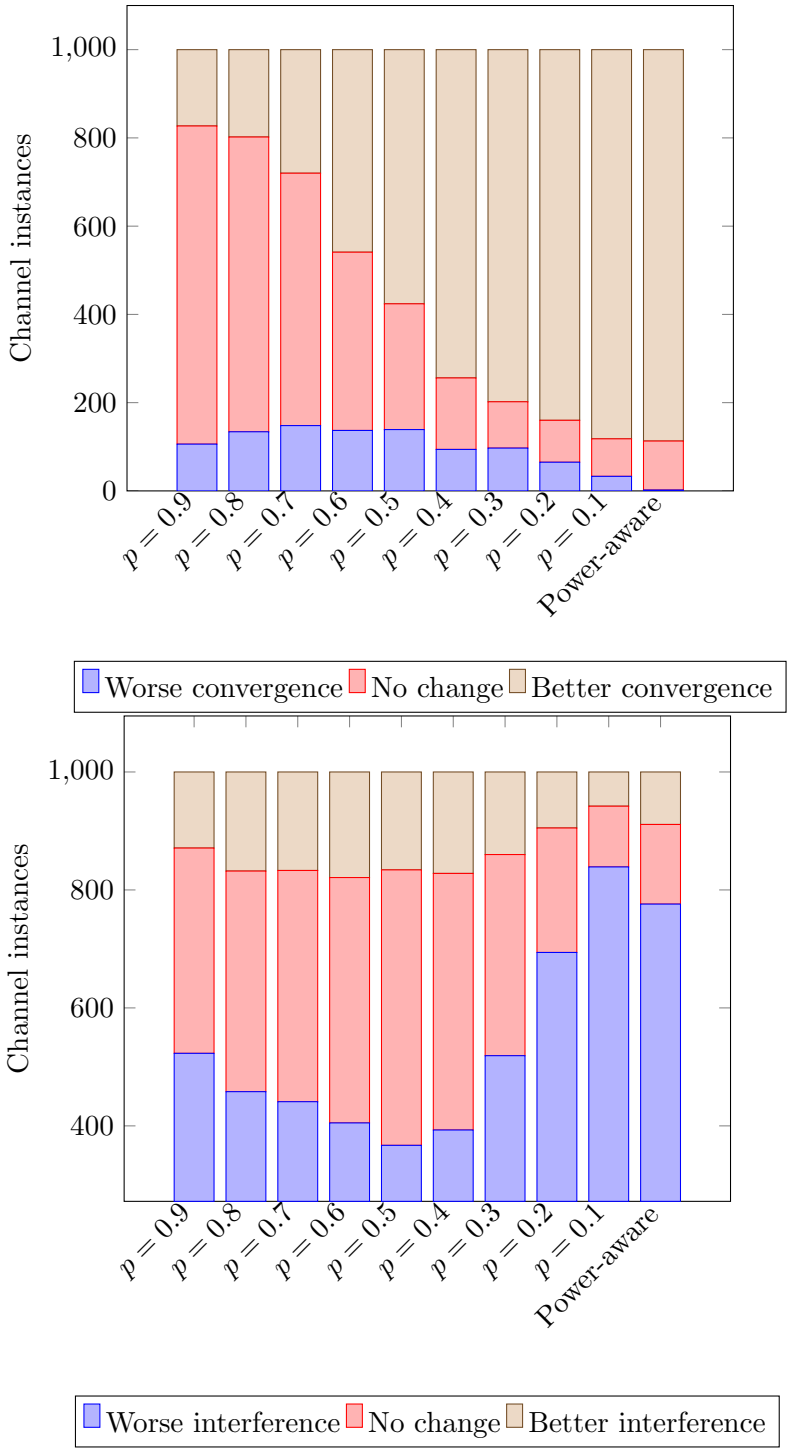

Figure 3.8: Effect of algorithm modifications on convergence time and sum interference compared to performance of original Iterative Alignment algorithm

4 Rank Estimation of Channels with unequal numbers of antennas

4.1 Motivation

A significant proportion of the literature on interference management and alignment lies in the context of centralised systems such as cellular networks, but this does not preclude the possibility that such techniques could be applied to decentralised networks as well. In fact, it could be suggested that dense unplanned networks such as those seen in rapidly deployable networks (or 'scatternets') and the emerging Internet of Things (IoT) have more to gain from alignment techniques; the potential to limit interference in networks that can easily become congested (becoming interference-limited, if not rendered totally unusable) is a significant application advantage.

In this chapter we investigate a channel training strategy that permits the receiving node to estimate the number of antennas a transmitting node possesses, using a specially structured training sequence. The actual sequence itself does not need to known by the receiver during channel estimation. This can be performed when the network starts up, or during an phase in the MAC scheme allotted for new nodes to join the network. The number of antennas each user possesses is a crucial piece of information, necessary for informing the later stages of channel estimation and for determining the optimal transmission strategy during the next phase of the networks operation. Much significant work has been done on investigating the area of neighbour discovery but some fundamental assumptions are often made in the name of tractability. Many transmission schemes assume that all receivers and transmitters within the network have the same number of antennas, or at least that the number of transmitting antennas M and receivers N is the same for all users within the same interference channel during each transmission period. However this is unlikely to be the case in heterogeneous networks, or in networks comprised of many devices created by different manufacturers and fulfilling different roles (for instance in the IoT).

The number of antennas a node possesses is a critical element of the MIMO transmission scheme; the additional antennas are what gives the node its ability to better control the way in which it transmits into the channel and as such are a key source of diversity. This diversity is quantified in the 'Degrees of Freedom' (DoF) metric. This is clear in Interference Alignment (IA) schemes where the symmetric GDoF of the channel (a measure of the channel's performance normalised against the equivalent AWGN channel) is defined as a function of DoF within the channel, i.e. $d_{sym} = \min(M_i, N_i)\ \forall i \in \mathcal{K}$. While all the devices are connected to the same network, there is the possibility that additional DoF accessible to better-equipped devices can offer an improvement to the simultaneous rate of the network. This is exemplified in the Karmakar alignment scheme described in [31], where the signal subspaces left 'empty' between users who cannot perceive the subspace is filled with side information or additional payload. Since the other users are unable to 'percieve' that signalling dimension the additional channel does not add to the sum interference. Without this knowledge a transmitter cannot be aware of these additional DoF available to it. Conversely, a transmitter that knows the DoF available to its neighbours is much better equipped to deal with interference, as is able to be less conservative in its own channel usage.

Collection of Channel State Information (CSI) is usually by means of a training sequence; simple equalisation of a known training sequence in the absence of interference is easily performed by zero forcing, but is only possible when the channel matrix is full-rank and well-conditioned. Naturally, the presence of noise and/or interference has a negative impact on the resulting channel estimate, which in turn affects the user's ability to make full use of the channel. Correlated noise and interference pose an additional challenge to the receiver [43].

Crucial to any estimation approach based on training sequences is knowledge of the training sequence; without this prior information it is not possible to perform the operation. The sequence itself might be known *a priori*, or it might be generated from a set of parameters known to the receiver before estimation commences. Such parameters that are necessary for effective channel estimation include the sequence length, the power allocation strategy, and the covariance matrix of the sequence. Implicit in this covariance matrix is the number of independent 'streams' of

symbols over which to calculate the covariance. This is also the signal rank, and in order to make the most effective use of the channel being estimated this signal should have as many sequences as the transmitting node's array has antennas, such that every spatial dimension (in the case of subspace-based estimation) contains a signal that can inform the channel estimator. While the length of the training sequence might be able to be inferred from inspection of the time correlation over a number of repetitions, the rank of the signal when the number of transmit antennas is unknown is a more challenging task. In order for training sequences to be an option without rank estimation, therefore, it is necessary to restrict the number of transmitted streams to a known quantity throughout the network. In a network with a variety of node capabilities this will be limited to the smallest number of antennas *any* user can feasibly be equipped with.

In [44] the authors demonstrate several training sequences that can be used by their joint detection and estimation algorithm to robustly estimate rank-deficient channels. However, the joint estimator-detector relies on the training segment of the frame to be composed of a number of *known* training sequences denoted by $\mathbf{S}$. The authors propose that the Maximum Likelihood solution for the channel coefficients can be derived from the received sequence $\mathbf{Y}$ by

$$\hat{\mathbf{H}}_{ML} = \mathbf{Y}\mathbf{S}^H(\mathbf{S}\mathbf{S}^H)^{-1} \tag{4.1}$$

The optimal training sequence that minimises the estimation error is therefore one that satisfies

$$\mathrm{Tr}(\mathbf{S}\mathbf{S}^H) = PM \tag{4.2}$$

where P is the transmit power and M is the number of transmit antennas.

The authors also propose a training sequence for channels with correlated interference (i.e. 'coloured' noise) that relies on secondary channel information, as does [45]. The optimal training sequence is derived from the decomposition of the temporal correlation matrix $\mathbf{Q} = \mathbf{U}\Lambda\mathbf{U}^H$ and the spatial correlation matrix $R_t = \mathbf{V}\Delta\mathbf{V}^H$ where $\mathbf{U}$ and $\mathbf{V}$ are orthonormal eigenvectors. The

optimal training sequence, referred to as the 'Liu' sequence is given by

$$\mathbf{S} = \mathbf{U}\Sigma\mathbf{V}^H \tag{4.3}$$

where Σ is a diagonal matrix with entries

$$\sigma_i = \max\left\{\sqrt{\frac{\lambda_i}{\mu}} - \frac{\lambda_i}{\delta_i}, 0\right\}^{1/2} \quad \text{for} 1 \leq i \leq \min(M, L) \tag{4.4}$$

with parameter μ maintaining the power limit of the transmitted signal.

While the temporal correlation of the channel could be measured through monitoring the channel, the need for information on the transmitter correlation (even if it was modelled) necessitates knowledge of the number of antennas the transmitter possesses. This would not be possible in a heterogeneous network.

A training sequence that is capable of both performing rank estimation and channel estimation would therefore be of significant advantage. In order to be applicable to all varieties of heterogeneous channels, the training sequence itself would be one that could be generated by the receiver given knowledge of the number of transmitted streams.

One such sequence is the 'chaotic' sequence proposed by the same authors:

$$\mathbf{S} = [\mathbf{c}_1 \ldots \mathbf{c}_M]^T \tag{4.5}$$

where the individual chaotic sequences are k-th order Chebyshev maps

$$c_{l+1} = \cos(k \arccos(c_l)), \qquad -1 \leq c_l \leq 1 \tag{4.6}$$

The chaotic sequence has the benefit of meeting the optimality requirement in (4.2) while

also being deterministic, given that the initial 'seed' values of the chaotic sequence can be shared amongst users.

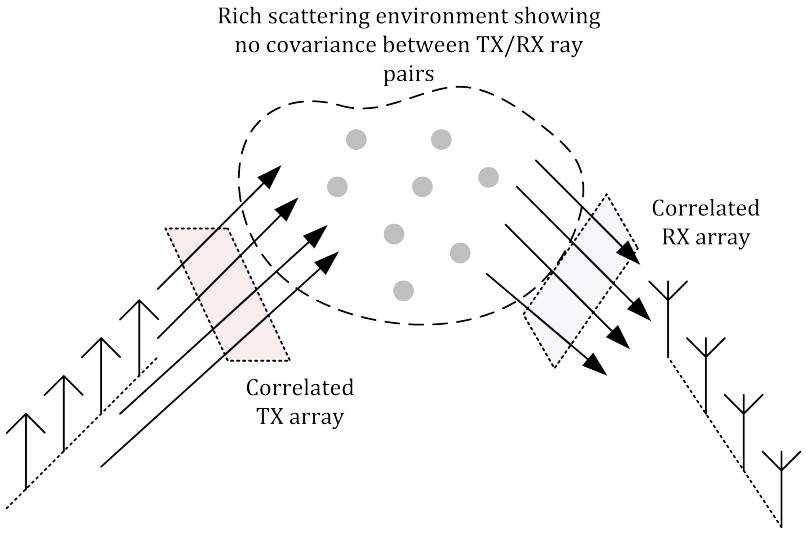

Figure 4.1: The Kronecker Channel

While temporal covariance can be manufactured by the use of repeated sequences, the spatial correlations of the channel are the result of physical properties of the channel. Without explicit measurement these must be modelled according so some assumption made about the channel. One such model (and that employed in [44]) is the *Kronecker Channel Model* [46]. This model represents the channel matrix as the product of the two 'one-sided' antenna correlation matrices at the receiver ($\mathbf{R}_r$) and transmitter ($\mathbf{R}_t$), such that:

$$\mathbf{H} = \mathbf{R}_r^{1/2}\mathbf{H}_{iid}\mathbf{R}_t^{1/2} \tag{4.7}$$

where $\mathbf{H}_{iid}$ is a matrix whose elements are i.i.d. zero-mean circular symmetric Gaussian random values with unity variance.

The defining feature of this model is that correlations at either 'end' of the channel are taken into account, but the correlations are separable and the channel exhibits no coupling between

the scatterers surrounding either side of the link. This is a reasonable assumption to make in an environment where scatterers are highly local to the transmitters and receivers, but the two 'ends' of the channel are sufficiently far away that there are no common scatterers that can cause correlation between the two arrays. The Kronecker model is widely used in modelling channels with antenna correlation [47], and it has been subjected to several real-world tests [48] to gauge its suitability in MIMO research.

In this chapter we investigate an approach that exploits the correlation properties imbued on the signal, both by its structure and by the correlation between the antennas that make up the arrays at either end of the channel. This chapter is organised as follows: Section 4.2 describes the transmission model and role of the rank estimation function in the context of a protocol that makes use of the channel rank as an input to the DoF-finding algorithm. Section 4.3 presents the derivation of channel rank from a theoretical standpoint. Section 4.4 describes the details of how a rank estimator was implemented and the simulation parameters defined. Finally, the performance of the estimator is evaluated in Section 4.5 and conclusions on its efficacy and applicability are drawn in Section 4.6.

4.2 System model

Consider again the two-user Interference Channel comprised of two pairs of devices, hereafter referred to as 'users'. This is depicted in Figure 2.3. Each user takes a turn to transmit a training sequence on the channel without interference from any other user (i.e. the transmitting members of each user pair). This coordination is performed by the MAC layer and is not considered here; it is assumed that during the transmission of training sequences no interference is encountered. As well as the transmitting devices, either or both receiving devices may possess more than one antenna. Channel coherence and multipath conditions are assumed to be such that for the duration of training the channel is frequency flat and invariant, allowing the full matrix between the transmitter and receiver to be described in a complex-valued $N \times M$ channel matrix $\mathbf{H}$, where N is the number of receive antennas and M the number of transmit antennas.

As part of training the transmitter transmits M independent sequences of length L on each of its antennas, represented by the $M \times L$ matrix $\mathbf{S}$. The sequences are transmitted as such that their power is limited to P_t on each antenna. This transmit power is fixed as part of the user discovery protocol and is therefore known to the receiving device. The received baseband sequence at the receiver can therefore be described by the expression

$$\mathbf{Y} = \sqrt{P_t}\mathbf{H}\mathbf{S}^T + \mathbf{N} \tag{4.8}$$

where $\mathbf{N}$ represents the additive white Gaussian noise apparent at the receiver, which has zero mean and unity power. We will use the covariance properties of the received sequence to estimate the channel's rank in the next section.

4.3 Estimation of channel rank

The channel matrix can be expressed in the Kronecker form in (4.7). The separability of the two covariance matrices allows us to extract information from the covariance of the received signal, as shown in the following theorem.

Theorem 1. *Given a suitable training sequence* $\mathbf{S}$*, the number of transmitting antennas* M *can be estimated at the receiver using only the training sequence properties, even if the channel is rank-deficient.*

This theorem is supported by the following two Lemma.

Lemma 1. *The covariance matrix of a signal passed through a Multiple Input Multiple Output (MIMO) Kronecker channel is the Kronecker product of the combined spatial-temporal covariance of the transmitted signal and the covariance matrix of the receiving antenna array.*

Following from [45], using the vector operator $\mathbf{a} = \text{vec}(\mathbf{A}) = [a_{11} \quad \dots \quad a_{m1} \quad a_{12} \quad \dots \quad a_{mn}]^T$ and applying the Kronecker identity $\text{vec}(\mathbf{ABC}) = (\mathbf{C}^T \otimes \mathbf{A})\text{vec}(\mathbf{B})$, the vectorised channel matrix can be expressed as

$$\mathbf{h} = \text{vec}(\mathbf{H}) = (\mathbf{R}_r^{1/2} \otimes \mathbf{R}_t^{1/2})\mathbf{h}_{iid} \tag{4.9}$$

where $\mathbf{h}_{iid}$ is a $LN \times 1$ complex Gaussian random variable with unity variance and $\otimes$ denotes the Kronecker product operator. From this the channel covariance matrix can be computed, i.e.

$$\begin{aligned}\mathbf{R_H} &= \mathbb{E}[\mathbf{h}\mathbf{h}^H] \\ &= \mathbf{R}_r \otimes \mathbf{R}_t \end{aligned} \tag{4.10}$$

Following from (4.8), the covariance matrix of the received training sequence can be found in a similar manner.

$$\begin{aligned}\mathbf{R_Y} &= \mathbb{E}[\mathbf{y}\mathbf{y}^H] \\ &= \mathbb{E}[\mathrm{vec}(\mathbf{Y})\mathrm{vec}(\mathbf{Y})^H] \\ &= \mathbb{E}[\mathrm{vec}(P_t^{1/2}\mathbf{H}\mathbf{S}^T + \mathbf{N})\mathrm{vec}(P_t^{1/2}\mathbf{H}\mathbf{S}^T + \mathbf{N})^H] \\ &= \mathbb{E}[P_t^{1/2}P_t^{1/2}\mathrm{vec}(\mathbf{H}\mathbf{S}^T)\mathrm{vec}(\mathbf{H}\mathbf{S}^T)^H + \mathbf{n}\mathbf{n}^H] \\ &= \mathbb{E}[P_t(\mathbf{S}\mathbf{R}_t^{1/2} \otimes \mathbf{R}_r^{1/2})\mathbf{h}_{iid}\mathbf{h}_{iid}^H(\mathbf{R}_t^{1/2}\mathbf{S}^H \otimes \mathbf{R}_r^{1/2})] + \mathbf{I} \\ &= \mathbb{E}[P_t(\mathbf{S}\mathbf{R}_t^{1/2}\mathbf{R}_r^{1/2}\mathbf{S}^H) \otimes (\mathbf{R}_r^{1/2}\mathbf{R}_r^{1/2})] + \mathbf{I} \\ &= \mathbb{E}[P_t(\mathbf{S}\mathbf{R}_t\mathbf{S}^H \otimes \mathbf{R}_r)] + \mathbf{I} \end{aligned} \tag{4.11}$$

We now introduce the covariance matrix

$$\mathbf{Q} = \mathbb{E}[\mathbf{S}\mathbf{R}_t\mathbf{S}^H] \tag{4.12}$$

which represents the combined temporal and spatial covariance matrix of the transmitted signal once it has passed through the transmit antenna array. Therefore we can express the received signal covariance as

$$\mathrm{R_Y} = \mathbb{E}[\mathbf{y}\mathbf{y}^H] = P_t(\mathbf{Q} \otimes \mathbf{R}_r) + \mathbf{I} \tag{4.13}$$

Lemma 2. *Using covariance matrix* $\mathbf{Q} = \mathbb{E}[\mathbf{S}\mathbf{R}_t\mathbf{S}^H]$ *the number of transmitting antennas can be*

estimated if the transmitted signal exhibits high temporal correlation and low spatial correlation.

The covariance matrix $\mathbf{Q}$ has the following structure [45]

$$\mathbf{Q} = \begin{bmatrix} \sum_{i=j}^{M}\sum_{j=1}^{N}\mathbf{R}_{ij}[0]\rho_{ij} & \dots & \sum_{i=1}^{M}\sum_{j=1}^{N}\mathbf{R}_{ij}[L-1]\rho_{ij} \\ \vdots & \ddots & \vdots \\ \sum_{i=1}^{M}\sum_{j=1}^{N}\mathbf{R}_{ij}[L-1]\rho_{ij} & \dots & \sum_{i=1}^{M}\sum_{j=1}^{N}\mathbf{R}_{ij}[0]\rho_{ij} \end{bmatrix} \tag{4.14}$$

where ρ_{ij} is the i,j^{th} element of the one-sided transmit antenna covariance matrix $\mathbf{R}_t$, i.e. the covariance between antennas i and j of the array. $\mathbf{R}_{ij}[n]$ represents the temporal covariance between the sequences observed in streams i and j at symbol n.

By selecting suitable training sequences, the structure of $\mathbf{Q}$ can be manipulated. Using orthogonal sequences for each 'stream' ensures that the signal exhibits low autocorrelation and cross-correlation the value of the main diagonal of the covariance matrix. The covariance can be expressed as

$$\begin{aligned} \mathrm{diag}(\mathbf{Q}) &= \sum_{\substack{i=1 \\ i=j}}^{M}\sum_{j=1}^{M}\mathbf{R}_{ii}[0]\rho_{ii} + \sum_{\substack{i=1 \\ i\neq j}}^{M}\sum_{j=1}^{M}\mathbf{R}_{ij}[0]\rho_{ij} \\ &= \sum_{i=1}^{M}\mathbf{R}_{ii}[0]\rho_{ii} + \sum_{\substack{i=1 \\ i\neq j}}^{M}\sum_{j=1}^{N}\mathbf{R}_{ij}[0]\rho_{ij} \\ &= \sum_{i=1}^{M}1 + \sum_{\substack{i=1 \\ i\neq j}}^{M}\sum_{j=1}^{M}\mathbf{R}_{ij}[0]\rho_{ij} \\ &= M + \sum_{\substack{i=1 \\ i\neq j}}^{M}\sum_{j=1}^{M}\mathbf{R}_{ij}[0]\rho_{ij} \\ &= M + \epsilon \end{aligned} \tag{4.15}$$

The second term represents the residual covariance between the individual streams of the training sequence and between the elements in the transmitting antenna array. If this term is the product of two sufficiently small values they can be treated as an error term, denoted by ϵ.

Gold sequences [49] are a set of pseudorandom noise sequences used in spread spectrum applications due to their simple derivation from a small number of initial parameters and easily predictable correlation properties. Gold sequences exhibit low and deterministic values for their temporal autocorrelation($\mathbf{R}_{ii}(\tau)\ \tau \neq 0$) and inter-stream cross-correlation($\mathbf{R}_{ij}(\tau)\ \forall\ \tau$) matrices. 1023 symbol codes are used in the Global Positioning System (GPS) C/A code [50] due to these properties. The synchronisation of receivers on the ground and orthoganalisation between messages sent from different clocks in the GPS are analogous to the detection of training messages and discrimination of multiple MIMO streams in the channel estimation attempted here, making them ideal for the purposes of rank estimation.

The distribution of this error term will be discussed later in this chapter, but for now can be assumed to have zero mean. An appropriate estimation of the channel rank would therefore be the mean value of the covariance matrix's diagonal.

$$\hat{M} = \mathbb{E}[\text{diag}(\mathbf{Q})]. \tag{4.16}$$

This concludes the proof, and demonstrates that the channel rank can be estimated using only local channel knowledge.

This estimate is independent of the number of receive antennas and in the next section will be demonstrated to work for various lengths of training sequence, blocks lengths, signal powers, and MIMO channel dimensions.

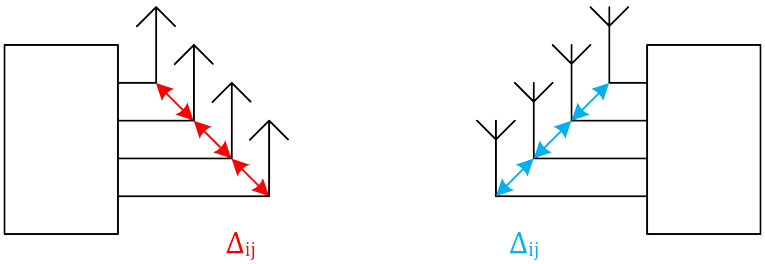

Figure 4.2: MIMO Channel during Training

4.4 Simulation

4.4.1 Rank Estimation

The performance of the rank estimation algorithm was assessed through the use of Monte Carlo simulations. Estimation of the signal rank is made over a training sequence composed of B blocks of Gold sequences L symbols in length. The received signal covariance matrix is formed by taking the expectation of the received signal over the B blocks, yielding an approximation of $\mathbf{Q}$ (denoted $\tilde{\mathbf{Q}}$) of dimension $L \times L$.

The M training sequences remain constant throughout the training process, selected randomly from the $2^L - 2$ sequences that are not the generating sequences. The generating sequences are omitted to avoid their potential use together, which would cause excessive covariance between the individual streams.

Since the algorithm depends on the equalisation of transmission power as part of the estimation process it is necessary that the transmit power of each stream is constant. For the purposes of simulation the transmit power will be defined relative to the noise power experienced within the channel, i.e. the transmit SNR:

$$\mathrm{SNR}_t = \frac{P_t}{N_r} \tag{4.17}$$

It is assumed that scatterers are sufficiently far away and distributed such that the channel model follows from the analysis in Section 4.2, where the two antenna correlation matrices are used with an Additive White Gaussian Noise (AWGN) matrix to generate a time invariant channel that remains constant for the duration of the training process. The antenna arrays at both ends of the link are Uniform Linear Arrays with inter-element spacing Δ_{ij}, which is expressed in wavelengths λ. The correlation matrices for both arrays may be approximated using a Bessel function of the first kind [51].

$$\rho_{ij} = J_0(2\pi\Delta_{ij}) = \frac{1}{2\pi}\int_0^{2\pi} e^{j2\pi\Delta_{ij}\cos(\phi)}d\phi \tag{4.18}$$

While this is a crude oversimplification of antenna array modelling (cf. [52] and [53]) it is sufficient to model the relevant structure of a ULA's correlation matrix, i.e. strictly decreasing correlation coefficients as the distance between antennas increases, but with oscillations due to critical spacings. Channel instances were constructed according to (4.7). The temporal component of the combined covariance matrix $\mathbf{Q}$ requires that the expectation in (4.11) be taken over multiple repetitions of the training sequence. The training period is therefore split into 'blocks' created by repeating the selected Gold sequences a number of times, inducing the required temporal correlation in the transmitted sequence. This temporal correlation permits the expectation in (4.11) to be taken over multiple copies of the same transmitted sequence, with the receiver able to identify the length of the sequence without prior knowledge at the receiver.

This enables the receiver to operate 'semi-blind', as it does not require knowledge of the sequence length to operate. As will be discussed later, simulations demonstrate that there is very little advantage to using long sequences, whereas shorter sequences reduce computation load and minimise the time spent exchanging training data.

At the receiver the Nearest Kronecker Product (NKP) is used to estimate $\mathbf{Q}$ from the covariance of the received signal. The receive antenna array configuration is assumed to be constant throughout the period of transmission (and likely the device's lifetime), so it can be assumed that

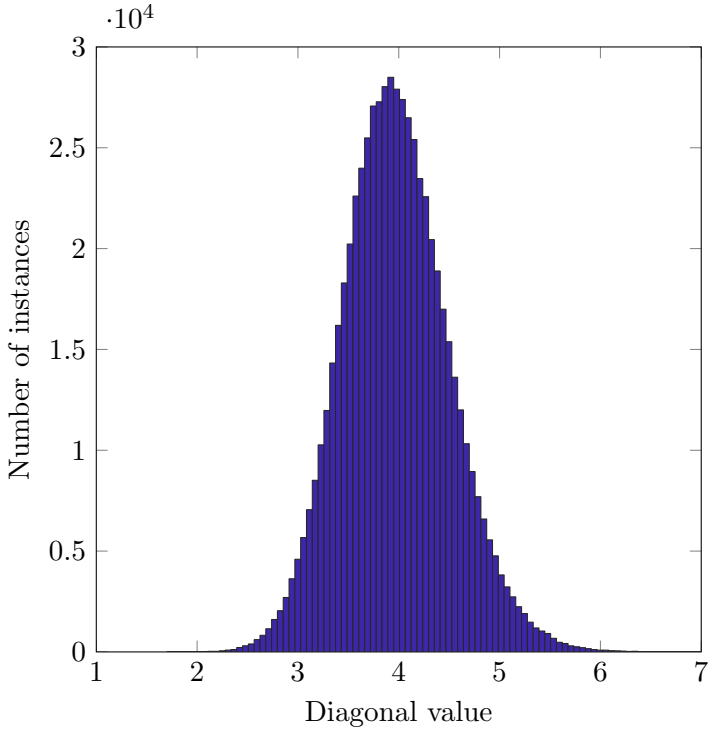

Figure 4.3: Histogram of diagonal values of covariance matrix $\tilde{\mathbf{Q}}$ over 10,000 instances

$\mathbf{R}_r$ is already known empirically or can be modelled depending on the MIMO array structure employed. The NKP can be found by solving the least squares problem [54] below

$$\tilde{\mathbf{Q}} = \min_Q \left(\| \left(\frac{\mathbb{E}\left[\mathbf{y}\mathbf{y}^H\right] - \mathbf{I}}{\mathrm{SNR}_t} \right) - \left(\mathbf{Q} \otimes \mathbf{R}_r\right) \|_F^2 \right) \tag{4.19}$$

which is minimised by:

$$\tilde{q}_{ij} = \frac{\mathrm{Tr}\left(\left(\frac{\mathbb{E}[\mathbf{y}\mathbf{y}^H] - \mathbf{I}}{\mathrm{SNR}_t} \right)^{[ij]T} \mathbf{R}_r \right)}{\mathrm{Tr}(\mathbf{R}_r^T \mathbf{R}_r)} \tag{4.20}$$

where $.^{[ij]}$ denotes the $ij^{th} N \times M$ submatrix of the larger matrix.

Figure 4.3 shows a histogram of the diagonal values of the estimated signal covariance $\tilde{\mathbf{Q}}$ matrix using (4.19) over 10,000 instances of a 4×4 MIMO Interference Channel (IC) at $P_t =$ 20dB. The covariance matrix was calculated over 32 blocks of a 63-symbol long training sequence. $\mathrm{diag}(\tilde{\mathbf{Q}})$ can be observed to possess a mean value approximately equal to the number of transmit

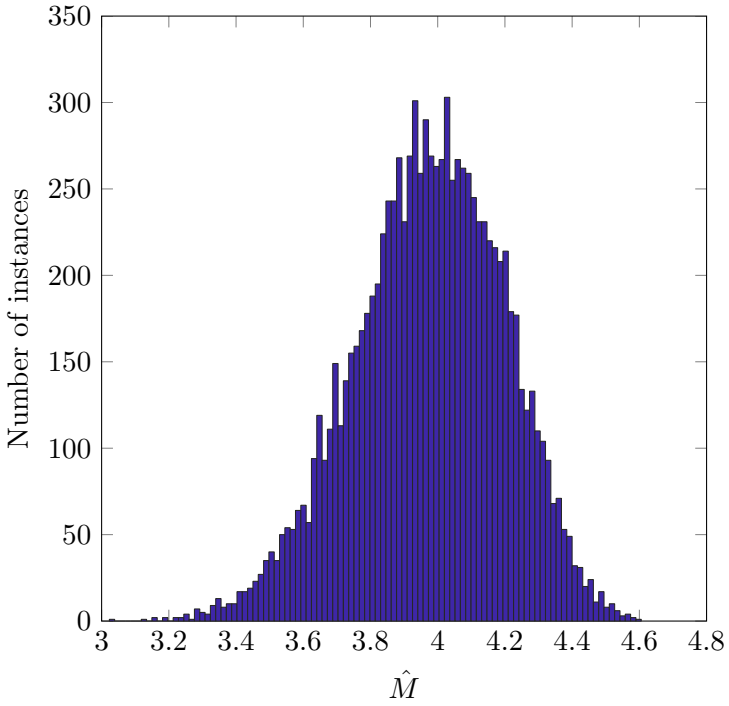

Figure 4.4: Histogram over 10,000 estimates of channel rank $\hat{M}$

antennas $M = 4$ but with a significant variance. From this it can be inferred that the error term ϵ is a random variable with normal distribution and a small mean value.

By performing the averaging operation over the entire diagonal in (4.16), $\mathbb{E}(\text{diag}(\tilde{\mathbf{Q}}))$ is observed in Figure 4.4 to exhibit very little variance.

In estimating the impact of error in the rank estimation we must consider the implications of over- or under-estimating the channel's rank on future transmissions.

- Over-estimating the channel rank (i.e. by rounding up to the nearest integer number) will have the effect of misleading a user into believing there are additional degrees of freedom to equalise and eventually use. Transmission of a multi-stream signal into a rank-deficient channel will cause the signals to be inseparable at the receiver and the channel will become unusable.
- Under-estimating the channel rank will cause the receiver to assume the transmitter has fewer antennas than it actually does. Any signal transmitted will therefore not make the

full advantage of the degrees of freedom available to it; this may negatively impact the throughput of the channel but does not render it unusable.

For this reason, the receiver should *underestimate* the channel rank, so as to avoid over-specifying the channel and the user transmitting an undecipherable signal in later stages of channel estimation.

If the training sequence is to be subsequently used for channel estimation, however, both kinds of error are equally negative and the estimated channel coefficients will be incorrect. In this case the rank estimation decision should be a simple rounding of $\hat{M}$ to the nearest integer value.

The decision to underestimate is algorithmic; for the purposes of assessing the effect of the parameters above on the rank estimate the error will be measured using the Mean Squared Error metric. The Mean Squared Error is an appropriate measure of error due to its relation to the variance and bias of the estimate:

$$\begin{aligned} \text{MSE} &= \mathbb{E}[(\hat{M} - M)^2] \\ &= \text{Var}_M(\hat{M}) + \text{Bias}(\hat{M}, M)^2 \end{aligned} \tag{4.21}$$

Since the effect of the error is absolute (i.e. an error of 1 on a rank-1 channel is just as severe as an error of 1 on a rank-10 channel) the MSE is not normalised against the value it is estimating.

4.4.2 Channel Estimation

It can be assumed that the receivers possess sufficient knowledge in order to be able to recreate the original training sequences for the purposes of channel estimation. In the case of the Gold sequences it is sufficient to know the length of the training sequence and the sequences selected

for each independent stream. Since all Gold sequences except the generating sequences exhibit similar levels of cross-correlation these can be selected as part of the algorithm without penalty to rank estimation. The number of Gold sequences contained within the training sequence is the rank of the channel and is estimated as in Section 4.3.

Similarly, the chaotic sequence can be recreated at the receiver if a common set of starting sequence values are shared as part of the channel estimation algorithm. For the purposes of channel estimation the rank of the chaotic training sequence is assumed to be known by the receiver through some other means.

As stated in [44], the Maximum Likelihood solution to the channel estimation problem is derived from the training sequence by $\hat{\mathbf{H}}_{ML} = \mathbf{Y}\mathbf{S}^H(\mathbf{S}\mathbf{S}^H)^{-1}$. This approach shall be used by both the chaotic sequence and Gold sequence for channel estimation.

Channel estimation performance is measured with the Normalised Mean Square Error (NMSE) as defined below:

$$NMSE = \frac{\|\mathbf{H} - \hat{\mathbf{H}}\|_F^2}{\|\hat{\mathbf{H}}\|_F^2} \tag{4.22}$$

where $\|\cdot\|_F$ is the Frobenius norm.

4.5 Numerical results

In this section we consider the performance of the rank estimation algorithm, using the Mean Squared Error (MSE) and frequency of making an erroneous rank estimation as an indicator of the quality of the estimate.

We first examine the effect on rank estimation of parameters the system designer can control within the transmitted sequence. These include the training sequence length L, the number of repetitions in a block B, and the transmitted power SNR_t. Manipulation of these parameters allows the designer to trade off speed of operation against performance.

We then examine the effect on rank estimation of parameters that are less under the control of the system designer, including the number of antennas the users have N, M and the physical configuration of the antenna arrays. This is modelled by defining the distance between antenna elements as a function of wavelength, which intuitively will have a significant effect on the levels of correlation between elements in the transmit and receive antenna correlation matrices $\mathbf{R}_t$ and $\mathbf{R}_r$.

This is followed by a comparison of the performance of the Gold sequences as training sequences for the purposes of channel estimation against an existing channel estimation technique. The 'chaotic' sequence detailed in Section 4.1 will be used as a comparison due to its ability to be reproduced deterministically from a small number of initial parameters, as opposed to training sequences that must be known verbatim between users in order to be usable.

4.5.1 Rank Estimation Performance

In this section we measure the performance of the rank estimation algorithm. As discussed in Section 4.4 there are two figures of merit relevant to the algorithm's performance.

The mean squared error (MSE) offers an insight into the confidence that the resulting estimate $\hat{M}$ from the covariance matrix is close to the actual number of transmit antennas M, and is defined in (4.21).

The frequency of erroneous rank estimation is calculated similarly, counting the proportion of channel instances incorrectly estimated. It is assumed that the rank estimate is required to inform the channel estimator, so underestimating the channel rank is not necessary and the rank estimate is a simple rounding of the mean of the diagonal values of $\tilde{\mathbf{Q}}$.

Training sequence length, block size, and transmit power

Figure 4.5 shows the MSE observed in three different channels with $\Delta_t = \Delta_r = 0.4\lambda$ for varying sequence lengths and block sizes. Beyond very low levels of transmit SNR (< -15dB)

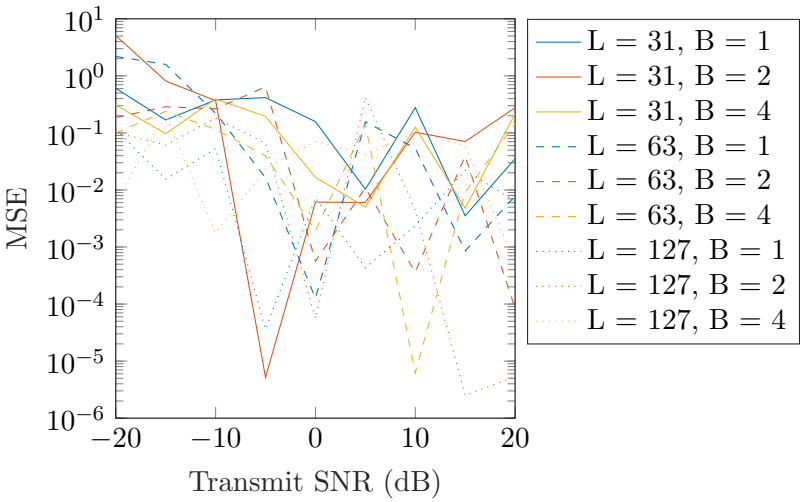

(a) $M = 3, N = 4$ (overdetermined) MIMO channel

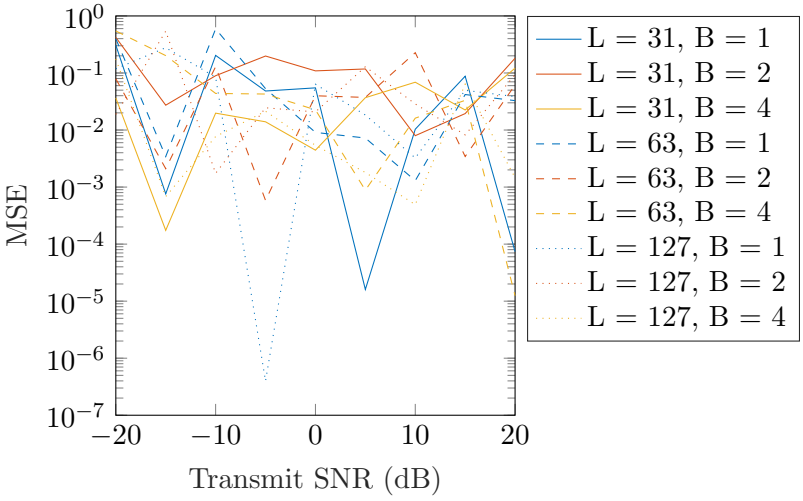

(b) $M = 3, N = 3$ MIMO channel

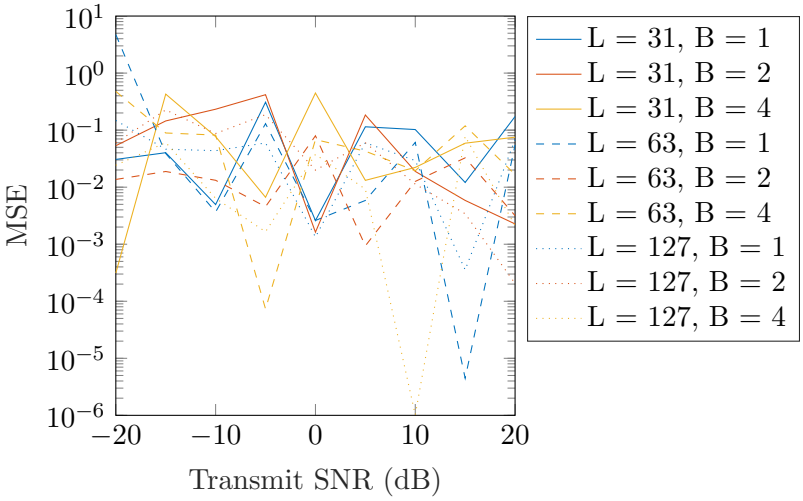

(c) $M = 4, N = 3$ (underdetermined) MIMO channel

Figure 4.5: Mean Squared Error of rank estimate observed in various MIMO Channels

there appears to be no discernible effect on MSE. Contrary to what would be expected, the MSE offers little insight into the performance of the estimator.

This in contrast with the error frequency graphed in Figure 4.6 for the same three channels, which shows a clear exponential relationship between transmit SNR and the performance of the estimator. It is observed that increasing levels of signal power correspond to a reduction in error probability.

Both sets of results point to the strong influence of the length of the overall training period – performance is similar between combinations of sequence length and block size that yield the same training period (e.g. 2 blocks of 31 and 1 block of 63) at low transmit SNRs, with the longer sequence offering slightly better performance at higher transmit SNRs (> 5 dB) for two of the three channels depicted here. Even in the under-determined channel the difference in performance at 20dB is only a fraction of 1%.

The improvements at high SNRs between overall training period lengths are marginal, and a canny system designer would be inclined to select the shortest combined training period length that offers the desired level of performance. For all three channels this would likely be the single block of the 63-symbol long training sequence.

It is also noted that the absolute level of error is higher in the channels with more receive antennas. This will be discussed in greater detail in the subsequent section.

From these results it can be concluded that the performance of the rank estimator is clearly sufficient for use in a practical channel estimator, particularly in under-determined channels where relatively short training periods (only 63 symbols) yield a very low frequency (less than 1% at 8 dB) of error. The system designer is afforded ample opportunity to trade transmit power and channel training time to achieve the desired performance.

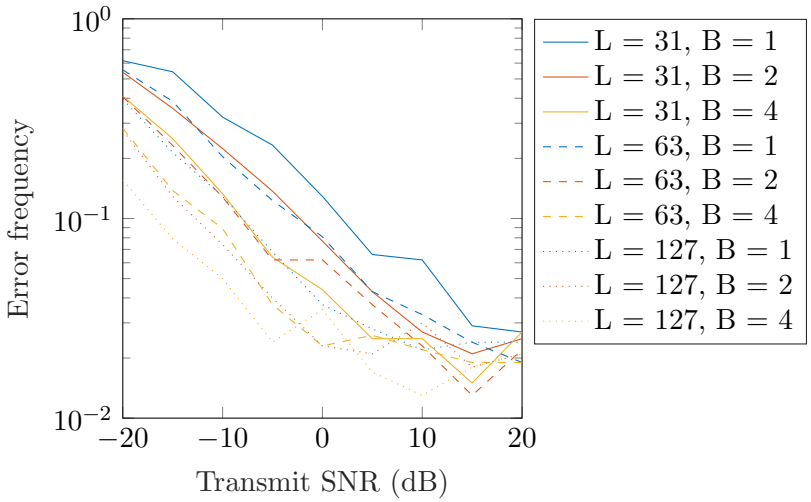

(a) $M = 3, N = 4$ (overdetermined) MIMO channel

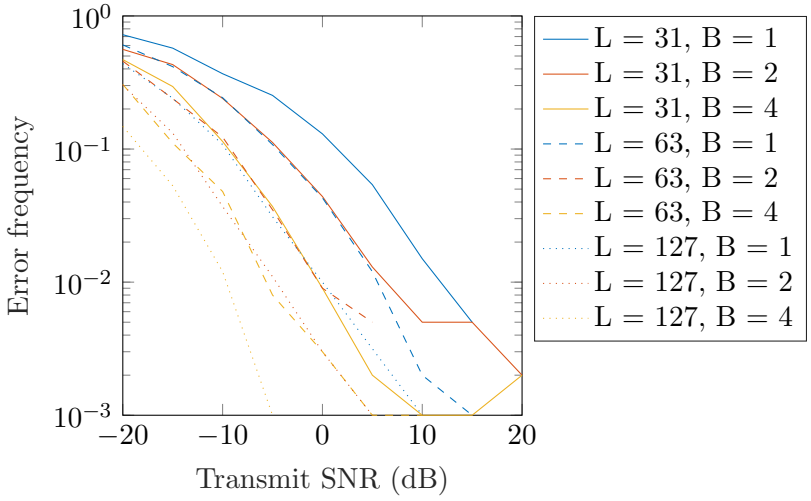

(b) $M = 3, N = 3$ MIMO channel

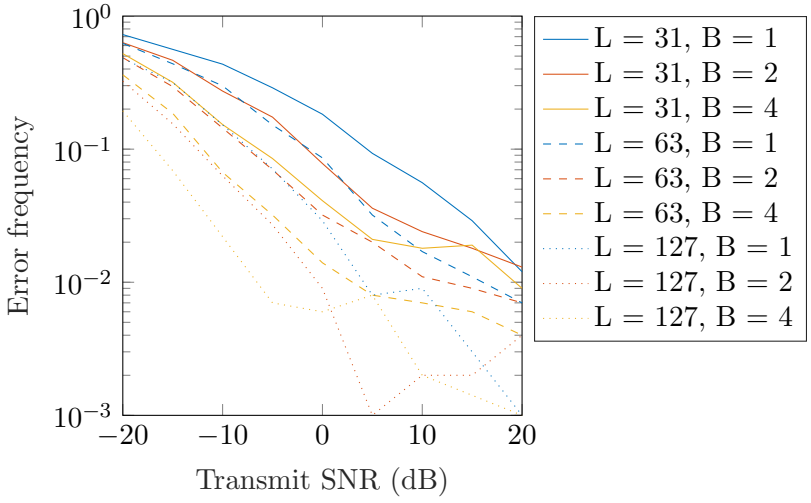

(c) $M = 4, N = 3$ (underdetermined) MIMO channel

Figure 4.6: Rank estimation error frequency observed in various MIMO Channels

Number of antennas

We now turn our attention to the effect of the size of the MIMO channel on rank estimator performance. The error frequency of the rank estimate against various size MIMO channels is shown in Figure 4.7 for three transmit SNR levels. These results were obtained over 1,000 channel instances using a training sequence of $L = 63, B = 1$ transmitted through arrays with $\Delta_t = \Delta_r = 0.4\lambda$.

These results demonstrate the ability of the estimator to correctly estimate the signal rank with a high rate of success (e.g. $> 99\%$ in a 4×2 MIMO channel) for various numbers of both transmit and receive antennas. As the number of antennas in the arrays on *either* side of the channel grows, however, it is observed when $\text{SNR}_t > 0\text{dB}$ that the error frequency *increases*. In contrast, a local minimum exists for the errors observed when $\text{SNR}_t < 0\text{dB}$. This can be directly attributed to the array gain of the MIMO channel increasing the signal power above the noise threshold, improving the receiver's ability to estimate the channel rank. This is observed in Figure 4.8 which shows the effect of the number of receive antennas on the estimate standard deviation at various power levels. While all but the strongest power levels see benefit in the initial array gain, the increase in variance encountered in $\tilde{\mathbf{Q}}$ induced by additional receive antennas overcomes the array gain to have a net detrimental effect on the variance of the estimate.

When implementing the channel estimation algorithm the system designer should take into account the expected power levels within the network, as this will influence the number of antennas that should be used to perform the channel estimation. As is shown in Figure 4.7 only in the weakest of channels would a practical system require to use more than two of three antennas.

At all power levels it is important to note that there is no error penalty for channels which are rank-deficient; this makes the estimation method suitable for all dimensions of MIMO channel.

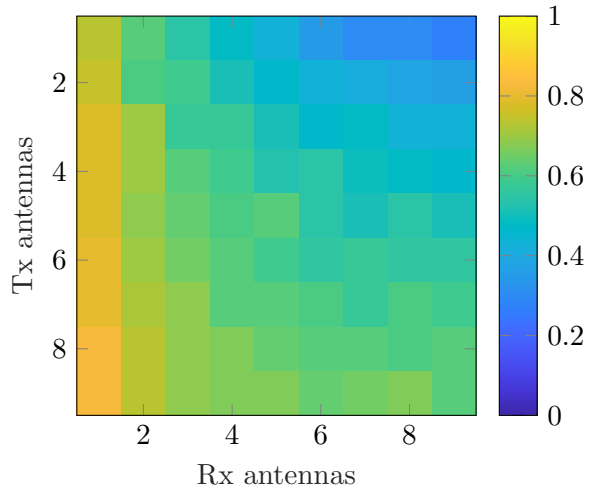

(a) $\mathrm{SNR}_t = -20\mathrm{dB}$

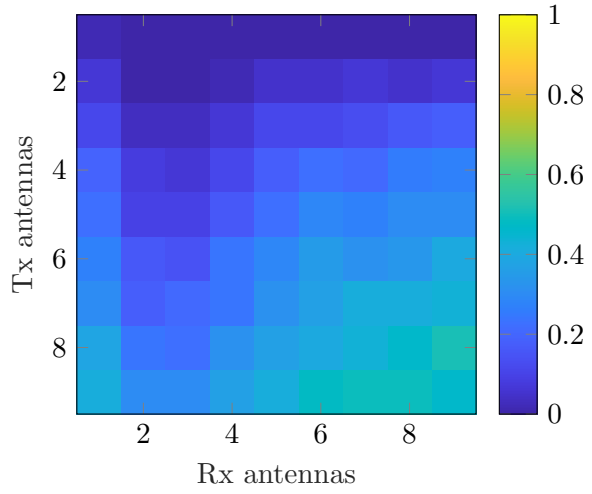

(b) $\mathrm{SNR}_t = 0\mathrm{dB}$

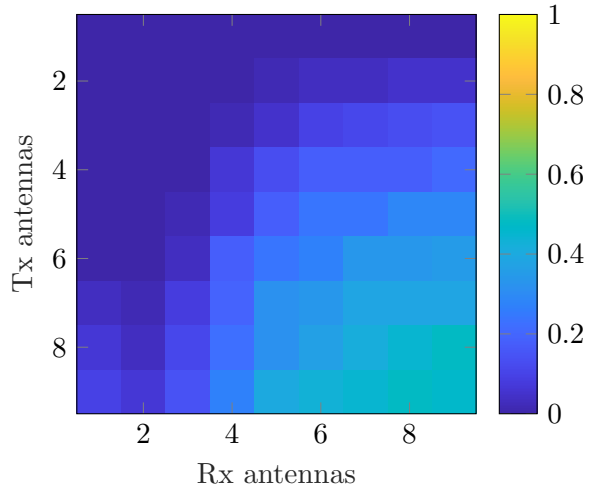

(c) $\mathrm{SNR}_t = 20\mathrm{dB}$

Figure 4.7: Error frequency of channel rank estimate for MIMO channels of dimension $M \times N$ at various power levels ($\mathrm{B} = 1$, $\mathrm{L} = 63$, $\Delta_r = \Delta_t = 0.4\lambda$)

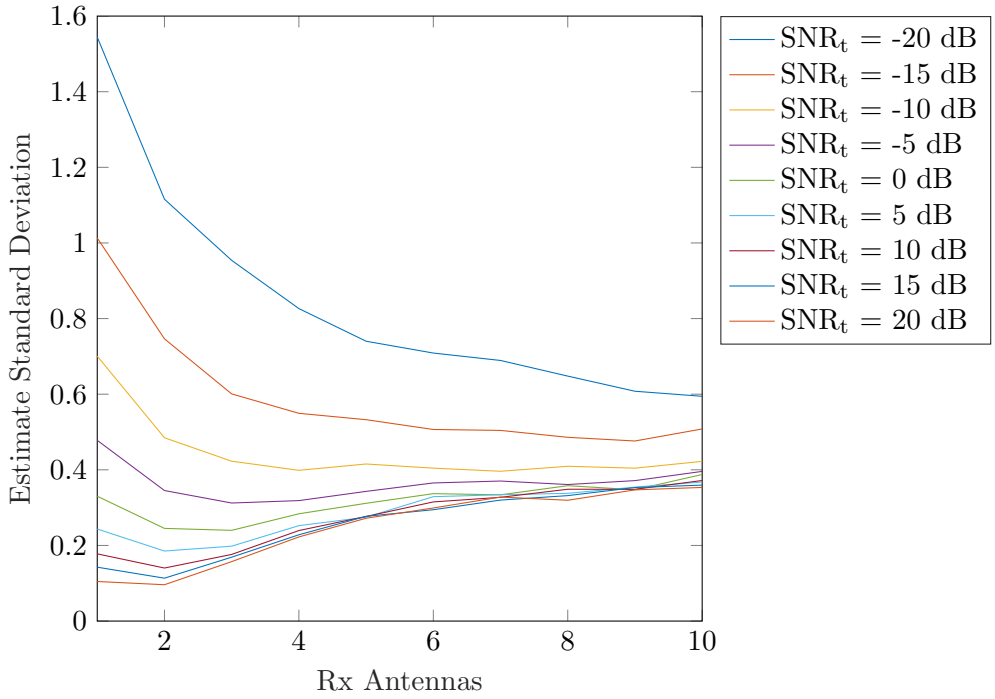

Figure 4.8: Effect of array gain on estimate standard deviation in $3 \times N$ MIMO channels at various transmit SNRs

Antenna spacing

Figure 4.9 shows the effect of antenna spacing on the estimate; since the value of transmit antenna cross-correlation ρ_{ij} determines the contribution the signal cross-correlation makes to the error term ϵ in the rank estimate, it follows that the MSE of the estimate should improve as the antennas move further away from the critical spacing of $\lambda/2$. This is in line with common wisdom that antennas should not be placed at critical intervals, causing greater correlation within the array. The receive antenna correlation can be observed to have no effect on the estimation error.

4.5.2 Channel Estimation Performance

For comparison purposes we assume that the channel estimators are in possession of perfect knowledge of the transmit power and channel rank. Figure 4.10 plots the NMSE for both the chaotic sequence described in [44] and the Gold sequence for MIMO channels of the same

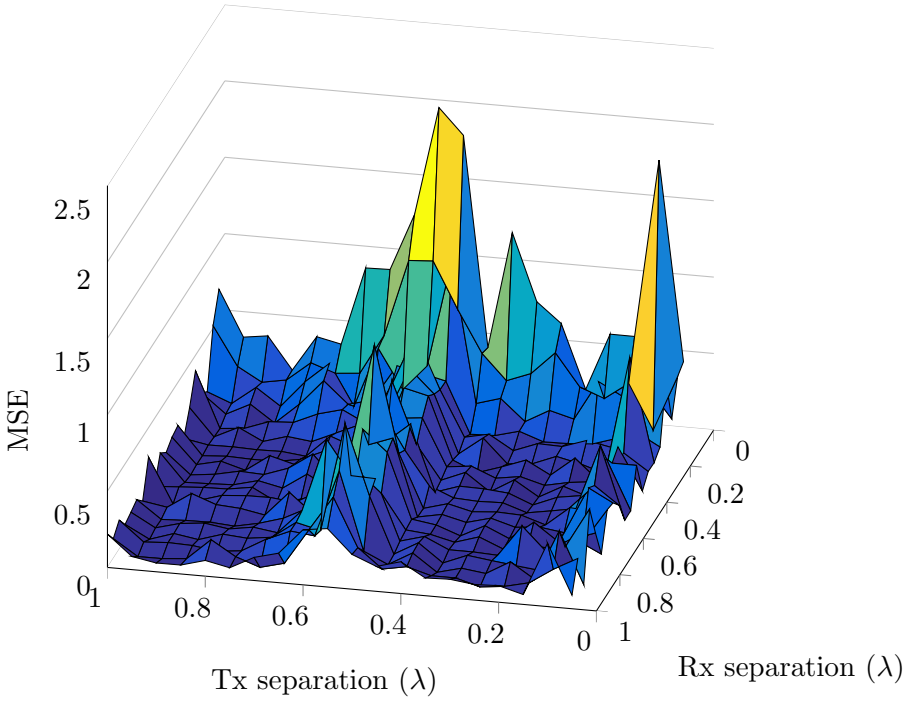

Figure 4.9: Effect of transmitter and receiver array element separation on estimate of channel rank $\hat{\mathbf{M}}$ (1000 iterations, 5×5 channel, $SNR = 30\text{dB}, B = 32, L = 31$)

dimensions as Figures 4.5 and 4.6.

It is observed that Gold sequences often provide *better* results than a chaotic sequence of the same length. This can be attributed to the predictable correlation properties of the Gold sequences, which will outperform chaotic sequences of the same length regardless of starting value. Chaotic sequences offer one advantage over Gold sequence in that they can be of any length, but this offers little when the performance of the equivalent Gold sequence is better.

These results further cement the channel rank estimator as a useful contribution to channel estimation, offering the ability to perform channel estimation with no prior channel knowledge required – other than the knowledge that the transmitter is employing Gold sequences for channel training.

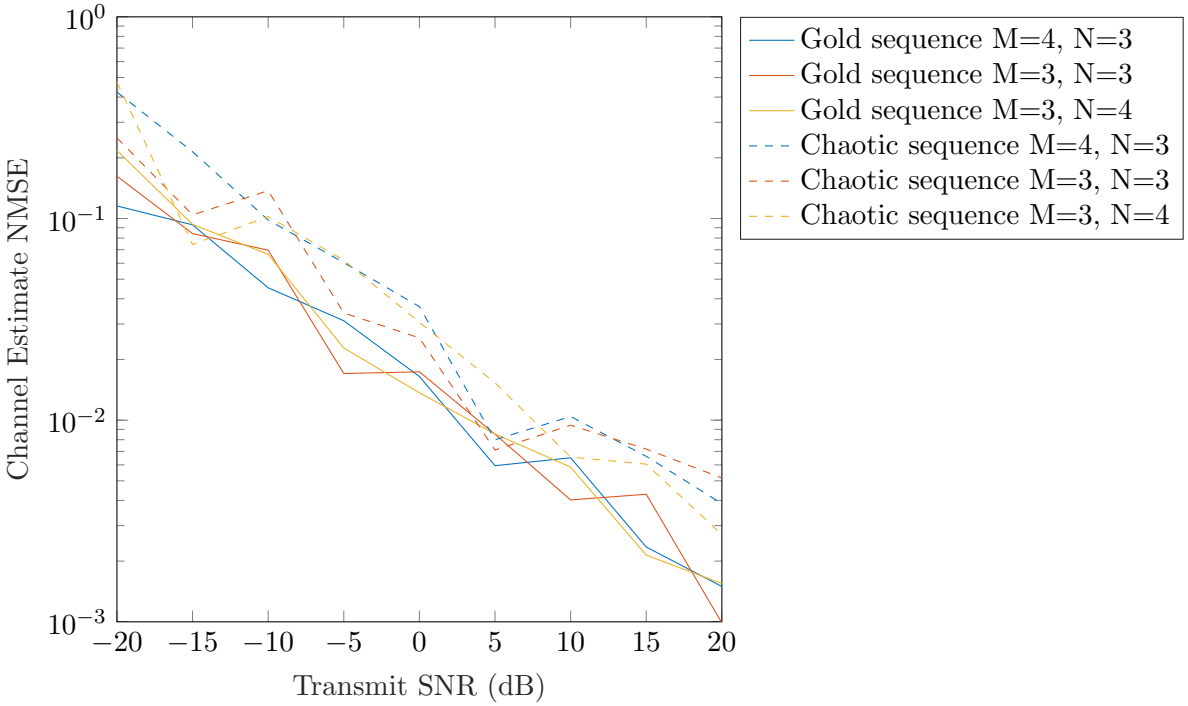

Figure 4.10: Comparison of channel estimation performance (B = 1, L = 63, $\Delta_r = \Delta_t = 0.4\lambda$)

4.6 Conclusions

In this chapter we have proposed an channel training sequence based on Gold sequences that is capable of estimating both the rank and coefficients of a MIMO channel with Kronecker structure. We find that the sequence offers a receiver with no knowledge of the transmitter's configuration to detect the number of transmit antennas a transmitter possesses, and then use that information to generate the training sequence that can then be used to perform channel estimation.

We observe that approximately equal performance can be achieved from combinations of blocks of repeated sequences with the same overall total training sequence length, and there is a clear relationship between sequence length, transmit power and estimator performance. This offers the system designer the ability to optimise the performance of the system against the time and power constraints imposed by the application.

Furthermore we observe that rank estimation is possible on all dimensionalities of MIMO

channel, including rank-deficient channels (i.e. fewer receive antennas than transmit antennas) with no penalty. The number of streams used to perform rank estimation can be arbitrarily selected to ensure adequate performance. This permits the rank estimation algorithm to be implemented in heterogeneous networks where users may be equipped with antenna arrays of different sizes. Where transmitters operate at low power levels or where attenuation in the channel is such that the received power is less than the noise encountered, better rank estimation is achieved by using a large number of receive antennas. Conversely, where transmitters operate at high powers the rank estimation error is minimised by using fewer receiver streams to perform estimation.

We find that for all channel dimensions and all power levels there exists a combination of sequence length and number of receive streams that enables robust rank estimation (probability of error $< 1\%$). This in turn leads to confidence in using this information to inform the channel estimation algorithm. The only limitation of the algorithm is that the transmit power per stream must be uniform and not scaled to fit a combined power limit. This has the effect that the transmit power scales with the number of antennas a user possesses, which may limit the applicability of the technique or force the power level to adhere to a certain assumed limit of number of antennas. In a planned network this is of little consequence and would simply become part of the implementation of the algorithm, but in an heterogeneous unplanned network may pose a challenge if the range of devices in the network is not adequately controlled.

We also confirm that Gold sequences work as well as chaotic sequences as channel estimation training sequences. Both types of sequences can be constructed at the receiver from a small initial data set, making them suited for use in low-power devices where storage is limited compared to more complex training sequences that would potentially be required to be stored in their entirety in device storage.

This offers the system designer a powerful tool in the implementation of unplanned networks; blind channel estimation is now possible between devices of differing antenna numbers with no *a priori* knowledge of the channel conditions or configuration of other devices.

5 Effect of Array Directivity of Neighbour Discovery in Unplanned Networks

5.1 Motivation

The process of neighbour discovery is a key aspect of network initialisation. In the absence of any centralised network architecture, nodes must communicate amongst themselves in order to pass data across the network. Depending on the application, nodes may simply communicate between each other or may establish a forwarding table towards a 'data sink' that possesses additional capabilities such an internet gateway. Data can then be collected at the gateway and forwarded elsewhere. These 'relay networks' are common amongst Wireless Sensor Networks (WSNs) [55] and other rapidly-deployed networks. In such networks the system operator relies on the node density being sufficiently high to provide a connected mesh of users.

A node's neighbours are not only relevant to the forwarding of information through the network, but also for the purposes of interference avoidance. The act of creating a network of known users and using interference management techniques to manage access to the network between them is a complex one, in what is now termed Topological Interference Management (TIM) [56, 57]. In order for TIM to be achievable, the users need to know more than just the presence of interference but be able to identify the user with which that interference is associated. This enables complex management schemes in which users can coordinate between themselves simultaneous use of the network without causing unrecoverable interference to each other. As such, users must not simply detect the presence of a signal but identify the source (through a unique ID, for instance). This necessitates that a coding scheme and a definition of 'success' that includes successful decoding of a signal from each interferer. This is achieved in this chapter by defining a successful detection as the receiver being able to detect and decode all k users for a given SIR.

The act of detecting neighbours is often posed as purely a MAC layer problem, where the

effect of a collision within the discovery slot is treated as total failure and the opportunity to detect a neighbour is lost. In the literature such interference is avoided by various schemes; for example embracing asynchronism between the distributed nodes [58], performing neighbour detection across multiple frequency bands [59] or by an incremental method where only a subset of nodes in the network are involved in the discovery process [60]. These are in contrast to the authors of [61] who embrace collisions, using the number of neighbours detected to estimate the number of nodes within the network. This allows the node to determine when it has detected a significant proportion of all its neighbours and can progress to the next stage of network initialisation. The time taken for neighbour discovery is the key measure of a protocol; spending excessive time discovering nodes leaves less time for the transmission of payloads, and a slow protocol is left open to the risk of node mobility invalidating the results before the process is even completed. A comprehensive albeit slightly dated review of the field is presented in [62].

In this chapter we examine the effect of antenna directivity on the neighbour discovery process, in order to determine the system parameters that govern the speed and quality of neighbour information collected. We determine the number of neighbours a receiver may be capable of detecting and in which network conditions knowledge of how the node will behave can influence how long neighbour discovery will take. The effects of these parameters are confirmed using the results of simulated neighbour discovery. This will allow system designers to achieve their system goals by optimising network parameters for their intended use case, taking into account conditions such as expected node density, path loss exponent, and node mobility.

5.1.1 Directional transmission in wireless sensor networks

Of particular interest is the challenge of neighbour discovery (and interference management in general) in networks with antenna directivity. The potential for interference from nearby nodes is reduced due to the narrower interference footprint in the azimuth around a transmitting node. Conversely, the addition of gain to the antenna due to directivity now means interference 'travels' further, increasing the potential for a transmitter to cause interference to a distant receiver. Antenna directivity has been proven to improve connectivity between nodes [63, 64, 65]

in mobile networks, and is seen as a key enabler in millimetre wave (mmWave) networks due to the hostility of the radio environment to mmWave transmissions [66]. Directional antennas have been shown to improve coverage in such networks as well [67]. In networks where the hosts are already equipped with MIMO arrays it is reasonable to expect they can also be used for the purposes of beamforming The analysis include in this section is equally valid for more conventional sectored antenna arrangements too, providing that selection of the direction of transmission has the same randomness properties as random main lobe steering.

5.2 Prediction of neighbour detection success

In this section we derive an analytical expression for the upper bound of the probability of a receiver detecting k of its neighbours using an omnidirectional receive pattern while the transmitters employ a Dolph-Chebyshev array pattern randomly distributed around the azimuth. This expression highlights the effect of several network parameters and their influence on the success probability is then assessed.

Each transmitter is equipped with a uniform circular array (UCA), with antenna coefficients calculated using the Dolph-Chebyshev method [68] further transformed to be applicable to the UCA by the authors of [69]. This approach has been chosen since the use of a circular array permits much simpler steering of the main lobe of the array pattern around the azimuth than convention linear arrays. Without utilising pattern-matching approaches (where an iterative algorithm is used to alter antenna weight coefficients in order to meet the desired arbitrary antenna pattern) linear arrays suffer a degree of main lobe widening as the direction of the beam is steered. It is also not possible to steer across the entirety of the azimuth plane using a linear array[70]. In contrast, once the transformation of the coefficients of the linear array to the circular has been performed, steering is simply a matter of applying a phase difference to the coefficients.

5.2.1 Modelling antenna array directivity

The Dolph-Chebyshev antenna pattern has a single parameter, controlling the level of gain suppression in the sidelobes compared to the centre of the main lobe. This can be arbitrary, with no limit on the level of sidelobe suppression imposed by the physical properties of the antenna array. The physical properties of the array determine the number (and therefore beamwidth) of the side lobes, but not their peak gain.

This is ably modelled by the typical 'flat top' or 'cone and ball' antenna pattern model commonly used in estimations of network coverage in wireless networks. In the cone and ball model shown in Figure 5.1 the main lobe is modelled as a flat gain across the azimuth angle $\Theta_{bw} \in [-\theta_{bw}, \theta_{bw}]$, while the side lobes are modelled as a flat gain across the rest of the antenna pattern.

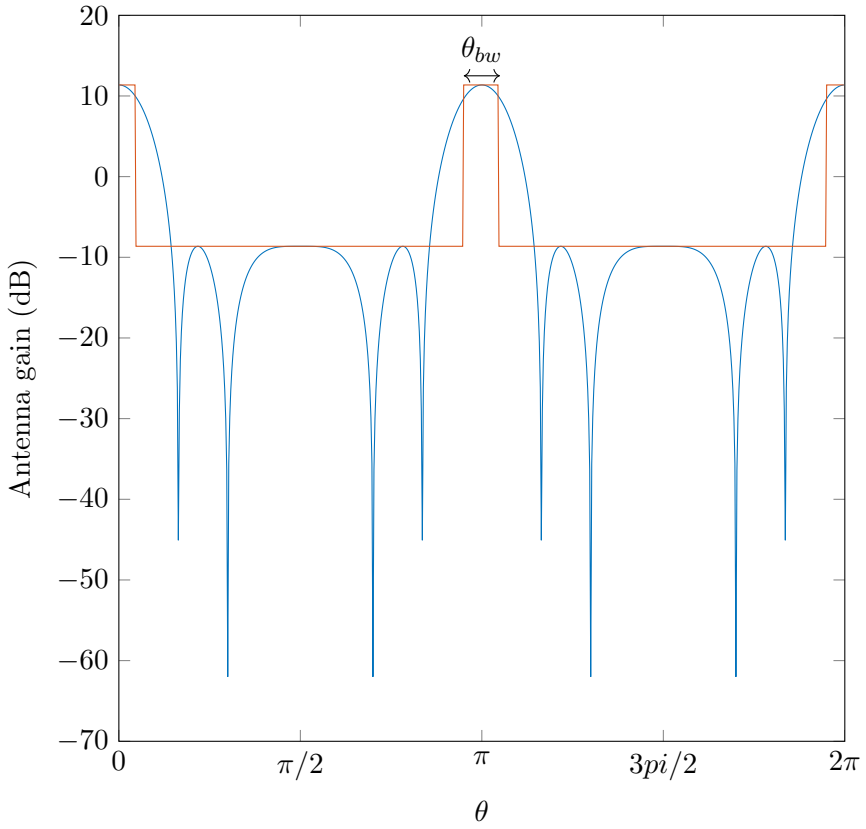

Figure 5.1: Azimuth antenna pattern calculated using the Dolph-Chebyshev technique (blue) and its 'cone and ball' approximate model(red)

The width of the 'cone' is determined by the half-power beamwidth (HPBW) of the array, which is known to be subjected to a broadening factor when the array factor is increased [71]. The cone width is given by the expression

$$\theta_{bw}(R) = 1 + \frac{0.56}{Nd}\left[\frac{2}{R}\cosh\sqrt{(\cosh^{-1}R)^2 - \pi^2}\right]^2 \tag{5.1}$$

where N is the number of array elements and d is the inter-element spacing given in fractions of the wavelength. $R = 10^{R_{dB}/20}$ is the linear side lobe suppression factor.

The Dolph-Chebyshev antenna array exhibits two main lobes, directed at 0 and π radians from the array's broadside. In the circular array form, the direction of these main lobes can be can be selected arbitrarily by phasing. The fraction of the azimuth plane illuminated by the main lobe is defined as $\frac{|\Theta_{bw}|}{2\pi}$ where

$$\Theta_{bw} = [-\theta_{bw}/2, \theta_{bw}/2] \bigsqcup [\pi - \theta_{bw}/2, \pi + \theta_{bw}] \tag{5.2}$$

5.2.2 Modelling of the wireless network with a Poisson Point Process

Stochastic Geometry is a field that has attracted significant interest for the purposes of modelling wireless networks in the past few years. It is a powerful tool that allows the positions of users in the network to be modelled using stochastic processes with well-understood statistical properties. Operations that preserve the 'Poisson-ness' of the network [36] allow for other features such as fading, antenna gain and interference to be modelled in a tractable way, often leading to closed-form expressions for the key parameters of the network. These include the distances between users, the distribution of signal powers and interference within the network, and ultimately the success likelihood of transmissions in a variety of interference scenarios.

We model the location and behaviour of nodes in the network with a marked Power Law Poisson Network with Fading Φ in $\mathbb{R}^d \times \mathbb{R}^+ \times [0, 2\pi)$, which was introduced in Haenggi's framework

[36]:

$$\Phi = \{(X_i, h_i, \theta_i), i \in \mathbb{N}\} \tag{5.3}$$

The intensity function of the ground process modelling the node locations in 2D-space (i.e. $d = 2$) is $\lambda(x) = a\|x\|^b$. a is a simple scaling coefficient while $b \in (-d, \alpha - d)$, where α is the path loss exponent, ensures that the interference received at the receiver is finite. Through Slivnyak's theorem a receiving node can be added at the origin of $\mathbb{R}^d$ without affecting the 'Poisson-ness' of Φ.

Each node determines whether it will transmit in this slot independently of all other nodes, therefore allowing the entire network of transmitters to be modelled as a thinned PPP with intensity $p\lambda(x)$, with the likelihood that a transmitter transmits in the slot $p \in [0, 1]$. This is one of the key transmission criteria that must be set by the system designer prior to deployment. Each transmitting node randomly selects a beamforming direction around the azimuth to transmit towards during this slot. The beamforming direction is thus modelled by a mark uniformly distributed in the interval $[0, 2\pi)$ Fading within the network is modelled by an iid fading mark $h_i \in \mathbb{R}^+$.

Φ can be split into two disjoint complementary point processes Φ_a and Φ_u, representing the aligned nodes and unaligned nodes respectively:

$$\Phi_a = \{(X_i, h_i, \theta_i) \in \Phi : \theta_i \in \Theta_{bw}\}$$
$$\Phi_u = \{(Y_i, h_i, \theta_i) \in \Phi : \theta_i \notin \Theta_{bw}\}$$

Alignment is determined by the mark attached to each transmitting node which represents its alignment in the azimuth plane, and is defined as when the angle between the centre of the font beam of the array and the receiver being within the main beam of the simplified antenna array model described in section 5.2.1, and represented by the mark θ_i being within the set Θ_{bw}.

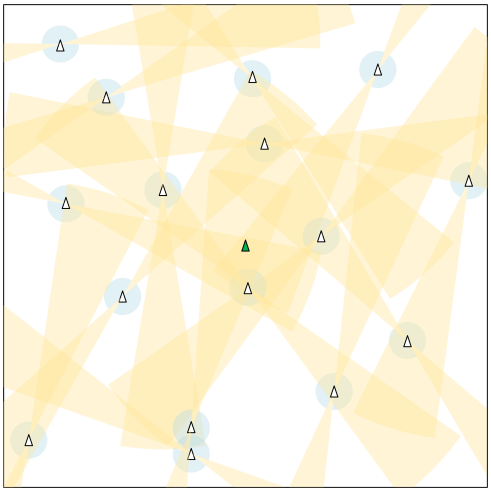

(a) Original PPP Φ

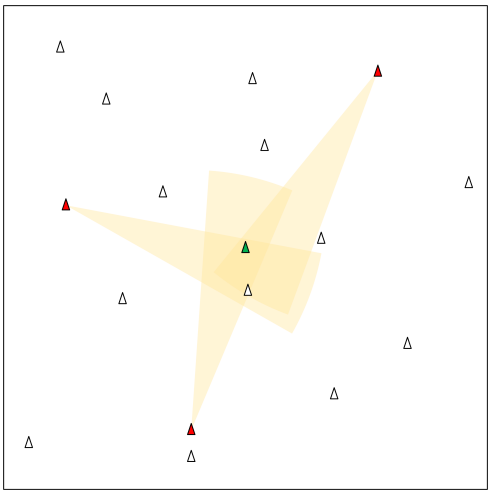

(b) PPP of aligned users Φ_a

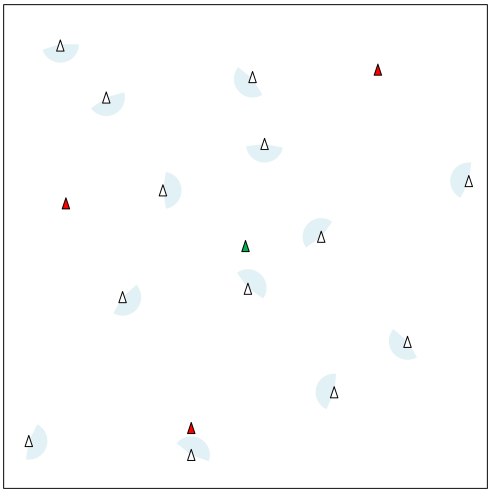

(c) PPP of unaligned users Φ_u

Figure 5.2: Poisson Point Process of intensity $p\lambda$ representing the locations of nodes in the network transmitting during a neighbour discovery slot and their array alignments. The receiver is at the origin of the PPP. PPPs Φ_a and Φ_u are thinned sub-processes representing the aligned users and unaligned users respectively

Due to the random and independent alignment of antenna arrays of the receivers, splitting the original process into two processes yields two heterogeneous PPPs with intensities related to the likelihood of a node's main lobes being aligned with the path between transmitter and receiver. The two processes therefore have the intensities $\lambda_a = p\lambda(x)\frac{|\Theta_{bw}|}{2\pi}$, $\lambda_u = p\lambda(x)\frac{2\pi-|\Theta_{bw}|}{2\pi}$.

Transmissions are subjected to path loss as they travel from the transmitting nodes to the receivers. Later we will select a value for α to aid tractability of the analytical equation.

$$\mathcal{L}(x,h) = \frac{\|x\|^\alpha}{h} \tag{5.4}$$

The two PPPs undergo a mapping from $\mathbb{R}^d \times \mathbb{R}^+ \times [0, 2\pi)$ to $\mathbb{R}^+$ using this function to represent the path loss, with the index i now imparting an ordering on the nodes within the new point processes Φ'_a and Φ'_u. In [36] this is referred to as a *Path Loss Process with Fading*.

$$\Phi'_a = \{\phi_i = G_t\mathcal{L}(x_i), \phi_i > \phi_j \qquad \forall i < j\} \tag{5.5}$$

$$\Phi'_u = \{\psi_i = \mathcal{L}(y_i), \psi_i > \psi_j \qquad \forall i < j\} \tag{5.6}$$

This yields two inhomogeneous PPPs with intensity measures

$$\Lambda'_a([0,r]) = pf(\Theta_{bw})\frac{ar^\beta \delta c_d \mathbb{E}(h^\beta)}{\beta} \tag{5.7}$$

$$\Lambda'_u([0,r]) = pf'(\Theta_{bw})\frac{ar^\beta \delta c_d \mathbb{E}(h^\beta)}{\beta} \tag{5.8}$$

where $f(\Theta_{bw}) = \frac{|\Theta_{bw}|}{2\pi}$ and $f'(\Theta_{bw}) = \frac{2\pi-|\Theta_{bw}|}{2\pi}$. The parameter $\beta = \frac{d-b}{\alpha}$ determines the behaviour of interference experienced by the receiving node.

These two point processes model the path loss experienced by transmissions from each trans-

mitting node during the time slot. Given uniform transmit power across the network the inverse of these point processes also describe the signal power experienced by the receiver. In both cases 'Poisson-ness' has been maintained, allowing the tools of Stochastic Geometry to be used to estimate the number and distribution of the points within. As models of signal powers they can be used to make predictions about the behaviour of nodes within the network.

5.3 Criteria for successful neighbour detection

Successive Interference Cancellation (SIC) is a powerful tool for dealing with interference; as a purely receiver-side process nodes are able to decode multiple users without cooperation from the transmitter. This is the case regardless of if the transmitter is a desired partner (for instance a potential neighbour in the network) or is to be treated as interference. Being able to decode multiple neighbours within the same transmission period has many benefits; the time spent discovering all adjacent neighbours can be shortened, and the proportion of slots lost to unrecoverable collisions is reduced. Both contribute to better energy efficiency for the nodes in the network, who are able to spend overall less time in the discovery phase (increasing payload throughput) and waste less energy on failed discovery attempts (requiring fewer discovery attempts to find the same number of neighbours). This is crucial for many rapidly-deployed networks which are often based on low-power nodes with limited energy storage and harvesting capabilities.

In this section we will determine bounds on the likelihood that k users can be successively decoded by the receiver, allowing them to be added to the receiver's list of neighbours for the purposes of routing, interference avoidance, or any other purpose.

The receiver is able to decode k neighbours when it is possible to use SIC to decode and cancel out interference from the $k-1$ most significant interferers, and it is possible to decode the k^{th} transmitter against the sum interference experienced by that transmitter. This interference is composed of the combined interference from all the unaligned users.

Consider the PPPs described in (5.5) and (5.6), which described the aligned and unaligned nodes respectively. In this network the probability of the receiver discovering k neighbours can be expressed as

$$p_k > \mathbb{P}(\bigcap_{i=1}^{k-1} A_i)\mathbb{P}(B_k) \tag{5.9}$$

where A_i and B_k are the events

$$A_i = \{\phi_i^{-1} > (1+\kappa)\phi_{i+1}^{-1}\} \tag{5.10}$$

$$B_k = \{\phi_k^{-1} > \kappa I_k\} \tag{5.11}$$

where κ is the SINR threshold required for successful decoding and I_k the interference observed by node k. A_i represents the event that the transmission from aligned node i is decodable and can therefore be removed from the aggregate signal, allowing the receiver to proceed to the transmission from aligned node $i+1$, and B_k represents the event that the aligned node k can be decoded against the interference it experiences.

5.3.1 Detection of k directional users using SIC

We first examine the simpler element of (5.9), the success likelihood of successively decoding k aligned users, expressed as the event A_i in (5.10). The probability that all $k-1$ users are separable using SIC $\mathbb{P}(\bigcap_{i=1}^{k-1} A_i)$ follows from the analysis of SIC's performance in networks with omnidirectional users by Zhang [72].

The aligned users that make up Φ_a all exhibit the same level of array gain in their transmissions towards the receiver. As such, the actual level of gain becomes irrelevant to the success likelihood of SIC since we are interested in the ratio between the signal powers of successive users. This is more rigorously proven in [72, Proposition 1] and termed 'scale invariance'. It

thus follows that the ratio between the aligned users' signal powers in Φ'_a is uniformly distributed and the success probability bounds for SIC between the signals from aligned transmitters is the same as [72].

$$\begin{aligned}\mathbb{P}(\bigcap_{i=1}^{k-1} A_i) &\geq \mathbb{P}\left(\frac{\phi_i}{\phi_{i+1}} > (1+\kappa) \qquad \forall i < k | \phi_k\right) \\ &= \prod_{i=1}^{k-1} \mathbb{P}(X^{i\beta} < (1+\kappa)^{-i\beta}) \\ &= (1+\kappa)^{-\frac{-\beta}{2}k(k-1)} \end{aligned} \tag{5.12}$$

Similarly the upper bound is found the same way

$$\mathbb{P}(\bigcap_{i=1}^{k-1} A_i) \leq \kappa^{-\frac{\beta k(k-1)}{2}} \tag{5.13}$$

5.3.2 Detection of the weakest aligned user

The event B_k (5.11) is the event that the k^{th} aligned user is decodable in the presence of the interference it experiences, which is by construction the sum interference from the unaligned users.

$$\text{SIR}_k = \frac{S_k}{I_k} = \frac{G_T \phi_k^{-1}}{\sum_{\psi \in \Phi'_u} \psi^{-1}} \tag{5.14}$$

The signal power from aligned user k is modelled by the PPP Φ'_a, where each point is the path loss experienced from the corresponding transmitter in Φ_a to the receiver. In order to find the distribution of the power received from any of these nodes it is sufficient to look at the positioning (i.e. path loss, and by extension the signal strength) of the k^{th} node in Φ'_a and compare it to the sum of the interference, itself a sum over the path loss process Φ'_u.

By construction the interference experienced by aligned user k is the sum interference from the PPP Φ_u, i.e.

$$I_k = \sum_{\psi \in \Phi'_u} \psi^{-1} \tag{5.15}$$

Using Campbell's theorem for sums we can calculate the mean interference from Φ'_u, initially conditioned on an arbitrary value for the path loss of the first unaligned user, then de-conditioned to give the true mean.

$$\begin{aligned}
\mathbb{E}[I_k|\psi_1 = \rho] &= \int_{\rho}^{\infty} x^{-1} \lambda'_u(x) dx \\
&= \int_{\rho}^{\infty} x^{-1} p f'(\Theta) a \delta c_d \mathbb{E}[h^{\beta}] x^{\beta-1} dx \\
&= p f'(\Theta) a \delta c_d \mathbb{E}[h^{\beta}] \int_{\rho}^{\infty} x^{\beta-2} dx \\
&= -\beta \Delta_u \frac{\rho^{\beta-1}}{\beta - 1}
\end{aligned} \tag{5.16}$$

By virtue of being based on two independent PPPs the two random variables are independent, so the derivation of $\mathbb{P}(S_k/I_k \geq \kappa)$ is straightforward.

$$\begin{aligned}
\mathbb{E}[I_k] &= \int_{-\infty}^{\infty} \mathbb{E}[I_k|\psi_1 = \rho] f_{\psi_1}(\rho) \\
&= \int_{0}^{\infty} -\beta \Delta_u \frac{\rho^{\beta-1}}{\beta - 1} \exp(-\Delta_u \rho) \Delta_u d\rho \\
&= -\beta \frac{\Delta_u^{2-\beta}}{\beta - 1} \Gamma(\beta)
\end{aligned} \tag{5.17}$$

where $\Delta_a = p f(\Theta) a \delta c_d \mathbb{E}[h^{\beta}]/\beta$ and $\Delta_u = p f'(\Theta) a \delta c_d \mathbb{E}[h^{\beta}]/\beta$

Applying the Markov inequality we achieve a upper bound for the likelihood of success:

$$\begin{aligned}
\mathbb{P}(G_T\phi_k^{-1} \geq \kappa I_k) &= 1 - \mathbb{P}(I_k > G_T\kappa\phi_k^{-1}) \\
&\leq 1 - \frac{\mathbb{E}[I_k|\phi_k = x]}{G_T\kappa x} \\
&= 1 - \frac{\mathbb{E}[I_k]}{G_T\kappa}\int_{-\infty}^{\infty} \exp(-\Delta_a x)\frac{(\Delta_a x)^k}{x\Gamma(k)}dx \\
&= 1 - \frac{\beta\Delta_u^{2-\beta}\Delta_a\Gamma(k-1)\Gamma(\beta)}{G_T\kappa\Gamma(k)\Gamma(\beta-1)} \\
&= 1 - \frac{p^2 f(\Theta)f'(\Theta)}{G_T\kappa}\frac{(a\delta c_d\mathbb{E}[h^\beta])^2\Gamma(k-1)\Gamma(\beta)}{\beta(\beta-1)\Gamma(k)}
\end{aligned} \tag{5.18}$$

Combining with (5.13) provides the main analytical result of this chapter:

$$p_k \leq \kappa^{-\frac{-\beta k(k-1)}{2}}\left(1 - \frac{p^2 f(\Theta)f'(\Theta)}{G_T\kappa}\frac{(a\delta c_d\mathbb{E}[h^\beta])^2\Gamma(\beta)}{\beta(\beta-1)(k-1)}\right) \tag{5.19}$$

5.4 Effect of network parameters on success probability

In this section we examine the influence of the network parameters on the upper bound presented in (5.19). It is clear from the expression that there are four parameters that can influence the likelihood of discovering neighbours; these are

- The physical density of the nodes in the network, which is reflected in a and b (and also, by extension, δ and β),
- The probability of each transmitter transmitting within the slot, represented by the transmission probability p,
- The level of sidelobe suppression applied to the antenna array pattern, reflected in G_T, $f(\Theta)$, and $f'(\Theta)$,
- and the SIR threshold of the MCS in use during the neighbour discovery process, reflected in κ

While the user density parameter of the network is determined by the physical deployment of users within the network, the designer is able to manipulate the performance of the neighbour discovery process through any one of the remaining three parameters independently of the others, offering a three-dimensional solution space in which to optimise the system for its expected operation.

In the following section we discuss the effects of each parameter on the upper bound of the success probability. We then investigate how closely these bounds reflect the actual behaviour of the network in simulations.

User density

The degree to which user density increases or decreases with distance from the receiving user is modelled by the parameter b, which influences the success probability through the parameter $\beta = \frac{d-b}{\alpha} = \delta + \frac{b}{\alpha}$.

Figure 5.3 shows the user density functions as a function of distance from the receiver for various values of b.

Various types of network can be modelled using the b parameter:

- Values of $b < 0$ represent networks with closely packed transmitters near the receiver. Such networks include 'Personal Area Networks' (PANs) where the network's range is effectively the personal space of one or a small number of humans. Devices much further than 2 m from the receiver are likely interferers from adjacent PANs. Networks in this category will expect medium to high data rates, typically used to transfer data such as high-definition audio or video between personal devices.
- A value of $b = 0$ represents a uniformly dense (i.e. homogeneous) network of intensity $\lambda = a$.
- A value of $b > 0$ represents networks with sparsely distributed transmitters near the receiver. Such networks exhibit low densities close to the receiver, with exponentially

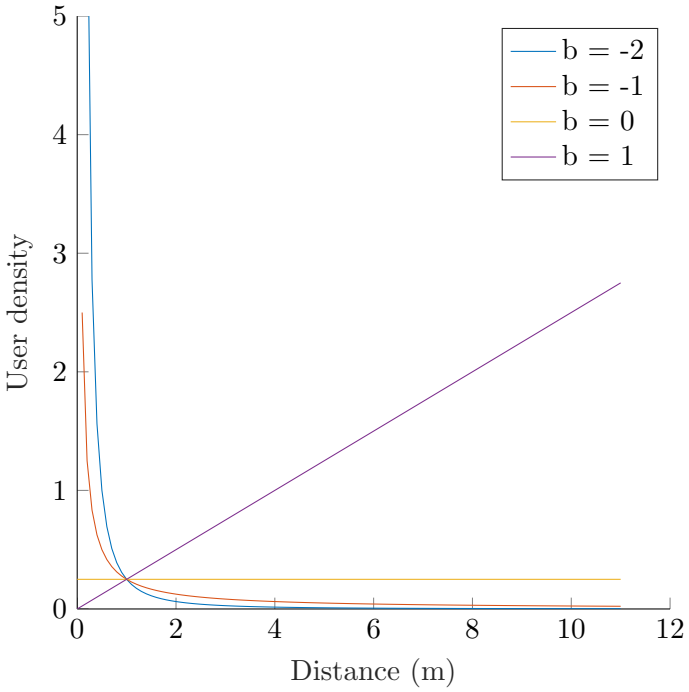

Figure 5.3: User density function $\lambda(x) = a\|x\|^b$ for various values of b, $a = 0.25$

growing densities as the distance from the user increases. Examples of these networks would be WSNs or 'scatternets' where the devices within the network are spread over a large area to enable wide coverage, with typically low data rates for sensor or diagnostic data.

As a consequence of the network's deployment as opposed to a configurable system parameter, we shall not investigate the effect of manipulating the scale factor in order to 'tune' system performance. It does however have a significant effect on the other parameters' ability to influence success likelihood. Figures 5.4 and 5.5 show the effect of the scaling factor b on the upper bound of $p_k, k = 2$. It is clear from these plots that the scaling factor has a profound effect on the ability of other parameters to achieve the full range of $p_k = [0, 1]$, with the likelihood of success increasing with network density.

In sparse networks the likelihood of detecting $k = 2$ users successfully is low. The ALOHA transmission probability and sidelobe suppression level are observed to have little effect - the likelihood of success is much more heavily dependent on the scale factor. In Figure 5.4a the

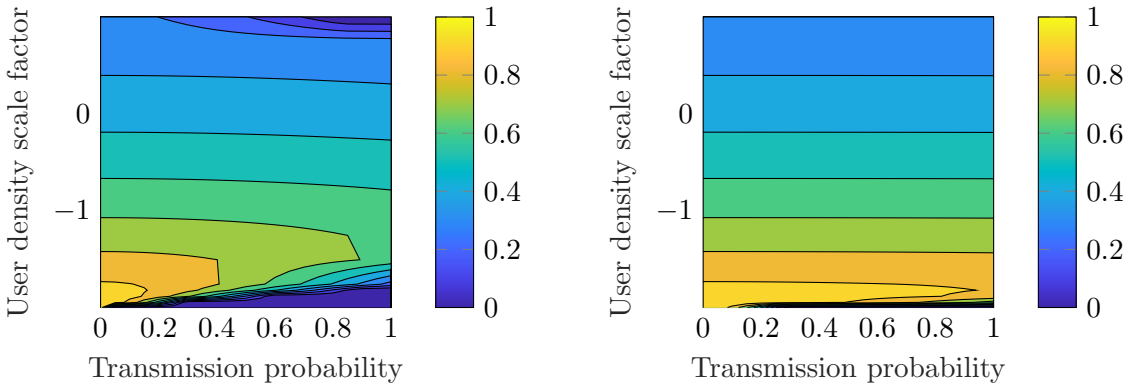

(a) $\kappa = 5\text{dB}, G_T = 5\text{dB}$ **(b)** $\kappa = 5\text{dB}, G_T = 35\text{dB}$

Figure 5.4: Effect of user density scale factor on $p_{k=2}$ in a simple MCS for different levels of sidelobe suppression

influence of transmission probability across the entire range [0,1] is only 8.6% when $b = 0.99$, i.e. in a homogeneous network. Similarly in Figure 5.6b the influence of sidelobe attenuation between 0 dB and 40 dB is minimal (an improvement in only 1.8%) when $b = 0.99$.

Conversely, in dense networks the likelihood of success is much greater. Additionally it becomes possible for parameters such as transmission probability and sidelobe suppression to influence the success likelihood. In sufficiently dense networks it is therefore possible that adjusting system parameters allows the designer to arbitrarily choose a desired success likelihood as hypothesised.

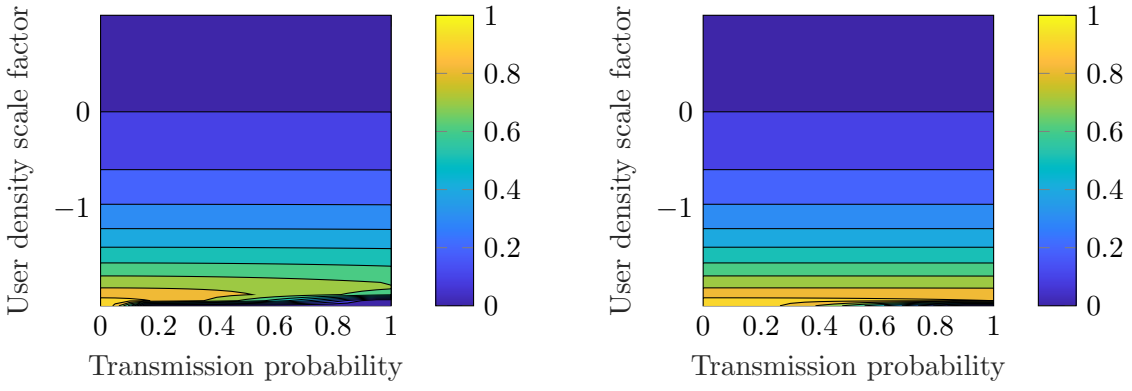

(a) $\kappa = 15\text{dB}, G_T = 5\text{dB}$ **(b)** $\kappa = 15\text{dB}, G_T = 35\text{dB}$

Figure 5.5: Effect of user density scale factor on $p_{k=2}$ in a complex MCS for different levels of sidelobe suppression

Both the scale factor and SIR threshold parameters dominate the success probability equation through their influence on both the A_i and B_k components of p_k. This is seen in Figure 5.5, where the impact of a more elaborate MCS (and thus requiring a higher SIR to achieve detection success) reduces the influence of the transmission probability at a given network density.

In very dense networks (i.e. where b approaches d) a reduction in success likelihood is observed, suggesting an 'optimal' user density that itself is a product of several network parameters. This is indicated by the differences between the area of low success brought about by altering the SIR threshold and sidelobe suppression level seen between the previous two figures.

SIR threshold

The SIR threshold is a secondary parameter determined by the MCS employed during the neighbour discovery phase of network operation. The tolerable Bit Error Rate (BER) of the MCS determines the level of SIR required before decoding can be considered successful in the analysis of A_i and B_k.

By selecting a simple MCS for the neighbour detection process (which may or may not be the same as that used for the rest of communication with neighbours once the network is set up) intuition suggests that the designer should be afforded the opportunity to tune the behaviour of the network to achieve the level of success required for smooth network operation.

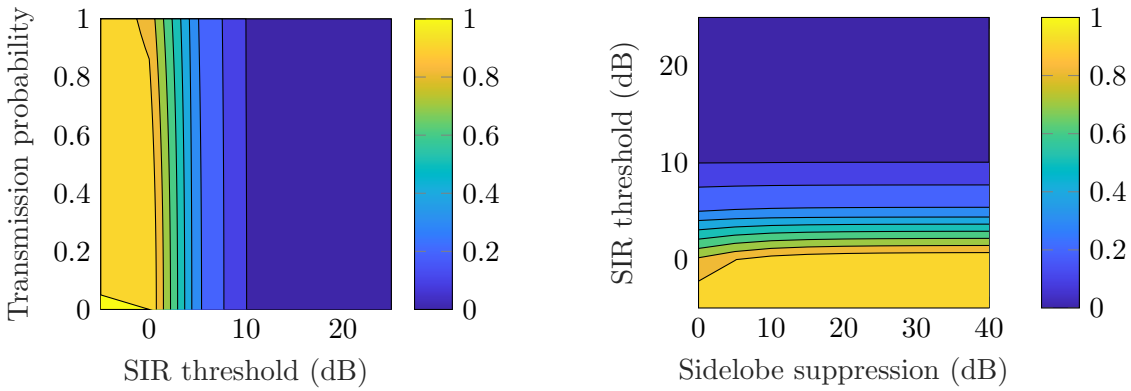

(a) $b = 0.99, G_T = 35\text{dB}$ **(b)** $b = 0.99, p = 0.2$

Figure 5.6: Effect of SIR threshold on $p_{k=2}$ for sparse networks

The influence of the SIR threshold on the upper bound of p_k is observed to be markedly different for different densities of network. In sparse networks it is observed in Figure 5.6 that the SIR threshold dominates the result, and it is unlikely that any significant tuning is possible through either the transmission probability (Figure 5.6a) or the sidelobe suppression level (5.6b). The only avenue open to the system designer is to pick a suitable MCS for the desired success likelihood. In these sparse networks adjusting the SIR threshold matches our intuition, in that increasing the SIR threshold necessary for success reduces the success likelihood.

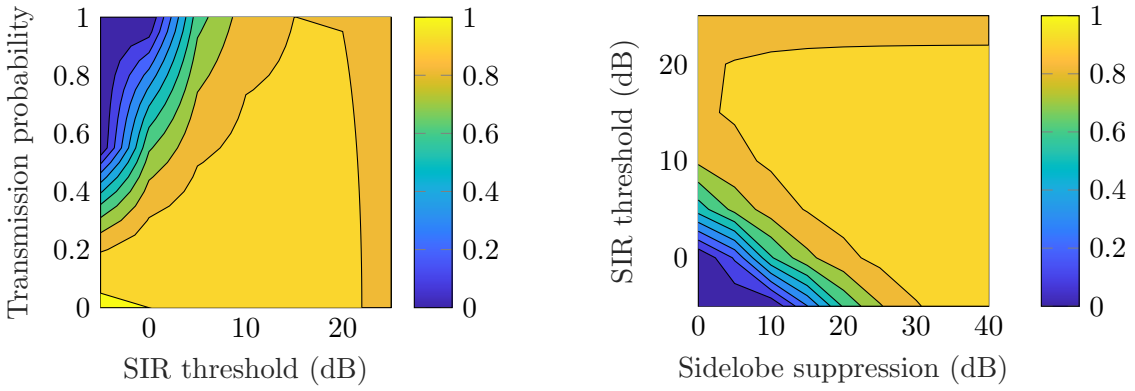

(a) $b = -1.9375, G_T = 35\text{dB}$ **(b)** $b = -1.9375, p = 0.2$

Figure 5.7: Effect of SIR threshold on $p_{k=2}$ for dense networks

Dense networks exhibit a different behaviour, where the choice of SIR threshold opens the possiblity of performance tuning to the system designer. As observed in Figure 5.7, there is now the potential to trade SIR complexity against the transmission probability (Figure 5.6a) or the sidelobe suppression level (5.6b). More complex schemes appear to be rewarded with a greater likelihood of success. This does not meet with our intuition that increasing the SIR threshold makes the chances of success lower howere, and the increase in success can be attributed to the loosening of the upper bound according to [72, Proposition 11].

Transmission probability

The transmission probability is a key parameter in system design by virtue of it being fully within the designer's control. Increased participation in the neighbour discovery protocol by transmitters increases the density of the PPPs describing the users, thus increasing the chance

of collision that cannot be recovered through SIC.

As observed previously in Figures 5.4 and 5.5, the transmission probability only influences the success likelihood significantly in dense networks. The *range* of network densities over which the transmission probability can influence the success likelihood is however determined by the SIR threshold of the MCS employed. This is observed in comparison between 5.4a and 5.5a, where the simpler MCS (with SIR threshold 5 dB) permits the transmission probability to influence success likelihood over the range of networks $b = [-2, -1]$, while the more complex MCS (with SIR threshold 15 dB) only exhibits a significant variation in likelihood over the range of networks $b = [-2, -1.75]$.

Furthermore, the *degree* to which the success likelihood can be influence by the transmission probability is determined by the directivity of the transmitter arrays. This is demonstrated by the comparison of 5.4a and 5.4b, where it is observed that the values over which a result of $p_{k=2} > 0.9$ is achievable is much larger in Figure 5.4b, indicating that increased directivity in dense networks yields more successful neighbour detection.

As expected, in networks where conditions are conducive to the transmission probability affecting success likelihood it is demonstrated that increasing the transmission probability has a negative effect on the likelihood of success. The system designer must then trade the speed at which neighbour discovery operates against the risk of a lost neighbour detection slot.

Sidelobe suppression

The level of sidelobe suppression is another key parameter that is within the system designer's control. This parameter affects neighbour discovery in two respects. Firstly, by increasing the power differential between aligned and unaligned users, the likelihood of decoding user k against the sum interference from the unaligned users should be improved. Secondly, but conversely, using the Dolph-Chebyshev approach increasing the level of sidelobe suppression employed will have a spreading effect on the mainlobe, increasing the proportion of aligned to unaligned users, negatively impacting the selectivity of the directional antenna array pattern employed.

Like the transmission probability, the impact that sidelobe suppression can have on the success likelihood is determined by other network parameters. The network density is a significant influence as demonstrated by the difference in behaviour exhibited between Figures 5.6b and 5.7b, where as before the sparse network observes little to no effect from variations in the directivity of transmitters. Conversely, in dense networks the sidelobe suppression is observed to have significant effect for simple coding schemes.

It is observed that increasing the transmitter directivity (and thus sidelobe suppression) has the effect of increasing success likelihood. Simpler coding schemes benefit the greatest from increasing transmitter directivity; more complex schemes with higher SIR demands exhibit high success likelihood regardless of antenna directivity. This again can be attributed to the loosening of the upper bounds in high SIR applications.

The effect of trading transmission probability against sidelobe suppression for various deployment scenarios is shown in Figure 5.8. They demonstrate the effect of the user density and SIR threshold have on the achievability of the full range of p_k using just the remaining two system parameters.

5.5 Effect of detected users k

The number of users detected at one time k will also have a significant effect on the expected success likelihood. A_i and B_k are both functions of k to different effects.

As discussed in the previous section the likelihood that the k aligned users are separable in power and SIC is possible (5.12) dominates the overall success likelihood in all but the most dense networks. In these networks k determines the influence of the SIR threshold κ has on the success likelihood through its effect on the exponent $-\frac{\beta k(k-1)}{2}$. With increasing k we expect that this effect increases and the success likelihood is a less linear function of κ. Its multiplicative effect on the user density in β will also yield a greater dependence on the user density.

This is demonstrated in Figure 5.9a which demonstrates that when $k = 3$, the same relation-

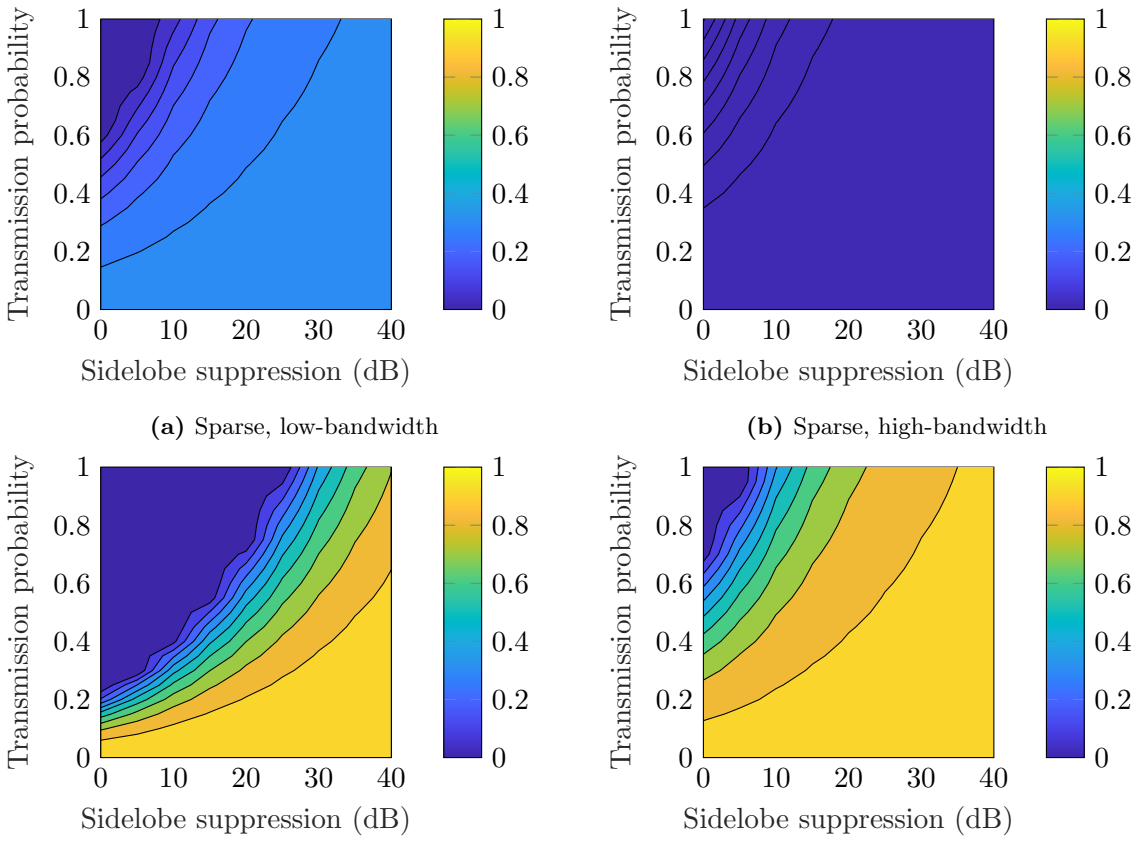

(a) Sparse, low-bandwidth

(b) Sparse, high-bandwidth

(c) Dense, low-bandwidth

(d) Dense, high-bandwidth

Figure 5.8: Effect of ALOHA transmission probability and sidelobe attenuation on theoretical upper bound $p_{k=2}$ for combinations of sparse ($b > 0$) and dense ($b < 0$) and low-bandwidth ($\kappa = 5$dB) and high-bandwidth ($\kappa = 15$dB) scenarios

ship between the parameters remains but the effect of user density is far greater, 'compressing' the achievable region into denser networks. This leads us to the conclusion that detecting higher numbers of users simultaneously is possible only in dense networks, and sparse networks are favoured by reducing the number of users detected at once.

Figure 5.9b demonstrates that the penalty to success likelihood incurred by the increased number of detected users can be recovered from; in order to detect a greater number of users simultaneously, the system designer may choose to reduce the transmission probability to move the system's performance back into a region of higher likelihood.

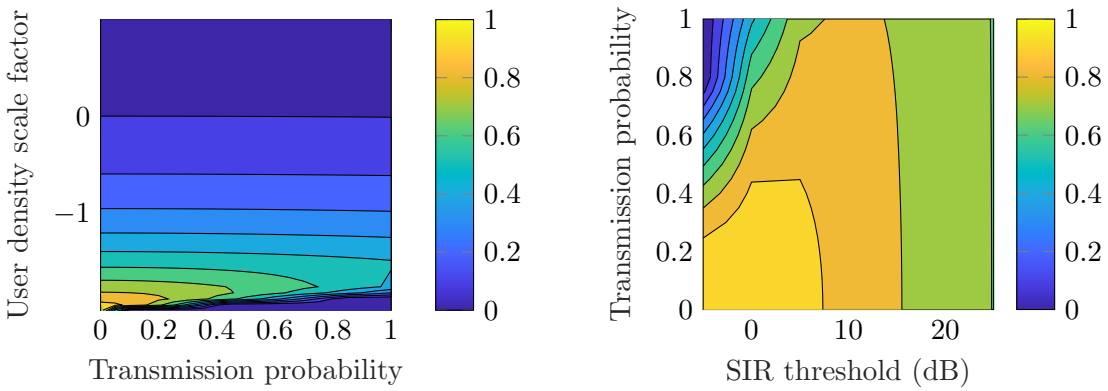

(a) $\kappa = 5\text{dB}, G_T = 5\text{dB}$ **(b)** $b = -1.9375, G_T = 35\text{dB}$

Figure 5.9: Effect of $p_{k=3}$ on influence of density and SIR threshold

5.6 Simulation of neighbour discovery

In this section we examine the performance of a simulated receiver employing neighbour detection, allowing the effect of the four parameters discussed in Section 5.4 to be observed on the likelihood of success. These are then evaluated by comparing the effect of the four parameters on the experienced system performance against that determined through the theoretical upper bound.

5.6.1 Simulation parameters

Results were collected over 500 network instances that meet the construction requirements set out in Section 5.2, with the aligned users and unaligned users in Φ_a and Φ_u generated in independent point processes.

Fading within the network is modelled as Rayleigh distributed with mean absolute value $\mathbb{E}[h] = 1$.

From Equations (5.7) and (5.8) it is observed the PPPs describing the aligned and unaligned users are both non-homogeneous. While the simulation of a homogeneous PPP is straightforward due to its constant user density measure, the simulation of a non-homogeneous PPP requires that the user density measure be quantised at multiple intervals in order to accurately model

the growth or decay in the user density.

A network of radius 10 m around the origin was simulated, quantising the user density measure at 0.25 m intervals. This interval avoids singularity at small values of r but offers reasonable granularity in the modelling of user intensity at distances less than 1 m.

5.6.2 Evaluation of simulation results

Figure 5.10 shows the effect of transmission probability and sidelobe suppression on the measured success frequency over 500 instances of the simulated neighbour discovery protocol. The effect of SIR threshold and network density are clear, with dense networks showing the expected penalty to overall success likelihood. However, the measured success of the high-bandwidth scenario (when SIR threshold is high) contradicts the indication that detection would be more likely in this scenario. This confirms that the upper bound becomes looser as the SIR increases, and the quality of the approximation of success likelihood therefore reduces as the MCS employed in the neighbour detection scheme grows in complexity.

However, the gradient of the success frequency in both Figures 5.10c and 5.10d suggests that the relationships between transmission probability, sidelobe suppression, and network user density match the prediction made by the upper bound. Examining these three in isolation and following the intuitive notion that higher SIR threshold yields a lower likelihood of success, the system designer is still able to use the upper bound as a design tool for planning the network.

From both the theoretical upper bounds and the simulation results it can be confirmed that in sufficiently dense networks the transmission probability can have a significant influence over the likelihood of successfully detecting multiple directional transmitters simultaneously. As the transmission probability of users within the network increases, the likelihood of successful detection reduces.

Likewise it can be confirmed that the level of directivity created by the transmitters' antenna arrays influences success likelihood. In sufficiently dense networks increasing the directivity of

the antenna arrays increases the likelihood of success.

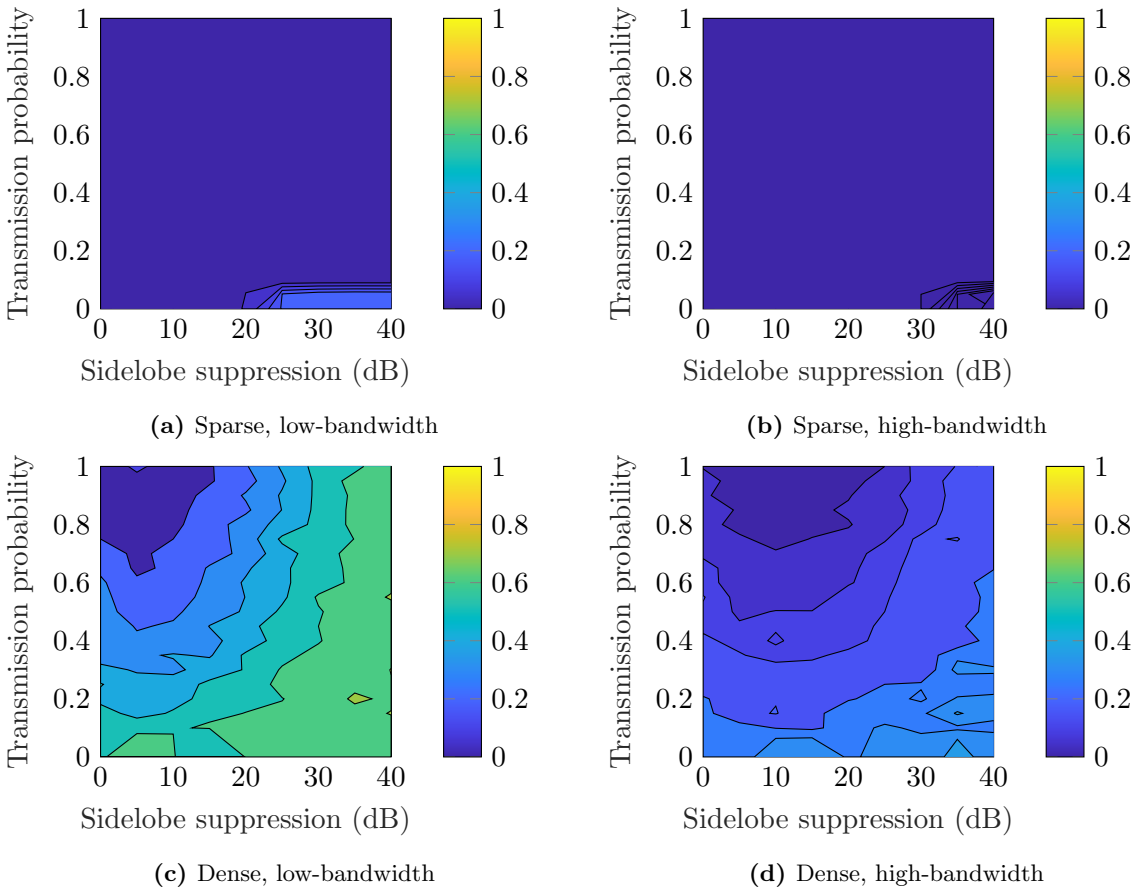

(a) Sparse, low-bandwidth

(b) Sparse, high-bandwidth

(c) Dense, low-bandwidth

(d) Dense, high-bandwidth

Figure 5.10: Effect of ALOHA transmission probability and sidelobe attenuation successfully detecting $k = 2$ users in simulation for combinations of sparse ($b > 0$) and dense ($b < 0$) and low-bandwidth ($\kappa = 5$dB) and high-bandwidth ($\kappa = 15$dB) scenarios

As the number of users to detect increases, the effect of k's influence on the success likelihood is also apparent in the simulation results. Figure 5.11 compares the upper bound of $p_{k=3}$ against the success frequency observed during simulation for the same system parameters. A blank area corresponding to $p = 0.05$ can be attributed to the lack of viable simulations at this transmission frequency; the low transmission probability yields too sparse a network for three aligned users to be present within the network within any reasonable frequency. For the purposes of all the simulations contained in this chapter the minimum frequency of a scenario to be considered feasible was one instance in 1000.

The reduced linearity of the influence of the SIR threshold is apparent here as it was in

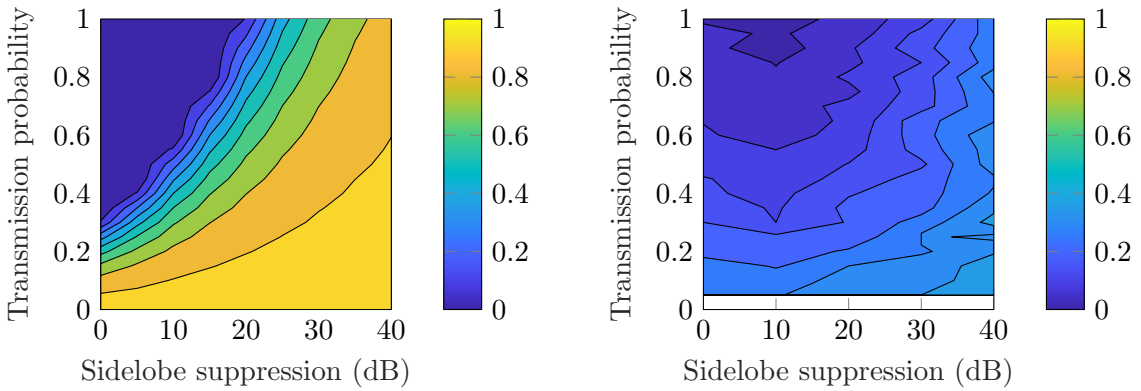

(a) Theoretical upper bound

(b) Simulated

Figure 5.11: Effect of ALOHA transmission probability and sidelobe suppression on $p_{k=3}$ in theoretical and simulated dense, low-bandwidth scenario ($b = -1.9375, \kappa = 5\text{dB}$)

Figure 5.9, which is manifested in the 'stretching' of the gradient of the probability regions in Figure 5.11a compared to 5.8a. This behaviour is confirmed through the results of simulations, exhibiting this same stretched relationship between transmission probability and sidelobe suppression. This has the effect of reducing the system designer's options for tuning the system – since the SIR threshold now has less effect on the success likelihood, the tradeoff that can be made between speed of operation (by increasing transmission probability) and array directivity is less favourable, and the range of success likelihood the designer is able to achieve with the same system parameters is reduced.

5.7 Conclusions

In this chapter we have derived an analytical expression for the upper bound of the likelihood of successfully detecting k users during neighbour discovery. This is achieved by employing directional antenna array patterns at the transmitters, while the receiver remains omnidirectional and able to receive across the entire azimuth. This allows the network, modelled by a Poisson Point Process, to be split into two independent processes. These two processes describe the aligned (i.e. illuminated by the main lobe of the transmitters' arrays) and unaligned (illuminated by the sidelobes of the transmitters' arrays) transmitters within the network. By applying a certain level of gain suppression to the sidelobes of the antenna array patterns using the Dolph-

Chebyshev model, it was hypothesised that it is possible to engineer the network's behaviour in order to meet arbitrary performance goals.

Four network parameters were identified from the success likelihood expression as candidates for use by a system designer to leverage in order to optimise the network to meet the design goals of the overall system. Of these four, two – the network user density scale factor and the coding scheme SIR threshold – were identified to dominate the other two. These parameters heavily influence the achievable region of $p_k = [0, 1]$ available through manipulation of the remaining two parameters – the ALOHA transmission probability and the level of sidelobe suppression in the directional transmitters.

While it was identified that the latter parameters exert an influence on the upper bound of the success likelihood in all networks, the greatest influence over the success likelihood these parameters have is in dense networks with simple coding schemes (the 'dense, low-bandwidth' regime in Figure 5.8).

In such circumstances it was determined that the system designer is able to increase the frequency at which users transmit in each slot of the neighbour detection scheme. As this frequency increases, the likelihood of irretrievable message collision increases and accordingly the likelihood of success decreases. This can be counteracted by increasing the directivity of the transmitter array, and this likelihood penalty recovered. The system designer is therefore capable of trading these two parameters against each other to reach the desired success likelihood.

The use of this upper bound as a method for estimating success likelihood is not without its drawbacks however, and it was demonstrated that the upper bound becomes looser as the SIR threshold increases. For more complex schemes this is reflected in an apparent improvement of system performance despite the higher SIR threshold. In reality, the effect of a more complex scheme matches our intuition that it has a negative effect on the likelihood of success.

6 Conclusions & Further Work

In this thesis we have considered the challenge of performing interference management in distributed, unplanned wireless networks. As well as the trend towards network densificiation increasing the level of interference in wireless networks in general, such networks pose an additional challenge to the system designer in being unable to provide reliable channels for users to receive channel information. This means that interference management becomes more necessary while being limited in what techniques are available for use.

While it is possible for future system designers to make use of the works presented in this thesis in their own planning and deployment of decentralised networks there remains ample opportunities to develop these ideas further.

'Cognitive' modifications to a distributed interference management scheme

The lack of a central base station or shared control channel significantly reduces the number and variety of interference management techniques available to unplanned networks. In Chapter 3 we investigate one technique that remains available, the Iterative Alignment algorithm. By iteratively changing the MIMO coding matrices on both transmitters and receivers it is possible to come to an alignment solution that minimises the levels of interference experienced by users. In ideal conditions this technique is capable of producing perfect interference alignment, eliminating interference altogether. However this algorithm is slow to operate and is limited by the fact it has no knowledge of signal power; the current needs of the network may not necessitate the levels of interference suppression it is capable of. In its original form, the Iterative Alignment algorithm rarely converges within less than 100 iterations. This may be unacceptably long in certain channel conditions.

The original algorithm was modified to selectively update user coding matrix coefficients randomly with some probability $p < 1$. Through simulation it was found that there is an in-

verse relationship between the speed of the algorithm's convergence and the likelihood of a user updating its coding matrix coefficients. It was found that when $p < 0.5$ the proportion of 3-user interference networks converging in less than 100 iterations is significantly increased. It was observed that solutions reached by this modified algorithm were often poorer from the perspective of interference suppression. Therefore it is clear that by reducing the frequency at which users update their coding matrix coefficients, the system designer is capable of improving convergence times at the expense of alignment solution quality. This permits interference suppression to be traded off against speed of operation.

More marked results were observed when the users were made aware of the desired signal's SINR and were allowed to not update their coding matrices when it was not necessary. The level of SINR desired is informed by the desire to avoid complex DoF-splitting coding schemes in favour of treating interference as noise or successive interference cancellation. This power-aware version performed even faster than the selective updates algorithm – it was observed in simulation that nearly all trials of the power-aware algorithm converge within ten iterations. This is achieved at the price of significantly higher interference levels, that ultimately have a negative impact on sum channel capacity. However, since the algorithm is steered by the observed SINR and not simply interference levels, it is also possible that in some channels the power-aware algorithm offers a net gain in network sum capacity compared to the original algorithm. In the conclusion to the chapter we discuss three potential use cases for the algorithm and determine the optimal algorithm choice for each case. This aids the system designer in their choice of an appropriate value for p in the case of the selective algorithm, and allows a comparison to be drawn between their choice and the potential time savings offered by the power-aware algorithm.

Iterative Alignment is only one of several distributed interference management algorithms, as well as the MaxSINR algorithm briefly discussed in Chapter 3. Other subspace-based or SINR-based algorithms may benefit from the same extension we that propose to provide better power control. This would be an immediate extension to the works presented in this chapter.

Channel estimation with unknown numbers of antennas

In the interference regimes where simple decoding practices like treating interference as noise and successive cancellation are not possible, it is necessary to use some kind of joint power control and coding approach. [6] deals with one such technique that also makes use of coding techniques to spread signals across subspaces, based on a modified Han-Kobayashi scheme. Such a technique permits high spectral efficiency by allowing the 'tactical' leaking of interference such that the receiving users are capable of removing it. Crucially, in networks with a variety of heterogeneous configurations a disparity of antennas permits interference to be steered along subspaces invisible to other users. Likewise these channels are also immune to interference caused by such users. In an unplanned network where the users may be equipped with a different number of antennas, conventional channel training techniques using a fixed training sequence leave these additional signalling dimensions to be left undiscovered.

Chapter 4 details a channel training technique based on Gold sequences that allows such users to be discovered without the need for *a priori* user information or a control channel to inform users of each others' configurations. We show that reliable estimates (with likelihood of error less than 1%) of other users' antenna array dimensions can be made at a wide range of transmit powers and channel dimensions. The method requires no prior knowledge of the channel matrix or number of transmit antennas and functions regardless of the size of the receiving user's antenna array. It is found that a combination of sequence length and number of receiver channels can be found that ensures a robust estimation of the channel for a wide range of transmitted signal powers.

This information is then used to inform a channel estimator that uses the same sequence to perform estimation of the channel coefficients. This estimator was found to perform better (roughly 50% reduction in NMSE) than equally-long codes proposed in the literature, at the expense that Gold sequences are only effective at certain fixed lengths. This offers a singificant advantage over other 'blind' techniques, in that it can operate in a heterogeneous network and achieve the full capability of an interference management technique such as [31].

A key limitation of the works in Chapter 4 is the channel model in which the rank estimation technique operates. The Kronecker channel has been demonstrated to underestimate the channel capacity of real channels [73]. This is due to the assumption that the scattering environment in which the channel resides exhibits no correlation between the paths taken from one group of transmit antennas to any group of receive antennas. In real-life scenarios this is not often the case, and physical objects in the channel environment create 'clusters' which induce correlation between the transmit and receive antennas arrays. This concept is introduced and modelled stochastically in Weichselberger, et al. [73], from which the model gets its name, the *Weichselberger Model*. Clustered correlation is also discussed and deterministic models for antenna correlations presented in [53]. This additional correlation between antennas will impact the estimator's ability to estimate the signal rank, as the transmit and receive antennas are no longer separable. It remains an open question if this additional correlation induced by clustering can be modelled and removed from the covariance matrix to recover the signal rank.

Directional antennas in neighbour discovery

Lastly, in Chapter 5 we examine a key element of establishing an unplanned network, the detection and identification of neighbouring nodes within the network. In this chapter we derived a closed-form, analytical result for the upper bound of the probability that k users can be successively decoded. These conditions are precipitated by employing directional circular antenna arrays on transmitters, causing them to be selective in their interference footprints. The delineation between aligned and unaligned users allows each category to be treated independently of each other, easing analysis.

We examine four key parameters of the network and identify where each can be traded off against each other in order to achieve a desired network performance goal. Two parameters are identified as being largely outside the system designer's control, being features of the desired application of the network. The expected user density model is defined by the physical distribution of nodes within the network, while the SIR threshold is defined by the Modulation and

Coding Scheme employed within the neighbour discovery protocol. The transmission probability and sidelobe suppression level are by contrast entirely under the system designer's control, and can be used (alongside the SIR threshold to a lesser extent) to 'tune' the network's operation in order to achieve the desired success probability. It was determined that the first two parameters are much more influential in the likelihood of success, and the latter parameters only exert a significant influence on system performance in a narrow range of scenarios.

While this work models the performance of neighbour discovery using the simplified model of the Dolph-Chebyshev array it is not a true reflection of the effect such an antenna pattern would have on the network. By assuming a flat top across the sidelobes we widen the range of angles of incidence across which interference would be received; a pattern containing many nulls is therefore much less likely to perform as predicted in the model. It is hypothesised that the same technique presented here can be used to apply the gains described by the CDF in each of the two regions (aligned and unaligned) as random mapping vectors to the gains in their respective PPPs. This would offer a more realistic modelling of the gains experience in each region of the antenna pattern, and thus provide a better estimate of the prediction of node degree during neighbour discovery. This would be an immediate and simple extension to the work in this chapter, due to the averaging effect of the mapping of the location-based PPP in $\mathbb{R}^2$ to $\mathbb{R}^+$.

Another immediate extension to this work would be to derive an analytical expression for the lower bound of success likelihood for p_k. This is key to recovering the use of the technique in the high-bandwidth scenario, as the upper bound is found to become loose as the SIR threshold increases, negatively impacting the bound's usefulness in predicting network behaviour.

Bibliography

[1] W. E. Forum. Why securing the Internet of Things is crucial to the Fourth Industrial Revolution. [Online]. Available: https://www.weforum.org/agenda/2019/04/why-securing-the-internet-of-things-is-crucial-to-the-fourth-industrial-revolution/

[2] "Ieee standard for information technology—telecommunications and information exchange between systems local and metropolitan area networks—specific requirements - part 11: Wireless lan medium access control (mac) and physical layer (phy) specifications," *IEEE Std 802.11-2016 (Revision of IEEE Std 802.11-2012)*, pp. 1–3534, Dec 2016.

[3] "Ieee standard for low-rate wireless networks," *IEEE Std 802.15.4-2015 (Revision of IEEE Std 802.15.4-2011)*, pp. 1–709, April 2016.

[4] N. Bhushan, J. Li, D. Malladi, R. Gilmore, D. Brenner, A. Damnjanovic, R. Sukhavasi, C. Patel, S. Geirhofer, S. V. Hattangady, R. G. Alley, G. G. Fountain, R. J. Markunas, G. Lucovsky, and D. Temple, "Network densification: the dominant theme for wireless evolution into 5G," *Communications Magazine, IEEE*, no. 2, pp. 1–8, 2014.

[5] B. Romanous, N. Bitar, M. Imran, and H. Refai, "Network densification: Challenges and opportunities in enabling 5g," 09 2015.

[6] K. Gomadam, V. R. Cadambe, and S. A. Jafar, "A Distributed Numerical Approach to Interference Alignment and Applications to Wireless Interference Networks," *Information Theory, IEEE Transactions on*, vol. 57, no. 6, pp. 3309–3322, 2011.

[7] C. Waters, S. Armour, A. Doufexi, W. H. Chin, and F. Tosato, "Mimo channel dimension estimation in interference channels with antenna disparity," in *2016 IEEE 84th Vehicular Technology Conference (VTC-Fall)*, Sep. 2016, pp. 1–5.

[8] N. Council, P. Affairs, T. Board on Science, C. Economy, C. Wessner, and D. Jorgenson, *Enhancing Productivity Growth in the Information Age: Measuring and Sustaining the New Economy.* National Academies Press, 2007. [Online]. Available: https://books.google.co.uk/books?id=o8qaAgAAQBAJ

[9] J. Luftman, P. Luftman, and O. U. Press, *Competing in the Information Age: Align in the Sand*, ser. Oxford scholarship online. Oxford University Press, 2003. [Online]. Available: https://books.google.co.uk/books?id=P23nCwAAQBAJ

[10] S. M. Alamouti, "A simple transmit diversity technique for wireless communications," *IEEE Journal on Selected Areas in Communications*, vol. 16, no. 8, pp. 1451–1458, Oct 1998.

[11] J. R. Hampton, *Introduction to MIMO Communications.* Cambridge University Press, Nov. 2013.

[12] K. Miller, A. Sanne, K. Srinivasan, and S. Vishwanath, "Enabling real-time interference alignment: promises and challenges," in *MobiHoc '12: Proceedings of the thirteenth ACM international symposium on Mobile Ad Hoc Networking and Computing.* New York, New York, USA: ACM Request Permissions, Jun. 2012, pp. 55–64.

[13] R. H. Etkin, D. N. C. Tse, and H. Wang, "Gaussian Interference Channel Capacity to Within One Bit: the General Case," *Information Theory, 2007. ISIT 2007. IEEE International Symposium on*, pp. 2181–2185, 2007.

[14] C. Rose, S. Ulukus, and R. D. Yates, "Wireless systems and interference avoidance," *IEEE Transactions on Wireless Communications*, vol. 1, no. 3, pp. 415–428, July 2002.

[15] W. Yu, W. Rhee, S. Boyd, and J. M. Cioffi, "Iterative water-filling for gaussian vector multiple-access channels," *IEEE Transactions on Information Theory*, vol. 50, no. 1, pp. 145–152, Jan 2004.

[16] S. A. Jafar and S. Shamai, "Degrees of freedom region of the mimo x channel," *IEEE Transactions on Information Theory*, vol. 54, no. 1, pp. 151–170, Jan 2008.

[17] H. Farhadi, "Interference Alignment and Power Control for Wireless Interference Networks," Ph.D. dissertation, 2012.

[18] G. Miao and G. Song, *Energy and Spectrum Efficient Wireless Network Design.* Cambridge University Press, 2014.

[19] N. Abramson, "The aloha system: Another alternative for computer communications," in *Proceedings of the November 17-19, 1970, Fall Joint Computer Conference*, ser. AFIPS '70 (Fall). New York, NY, USA: ACM, 1970, pp. 281–285. [Online]. Available: http://doi.acm.org/10.1145/1478462.1478502

[20] M. A. Charafeddine, A. Sezgin, Z. Han, and A. Paulraj, "Achievable and crystallized rate regions of the interference channel with interference as noise," *IEEE Transactions on Wireless Communications*, vol. 11, no. 3, pp. 1100–1111, March 2012.

[21] C. Geng, N. Naderializadeh, A. S. Avestimehr, and S. A. Jafar, "On the optimality of treating interference as noise," *IEEE Transactions on Information Theory*, vol. 61, no. 4, pp. 1753–1767, April 2015.

[22] T. Han and K. Kobayashi, "A new achievable rate region for the interference channel," *IEEE Transactions on Information Theory*, vol. 27, no. 1, pp. 49–60, January 1981.

[23] X. Shang, B. Chen, and M. J. Gans, "On the achievable sum rate for mimo interference channels," *IEEE Transactions on Information Theory*, vol. 52, no. 9, pp. 4313–4320, Sep. 2006.

[24] M. Zheng, C. Ling, W. Chen, and M. Tao, "Polar coding strategies for the interference channel with partial-joint decoding," *IEEE Transactions on Information Theory*, vol. 65, no. 4, pp. 1973–1993, 2019.

[25] D. Tse and P. Viswanath, *Fundamentals of Wireless Communication.* New York, NY, USA: Cambridge University Press, 2005.

[26] H. Chong, M. Motani, H. K. Garg, and H. E. Gamal, "On the han–kobayashi region for theinterference channel," *IEEE Transactions on Information Theory*, vol. 54, no. 7, pp. 3188–3195, July 2008.

[27] S. A. Jafar, S. Shamai, A. Zaidi, Z. H. Awan, L. Vandendorpe, S. S. Shitz, C. S. Vaze, M. K. Varanasi, S.-H. Park, Y.-c. Ko, A. Agustin, J. Vidal, M. Ashraphijuo, V. Aggarwal, X. Wang, R. V. Cadambe, Z. Wang, X. Chen, S. H. Song, and K. Ben Letaief, "Degrees of Freedom Region of the MIMO X Channel," *Information Theory, IEEE Transactions on*, no. 1, pp. 1–20, 2008.

[28] V. Cadambe, S. A. Jafar, and S. Shamai, "Interference alignment on the deterministic channel and application to fully connected AWGN interference networks," *Information Theory Workshop, 2008. ITW '08. IEEE*, pp. 41–45, 2008.

[29] H. Maleki, S. A. Jafar, and S. Shamai, "Retrospective Interference Alignment Over Interference Networks," *Selected Topics in Signal Processing, IEEE Journal of*, vol. 6, no. 3, pp. 228–240, 2012.

[30] S. A. Jafar, "Interference alignment: A new look at signal dimensions in a communication network," *Foundations and Trends in Communications and Information Theory*, pp. 1–136, 2011.

[31] S. Karmakar and M. K. Varanasi, "The generalized degrees of freedom region of the mimo interference channel and its achievability," *IEEE Transactions on Information Theory*, vol. 58, no. 12, pp. 7188–7203, Dec 2012.

[32] H. Maleki, S. A. Jafar, and S. Shamai, "Retrospective interference alignment," in *Information Theory Proceedings (ISIT), 2011 IEEE International Symposium on*. IEEE, 2011, pp. 2756–2760.

[33] S. A. Jafar, "Blind Interference Alignment," *Selected Topics in Signal Processing, IEEE Journal of*, vol. 6, no. 3, pp. 216–227, 2012.

[34] T. Gou, C. Wang, and S. A. Jafar, "Aiming Perfectly in the Dark-Blind Interference Alignment Through Staggered Antenna Switching," *Signal Processing, IEEE Transactions on*, vol. 59, no. 6, pp. 2734–2744, 2011.

[35] B. Nazer, M. Gastpar, S. A. Jafar, and S. Vishwanath, "Ergodic Interference Alignment," *Information Theory, IEEE Transactions on*, vol. 58, no. 10, pp. 6355–6371, 2012.

[36] M. Haenggi, *Stochastic Geometry for Wireless Networks*, 1st ed. New York, NY, USA: Cambridge University Press, 2012.

[37] F. Baccelli, B. Błaszczyszyn *et al.*, "Stochastic geometry and wireless networks: Volume ii applications," *Foundations and Trends® in Networking*, vol. 4, no. 1–2, pp. 1–312, 2010.

[38] F. Baccelli and B. Błaszczyszyn, "Stochastic geometry and wireless networks: Volume i theory," *Foundations and Trends® in Networking*, vol. 3, no. 3–4, pp. 249–449, 2010. [Online]. Available: http://dx.doi.org/10.1561/1300000006

[39] J. W. Massey, J. Starr, S. Lee, D. Lee, A. Gerstlauer, and R. W. Heath, "Implementation of a real-time wireless interference alignment network," in *2012 Conference Record of the Forty Sixth Asilomar Conference on Signals, Systems and Computers (ASILOMAR)*, 2012, pp. 104–108.

[40] S. Lee, A. Gerstlauer, and R. W. Heath, "Distributed real-time implementation of interference alignment with analog feedback," *IEEE Transactions on Vehicular Technology*, vol. 64, no. 8, pp. 3513–3525, Aug 2015.

[41] O. Popescu, D. C. Popescu, and C. Rose, "Interference avoidance for capacity optimization in mutually interfering wireless systems," in *VTC-2005-Fall. 2005 IEEE 62nd Vehicular Technology Conference, 2005.*, vol. 1, Sep. 2005, pp. 593–597.

[42] C. Geng, N. Naderializadeh, A. S. Avestimehr, and S. A. Jafar, "On the optimality of treating interference as noise," in *Communication, Control, and Computing (Allerton), 2013 51st Annual Allerton Conference on*. IEEE, 2013, pp. 1166–1173.

[43] R. K. Mallik and Q. T. Zhang, "Optimum combining with correlated interference," *IEEE Transactions on Wireless Communications*, vol. 4, no. 5, pp. 2340–2348, Sep. 2005.

[44] J. L. L. Morales and S. Roy, "Training sequence design for robust joint detection and channel estimation over rank-deficient mimo links," in *2012 International Conference on Computing, Networking and Communications (ICNC)*, Jan 2012, pp. 221–226.

[45] Y. Liu, T. F. Wong, and W. W. Hager, "Training signal design for estimation of correlated mimo channels with colored interference," *IEEE Transactions on Signal Processing*, vol. 55, no. 4, pp. 1486–1497, April 2007.

[46] J. P. Kermoal, L. Schumacher, K. I. Pedersen, P. E. Mogensen, and F. Frederiksen, "A stochastic MIMO radio channel model with experimental validation," *IEEE J. Sel. Areas Commun.*, vol. 20, no. 6, pp. 1211–1226, 2002.

[47] E. Dahlman, S. Parkvall, J. Skold, and P. Beming, *3G Evolution, Second Edition: HSPA and LTE for Mobile Broadband*, 2nd ed. Orlando, FL, USA: Academic Press, Inc., 2008.

[48] M. Ozcelik, N. Czink, and E. Bonek, "What makes a good mimo channel model?" in *2005 IEEE 61st Vehicular Technology Conference*, vol. 1, May 2005, pp. 156–160 Vol. 1.

[49] R. Gold, "Optimal binary sequences for spread spectrum multiplexing (corresp.)," *IEEE Transactions on Information Theory*, vol. 13, no. 4, pp. 619–621, October 1967.

[50] J. Holmes, *Spread Spectrum Systems for GNSS and Wireless Communications*, ser. GNSS technology and applications series. Artech House, 2007, no. v. 45. [Online]. Available: https://books.google.co.uk/books?id=-AUfAQAAIAAJ

[51] H. T. Hui. Multiple Antennas for MIMO Communications - Channel Correlation. [Online]. Available: https://www.ece.nus.edu.sg/stfpage/elehht/Teaching/EE6832/Lecture%20Notes%5CMultiple%20Antennas%20for%20MIMO%20Communications%20-%20Channel%20Correlation.pdf

[52] L. Schumacher, K. I. Pedersen, and P. E. Mogensen, "From antenna spacings to theoretical capacities - guidelines for simulating mimo systems," in *The 13th IEEE International Symposium on Personal, Indoor and Mobile Radio Communications*, vol. 2, Sep. 2002, pp. 587–592 vol.2.

[53] A. Forenza, D. J. Love, and R. W. Heath, "Simplified spatial correlation models for clustered mimo channels with different array configurations," *IEEE Transactions on Vehicular Technology*, vol. 56, no. 4, pp. 1924–1934, July 2007.

[54] C. F. Van Loan and N. Pitsianis, *Linear Algebra for Large Scale and Real-Time Applications*. Dordrecht: Springer Netherlands, 1993, ch. Approximation with Kronecker Products, pp. 293–314.

[55] Z. Gu, A. Wang, W. Shi, Z. Tian, K. Ren, and F. Lau, "A practical neighbor discovery framework for wireless sensor networks," *Sensors*, vol. 19, p. 1887, 04 2019.

[56] S. A. Jafar, "Topological interference management through index coding," *IEEE Transactions on Information Theory*, vol. 60, no. 1, pp. 529–568, 2014.

[57] H. Sun, C. Geng, and S. A. Jafar, "Topological interference management with alternating connectivity," *2013 IEEE International Symposium on Information Theory (ISIT)*, pp. 399–403, 2013.

[58] F. Tian, B. Liu, H. Cai, H. Zhou, and L. Gui, "Practical asynchronous neighbor discovery in ad hoc networks with directional antennas," *IEEE Transactions on Vehicular Technology*, vol. 65, no. 5, pp. 3614–3627, May 2016.

[59] H. Park, Y. Kim, T. Song, and S. Pack, "Multiband directional neighbor discovery in self-organized mmwave ad hoc networks," *IEEE Transactions on Vehicular Technology*, vol. 64, no. 3, pp. 1143–1155, March 2015.

[60] R. A. Santosa, B. Lee, C. K. Yeo, and T. M. Lim, "Distributed neighbor discovery in ad hoc networks using directional antennas," in *The Sixth IEEE International Conference on Computer and Information Technology (CIT'06)*, Sep. 2006, pp. 97–97.

[61] A. Russell, S. Vasudevan, B. Wang, W. Zeng, X. Chen, and W. Wei, "Neighbor discovery in wireless networks with multipacket reception," *IEEE Transactions on Parallel and Distributed Systems*, vol. 26, no. 7, pp. 1984–1998, July 2015.

[62] R. Pozza, M. Nati, S. Georgoulas, K. Moessner, and A. Gluhak, "Neighbor discovery for opportunistic networking in internet of things scenarios: A survey," *IEEE Access*, vol. 3, pp. 1101–1131, 2015.

[63] C. Bettstetter, C. Hartmann, and C. Moser, "How does randomized beamforming improve the connectivity of ad hoc networks?" in *IEEE International Conference on Communications, 2005. ICC 2005. 2005*, vol. 5, May 2005, pp. 3380–3385 Vol. 5.

[64] O. Georgiou, S. Wang, M. Z. Bocus, C. P. Dettmann, and J. P. Coon, "Directional antennas improve the link-connectivity of interference limited ad hoc networks," in *2015 IEEE 26th*

Annual International Symposium on Personal, Indoor, and Mobile Radio Communications (PIMRC), Aug 2015, pp. 1311–1316.

[65] L. T. Dung, T. D. Hieu, B. An, and B. Kim, "How does beamforming influence the connectivity of cognitive radio ad-hoc networks?" in *2016 International Symposium on Computer, Consumer and Control (IS3C)*, July 2016, pp. 227–230.

[66] Y. Wang, S. Mao, and T. S. Rappaport, "On directional neighbor discovery in mmwave networks," in *2017 IEEE 37th International Conference on Distributed Computing Systems (ICDCS)*, June 2017, pp. 1704–1713.

[67] X. Yu, J. Zhang, M. Haenggi, and K. B. Letaief, "Coverage analysis for millimeter wave networks: The impact of directional antenna arrays," *IEEE Journal on Selected Areas in Communications*, vol. 35, no. 7, pp. 1498–1512, July 2017.

[68] C. L. Dolph, "A current distribution for broadside arrays which optimizes the relationship between beam width and side-lobe level," *Proceedings of the IRE*, vol. 34, no. 6, pp. 335–348, June 1946.

[69] B. K. Lau and Y. H. Leung, "A dolph-chebyshev approach to the synthesis of array patterns for uniform circular arrays," in *2000 IEEE International Symposium on Circuits and Systems (ISCAS)*, vol. 1, 2000, pp. 124–127 vol.1.

[70] T. Das, A. Ghosh, S. Chatterjee, and S. Chatterjee, "Closed-form expression for first null beamwidth of a beam-steered dolph–tschebysheff array," *Electromagnetics*, vol. 36, no. 1, pp. 1–16, 2016.

[71] T. Milligan, *Modern Antenna Design*, ser. Wiley - IEEE. Wiley, 2005. [Online]. Available: https://books.google.co.uk/books?id=PPyDQXAd09kC

[72] X. Zhang, "Managing randomness in wireless networks: Random power control and successive interference cancellation," Ph.D. dissertation, University of Notre Dame, 2013.

[73] W. Weichselberger and M. Herdin, "A stochastic MIMO channel model with joint correlation of both link ends," *IEEE Trans. Wireless Commun.*, 2006.